Additive Manufacturing 51 (2022) 102642

Contents lists available at ScienceDirect

Additive Manufacturing

journal homepage: www.elsevier.com/locate/addma

Field-assisted additive manufacturing of polymeric composites

Shahriar Safaee [a], Matthew Schock [a], Erina B. Joyee [b], Yayue Pan [c], Roland K. Chen [a,*]

[a] School of Mechanical and Materials Engineering, PO Box 642920, Washington State University, Pullman, WA 99164, USA
[b] Department of Mechanical Engineering and Engineering Science, University of North Carolina at Charlotte, Charlotte, NC 28223, USA
[c] Department of Mechanical and Industrial Engineering, University of Illinois at Chicago, Chicago, IL 60607, USA

ARTICLE INFO

Keywords:
Additive manufacturing
3D printing
Polymeric composites
Field-assisted
Selective anisotropy

ABSTRACT

Additive manufacturing (AM) is a transformative manufacturing approach capable of building parts with free-form and complex geometries. Polymers come with a wide range of material properties and can be processed via several different AM processes. Adding anisotropy to polymeric composites opens new applications for polymer AM by earning additional functionality and creating composites with tailored properties. One of the new approaches in creating tailored anisotropic composites is pairing external fields that can exert force on fillers and manipulate them inside polymeric matrices. Four main types of external fields - shear, acoustic, magnetic, and electrical - are devised to control filler orientation and concentration in polymeric composites. This review highlights the recent research advances in field-assisted additive manufacturing technologies with the goal of creating polymeric composites with controlled anisotropy orientation and concentration.

1. Introduction

Additive manufacturing (AM), also known as 3D printing (3DP), rapid prototyping (RP), and solid freeform fabrication (SFF), is admittedly acknowledged as one of the most important industrial revolutions of the last 50 years [1]. Using this manufacturing niche, a digital computer-aided design (CAD) model is turned into a physical part by using a single machine without the need for going through multiple conventional manufacturing methods. In contrast to traditional subtractive manufacturing, which typically starts from a solid block of raw material and cuts excess areas away to generate the desired geometries, AM is a free-form process that builds 3D structures by adding materials generally one layer at a time. Utilizing its unique ability of rapidly generating near net-shaped products built upon multiple materials and theoretically no geometric limitations, AM introduces a wide and rapidly expanding range of applications from customized biomedical devices [2] to jet engine components [3] and mass-produced wearables [4]. Considering the advances in cyber-physical systems, AM also provides a flexible manufacturing platform in which people from all around the world have the opportunity to contribute to the design process and build parts with virtually no limitations [5].

AM was initially developed using single-phase materials and to date, most of the progress in additive manufacturing has been achieved on single-material processes. Due to a wide range of technologies and methods developed based on the additive concept, these manufacturing processes can be formulated to build components from various materials with different functionalities. However, the inability of single-material AM in creating structures that possess advantages of multi-material components, such as the low strength to weight ratio or the need for added functionality, has led to increasing attention towards AM of multi-material and composite structures. Composite materials are engineered or naturally built from more than one constituent component, each of which have significant differences in their properties and remain distinct from each other in the final structures [6]. Nature has developed this class of materials by embedding reinforcing particles into architectured structures. This approach helps natural materials such as cortical bone [7], dactyl clubs of the stomatopods [8], and spiders web [9], to generate superior physical and mechanical properties. While building natural composites is linked to complex biological structures and molecular behavior, they also have a far broader diversity compared to synthetic composites. Rather than the limited materials used in synthetic composites, this issue also originates from the inability in local control of concentration and orientation of reinforcing elements [10].

Owing to their relative availability and ease of processing and synthesis, polymers have received immense attention compared to other materials in this field [11]. While polymeric materials possess many advantages such as being lightweight, biocompatible, and responsive to external stimuli [12], they frequently lack mechanical strength

* Corresponding author.
E-mail address: roland.chen@wsu.edu (R.K. Chen).

https://doi.org/10.1016/j.addma.2022.102642
Received 7 September 2021; Received in revised form 21 January 2022; Accepted 24 January 2022
Available online 29 January 2022

compared to other materials. As such, this is where polymeric composites are introduced by adding continuous or discontinuous fillers to the polymeric matrix, which allows additional functionalities or enhanced mechanical properties [13]. Additive manufacturing of polymeric composites has been widely used for building 3D structures [14]. One of the superior advantages of AM compared to traditional manufacturing processes is the ability to build multi-material structures [15]. However, because of the relative infancy of this research area as well as limitations in most of the commercial printers, multi-material function of additive technologies is just beginning to be utilized in many industries. Using the multi-material approach, region-specific properties can be engineered in the structures fabricated in a single machine. Composite structures with local changes in the building unit blocks or graded distribution of the fillers, are also categorized under multi-material structures in AM [14]. Considering the abilities of multi-material additive manufacturing, one of the current topics for research in additive manufacturing of polymeric composites is controlling the direction of anisotropy in the structure [16]. Aligned fillers in polymeric composites leads to improved functionalities such as strengths and electrical conductivity. From a mechanical behavior point of view, controlling anisotropy in composite structures is critical as it helps the highly concentrated loads become dispersed in larger areas which leads to smaller stresses and eventually less chance of material failure [17].

Current limitations in aligning the reinforcing elements in polymeric composites can be, to some extent, addressed by the natural flow behavior of the materials in extrusion-based AM processes, in which the shear force between the extrusion channel and viscous material induces stresses into the flow and leads to a partial filler alignment [18,19]. The initial research related to this approach is dated back to about 50 years ago, where Bell [20] and Murty and Modlen [21] noticed that in a convergent channel, particles that are suspended in a fluid have a tendency to be aligned in the same direction as the flow. With the emergence of extrusion-based additive manufacturing technologies and the need to develop more advanced materials and improve the control over local structural properties, researchers have used the same concept in aligning the embedded fibers in AM of fiber-reinforced composites (FRCs) [22]. From a current industrial point of view, different companies such as Markforged and Fortify have tried to develop both their machines and materials for printing composite and multi-material structures with a goal of optimizing mechanical properties. As most of the multi-material or composite 3D printing machines work with extrusion-based technologies, they also work towards aligning the fibers along with the extrusion direction, which still does not give a selective control over anisotropy orientation.

Aside from the natural tendency of the fillers to be aligned in the flow direction during extrusion-based processes, other AM technologies do not possess such an intrinsic control over filler orientation. Therefore, controlling the anisotropy that originates from filler orientation in AM of composite structures remains to be one of the major challenges of this field [14]. Moreover, commercial polymer AM machines such as PolyJet and Multi Jet Fusion are very limited in terms of material choices and do not have the ability to control the fillers' orientation or concentration. Addressing the anisotropy alignment problem, however, is a promising research area in different additive technologies. By utilizing AM methods, precise control over the fillers within a layer can be achieved, which leads to better control over mechanical and physical properties of the product such as Young's modulus, toughness, thermal properties, and electrical conductivity [23]. These effects have been widely studied by different groups [24–27]. Variation in the anisotropy orientation in AM also adds a new dimension in design and opens additional avenues to develop new functional materials with customized and locally engineered properties such as thermal and electrical conductivity and mechanical properties [28].

The distribution of fillers in polymeric composites determines the bulk material behavior. Random distribution of the fillers leads to a merely isotropic structure, and by selectively aligning the fillers, certain material properties can be controlled. In last two decades, a new approach has been explored in controlling the anisotropies in polymeric composites which consists of using an external source of energy paired with the additive technology to control the fillers independently from the manufacturing process [29–32]. In this manufacturing approach, the external energy is generated from different fields such as magnetic [33], acoustic [34], electric [31], and shear fields [19], and is paired with AM technologies such as extrusion-based and vat photopolymerization processes (Fig. 1). In this context, a field is defined as a physical phenomenon that is capable of exerting a real-time force on materials, leading to an unmediated change in materials orientation or motion. This approach has been proven to be promising in controlling the filler orientation and in some cases, the filler concentration, while used concurrently with additive manufacturing technologies.

Field-assisted AM processes are used to reach customized polymeric composites with tuned properties. Using different fields gives the ability to locally control the fillers and fine-tune their location and orientation. This also helps with building programmable devices [33], shape shifting structures [35], self-assembled nanostructures [28,36], and efficient thin films [37]. Field-assisted additive manufacturing methods have been discussed in other works [38–42]. A comprehensive review on nanomaterial patterning in AM of polymeric composites has been done by Elder et al., where the focus is on integrating different physical phenomena such as thermal, mechanical, magnetic, electrical, evaporation, shear, optical, and electrical effects with AM technologies to develop functional architectures [40]. In another review, a thorough study on recent advances in using external force-generating fields in AM processes of polymers, metals, and ceramics is represented [41]. Current work will provide a detailed review on different field-assisted AM processes to build polymeric composites, previous research in this field, and its current state-of-the-art methodology. This review is organized as follows. In Section 2, a brief overview on the AM technologies used in field-assisted AM of polymeric composites is provided. In Sections 3–6, different assistive fields including shear, acoustic, magnetic, and electric fields are reviewed, and their contribution to AM of polymeric composites with selective alignment of reinforcing components is discussed. In each of these sections, a survey on how each field works, and how the assisted field is integrated to an AM process is provided and applicable materials, state-of-the-art implementation, potential and current

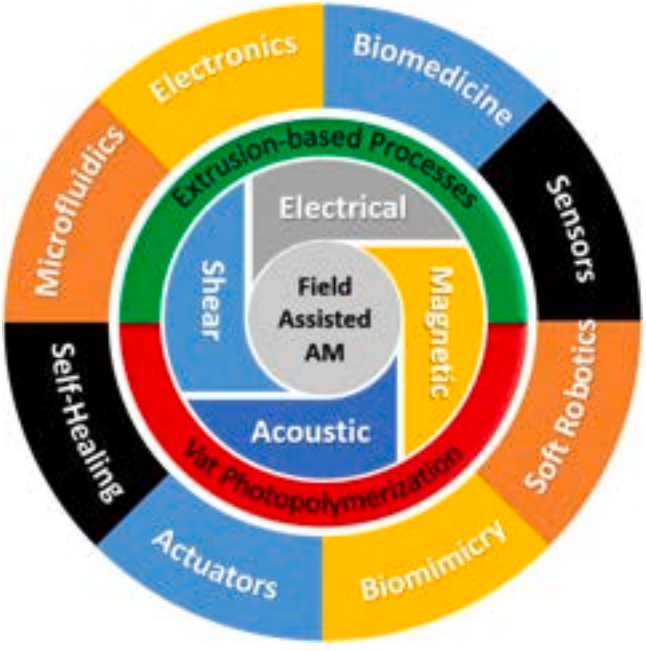

Fig. 1. Integration of external fields to additive manufacturing technologies can generate new categories and applications for polymeric composites.

applications and limitations of these processes, as well as possible future directions for each field are discussed. Due to the more complex integration or electrical and magnetic fields into AM technologies and the providing better insights into possible applications and future works, a brief section is dedicated to discussing the integration of these two fields into conventional manufacturing processes such as casting and molding.

2. Additive manufacturing technologies

AM technologies can be classified into seven categories according to the general principles and terminology for additive manufacturing published by the American Society for Testing and Materials (ISO/ASTM 52900:2015) [43]. These categories are binder jetting, directed energy deposition, material extrusion, material jetting, powder bed fusion, sheet lamination, and vat photo-polymerization. Among all of the AM technologies, material extrusion and vat photo-polymerization are two categories that are more widely integrated with an assisted field for AM of polymeric composites, and as a result, this review will focus on these two methods paired with external fields to control anisotropy in polymeric composites. Based on ISO/ASTM 52900:2015, these two processes are defined as follows:

> "*material extrusion* — an additive manufacturing process in which material is selectively dispensed through a nozzle or orifice."

> "*vat photopolymerization* — an additive manufacturing process in which liquid photopolymer in a vat is selectively cured by light-activated polymerization."

In the following two subsections, these two processes are briefly introduced to provide adequate context for the review in the later sections. It should be noted that there are a few studies using the material jetting process with an assisted field. Given the small number of references on field-assisted material jetting processes, these studies are reviewed together with the extrusion-based processes without a dedicated section.

2.1. Extrusion-based processes

Material extrusion is the most commonly used category of additive manufacturing processes. Popular AM processes in this category include Fused Filament Fabrication (FFF), also known as Fused Deposition Modeling (FDM), and Direct Ink Writing (DIW), also known as Liquid Deposition Modeling (LDM). Extrusion-based AM was first developed and introduced into the market based on the US patent 5121,329 by Scott Crump for the trademarked FDM process [44]. Since the expiration of this patent, many small and big companies have focused on developing 3D printer machines that utilize this FFF process. Fig. 2a illustrates the concept of material extrusion AM, which builds 3D objects by pushing a liquid-phased material, which can be a melt or ink, through the nozzle in a mostly continuous manner and deposit the extruded material selectively. Currently, various materials ranging from concrete to soft biomedical hydrogels that contain living cells are being printed using extrusion-based AM technology.

Two major limitations of extrusion-based AM technologies are the low surface quality and anisotropic mechanical properties, which are basically due to the nozzle size that is used in these processes [45]. However, using post-processing methods and smaller nozzle diameters, these issues have been addressed to some degree. The dimensional resolution of this process normally depends on the nozzle diameter, material deformation, flowability after extrusion, and the accuracy of the motion system in the 3D printing machine. In order to use the extrusion-based processes for AM of composite structures, two different approaches can be used: multi-nozzle processes, in which different materials are selectively extruded in different areas, or single-nozzle processes that use a mixture of matrix and reinforcing elements as the extruded material [14]. Process-specific considerations need to be taken when using either approach with many ongoing studies covering them. For the first approach, the control over multi-material properties and adhesion between different materials could still be challenging. For the second approach, preparing a filament or ink with desired filler and/or porosity distribution is also a challenge [46].

2.2. Vat photopolymerization

Vat photopolymerization was the first additive manufacturing concept that made its way to the market, developed and commercialized by Chuck W. Hull based on the US Patent 5,554,336 [47]. In this process, the resin vat contains a liquid photopolymer as the initial raw material for building the final product. This process is based on solidifying or curing a photosensitive liquid polymer by using a light source to provide the energy required to induce the curing chemical reaction [48]. At each step, a thin layer of a photocurable liquid resin is cured and solidified using different wavelengths of light. After each layer is formed, the print bed will move up or down (depending on the top-down or bottom-up nature of the process), and because of the void created from moving the cured layer, the fresh uncured resin flows to the print area and will be used to print the next layer. In the top-down approach, as shown in Fig. 2b, where the resin is cured by a light source above the build plate and resin vat, the printed part is exposed to more mechanical forces due to the separation from the bottom of the resin vat, while using less resin. This approach also provides a smoother surface in printed layer owing to minimal oxygen inhibition during the print process [49]. On the other hand, in bottom-up process (Fig. 2c), the resin is cured through a window at the bottom of the vat using a light source located below the vat, while the print bed is moving upwards for building the layers. In order to use vat photopolymerization process for building composite parts, the reinforcing elements might be added to the resin mixture from the beginning of the process, or they might be locally added using a secondary technology such as material extrusion.

In vat photopolymerization, the dimensional accuracy of the part is determined by the platform accuracy in the z direction, material curing properties, light wavelength, and the quality of the projected image into

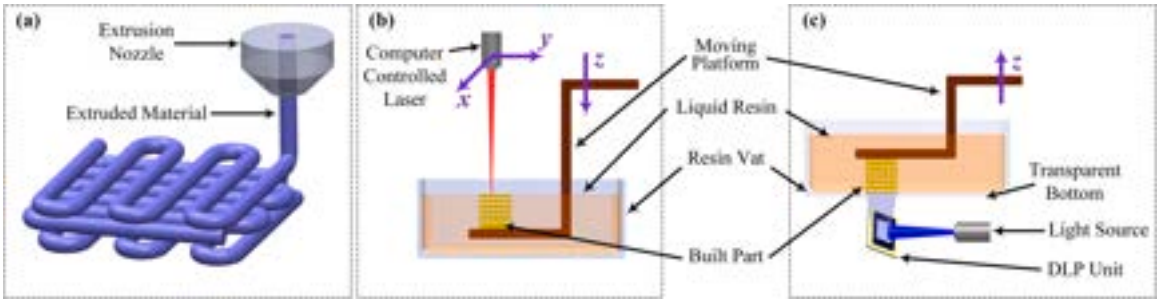

Fig. 2. (a) The basic concept in extrusion-based AM processes, (b) and (c): Different approaches in vat photopolymerization: (b) Laser-based top-down approach, and (c) DLP-based bottom-up approach.

the vat in the *x-y* plane. Light can be illuminated in two different forms: laser light that scans the pattern in each layer (laser-based stereolithography) or a projection of the digital mask image corresponding to each layer of the model. The projection method has been developed as an outcome of recent developments in LCDs (Liquid Crystal Displays) and DMDs (Digital Micromirror Devices) which can help with processing the light and reflecting the light-beam in different given patterns and, as a result, increasing the dimensional resolution of the process [50]. In this approach, which is a more novel method and uses the Digital Light Processing (DLP) technology, the LCD or DMD reflects the light beam pattern of a layer immediately into the resin vat and as a result, one layer is cured at a time. This approach leads to larger build sizes and faster manufacturing processes. Depending on the optical components used in DLP, this process can have a better dimensional accuracy than the laser-based approach. Fig. 2b-c shows the schematics of top-down and bottom-up approaches with laser- and DLP-based vat photopolymerization, respectively.

3. Shear field-assisted AM

Based on the concepts of fluid mechanics, shear stress in a flow originates from the difference between velocity of the walls and the fluid [51,52]. Therefore, a shear stress field is generated in a flow as a result of a no-slip boundary condition on the channel walls (Fig. 3a). About a century ago, shear-induced alignment of particles in a flow was first reported and modelled by Jeffery [53]. His work led to introducing the Jeffery orbits, a phenomenon causing the particles to experience continuous rotation during extrusion in a close channel and subsequently not achieving desired short-fiber alignment. Since then, more precise and sophisticated models regarding this matter have been studied and developed both theoretically and experimentally with a goal of synthesizing advanced composite materials with tailored properties, and shear forces have been employed to gain more desired composites with better mechanical characteristics [20,21,54].

Shear force has been used to synthesize nanoscale materials and develop customized polymeric composites. Chen et al. were among the first teams to develop the shear exfoliation process to transform graphite to graphene [55]. In this process, exposing the vortex fluidic films of the liquid to shear derived from centrifugal forces leads generating graphene in the solution (Fig. 3b). Expanding on the footsteps of this work, other researchers have developed similar processes such as turbulence-assisted exfoliation, which uses shear forces to produce graphene from liquid solutions [56,57]. Aside from material synthesis, different approaches have been used to apply shear forces that encourage alignment of nanoparticles in a polymeric matrix. In some studies, pure shear force in a solid media has been applied to align individual nanofibers in a single direction. Due to their interesting physical properties, a substantial portion of the research on shear-assisted alignment is focused on carbon nanotubes (CNTs) as the reinforcing components [58], where methods such as peeling-off [59], lateral shear (domino pushing) [60], and cutting has been used (Fig. 3c-e). Other methods of shear-assisted alignment in composite materials utilize flow-induced and extrusion-induced shear forces. Flow-induced shear forces emerge in a process such as chemical vapor deposition (CVD), in which the fillers within a coating layer grow in the direction of flow deposition on the surface and subsequent natural assembly of the nanomaterials from the same composition [61–63]. Extrusion-induced shear originates from the flow conditions in a channel and occurs following the no-slip boundary condition. Although these shear-induced alignment approaches have been widely used in manufacturing of composite materials with tailored properties, only the concepts of shear-assisted and peeling-assisted shear-induced alignment are used in AM of polymeric composites.

With increasing advancements in fluid mechanics and manufacturing processes, different approaches have been adopted to control shear-assisted alignment by introducing solutions that overcome Jeffery orbits. In conventional manufacturing processes such as casting and injection molding, depending on the geometry of the mold, sprues, or inlets, shear-alignment can act as a dominant intrinsic factor for re-orienting the fillers. More advanced manufacturing processes have also utilized shear-assisted particle alignment and control the Jeffery orbits using approaches such as controlling flow velocity, material properties, channel geometry, and surface properties [64–67]. Using the shear-assisted alignment for developing advanced materials is not only limited to where bulk flows of the materials run into a closed or open channel. Even in small volumes of a viscous fluid, using shear forces can lead to selective alignment of reinforcing elements along the shear direction, as reviewed by Hu et al. in developing shear coating and dip-coating processes to create 1D or 2D materials with selective anisotropy alignment [68].

Thanks to the undebatable advantages of additive manufacturing in building freeform structures, shear-assisted alignment is paired with AM to develop more advanced and tailored polymeric composites and enhance material properties such as electrical behavior, mechanical strength, and thermal conductivity. About twenty years ago for the first time, shear-assisted additive manufacturing was studied and

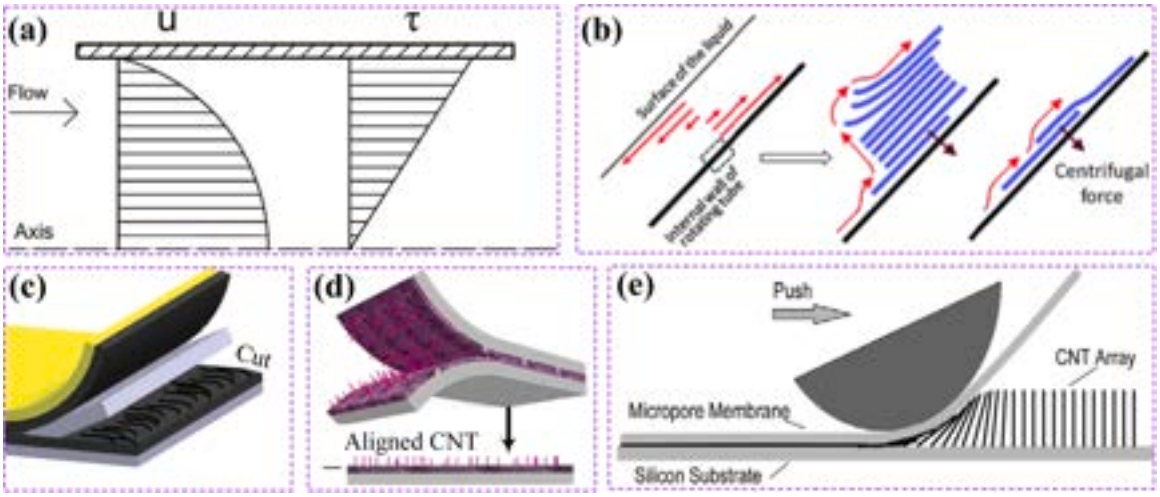

Fig. 3. Different concepts of shear field used in material development: (a) Profiles of velocity and shear stress for laminar flow [52]. (b) Microfluidic centrifugal flow velocity and the shear profile leading to exfoliation [55]. (c) Schematic of the method to align nanofibers using cutting method [58]. d) Peel-off method [59]. (e) Lateral shear method [60].

investigated by Dr. Jennifer Lewis and her team using a DIW ink consisting of a mixture of deionized water and silica particles with a surface treatment of poly(ethylenimine) as a DIW ink [69,70]. Although these works aimed at building ceramic materials rather than polymeric composites, they proved that by optimizing the extrusion process and material characteristics, customized composite structures can be achieved. This work pioneered other researchers to develop better materials and processes that can be more effective in term of shear-assisted alignment for building 3D composite structures. Since shear-assisted particle alignment is an intrinsic behavior that happens in many fluidic environments, shear field has been devised by many researchers to induce filler alignment into the polymeric composites made by AM. Unlike other fields discussed in this review, pairing the AM process with shear-assisted alignment does not require adding any additional equipment to the process and focuses on optimizing the material properties and process parameters to accentuate the applied shear force to the fillers. The following two sections will describe advances in shear-assisted AM processes in aligning reinforcing elements in polymeric composites and includes the extrusion-based and photopolymerization-based AM, which are the main processes that benefit from shear-assisted alignment.

3.1. Shear field-assisted extrusion-based AM

In extrusion-based manufacturing processes, shear-alignment occurs when anisotropic nanofillers experience the shear stress that originates from the boundary conditions of the flow. As a result of this shear force, fillers align themselves along the principal axis of the flow. Using short fibers inside the printed material in a process like FDM leads to partial flow-induced alignment within the nozzle during extrusion [18], as fibers want to re-orient in the direction of the extrusion [19,71] (Fig. 4a). Depending on where and how the shear stress is applied the most to the fillers, shear-assisted alignment of the particles in extrusion-based AM happens in two different ways [40]. In the first approach, which is predominantly used, the shear force is applied to the flow from the nozzle walls. When the fluid is moving inside a nozzle, due to the no-slip boundary condition, the flow undergoes a shear stress leading to particle/fiber realignment in the direction of the flow. In the second approach, which is less commonly used, the shear force might be applied after the material is extruded. An example of this phenomenon has been observed by Roskov et al. in the electrospinning process [64]. In electrospinning, aside from the electric field that helps with extrusion of the filament and realigning the reinforcing materials with extrusion direction, shear force can also play an important role. In this process, after the material is extruded towards the collector, owing to the minimal cross-sectional area of the filament, particles will experience a shear force along the extrusion direction which leads to intrinsically aligning the particles in the same direction.

When it comes to particle/fiber alignment in polymeric composites, enhancing mechanical properties is one of the primary goals that has been sought by different research studies. To reach this goal by using shear field, FFF was used to print nanocomposites of acrylonitrile

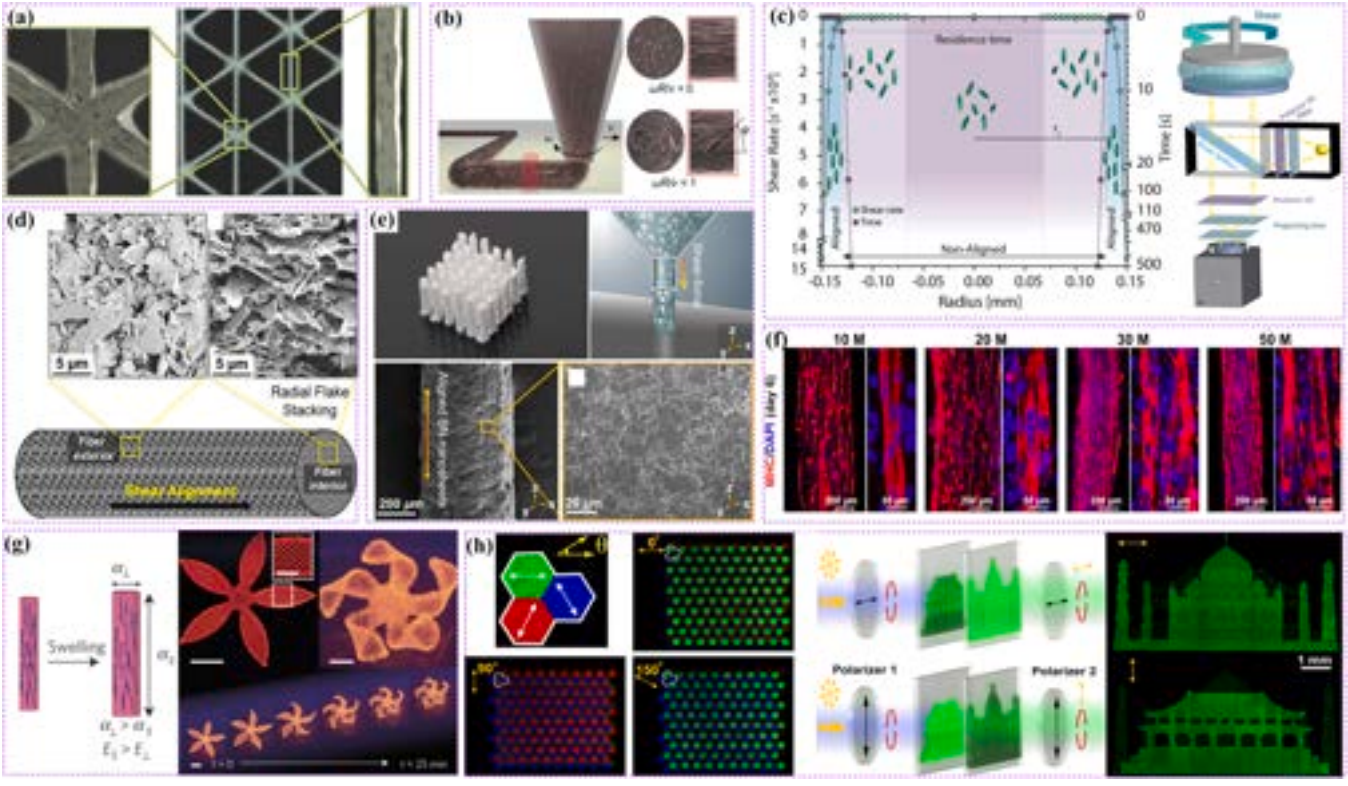

Fig. 4. Extrusion-based shear-alignment in AM: (a) Optical images of a triangular honeycomb 3D printed by SiC/C filled epoxy, showing how particles are aligned along the extrusion direction is different areas [19]. (b) Filler re-orientation mechanism during the 3D printing processes paired with nozzle rotation and the ideal outcoming orientation [72]. (c) The relationship between shear rate profile and corresponding required alignment time in radial direction of the nozzle and in situ polarization rheological setup [74]. (d) SEM images of the 3D printed sample showing how shear-assisted alignment led to aligning the graphene flakes along the fibers [79]. (e) The shear-assisted AM and 6 × 6 array of boron nitride rods and the SEM image of the rod's surface showing aligned nanosheets [81]. (f) Immunofluorescent images of 3D printed constructs containing human cells show that on a time period of 5 days after differentiation, cells start growing in longitudinal direction due to shear forces that act at the same direction [94]. (g) The mechanism of time-dependent swelling behavior as an outcome of shear-induced particle orientation during the print process and how it can lead to building smart stimuli-responsive devices [96]. (h) Printed pixel arrays with polarization-dependent emission multiplexing: To illustrate the polarized nanocomposites, when looking at the 3D printed polarized perovskite nanocomposites using two-layer device, patterns related to Taj Mahal and Forbidden city are seen, which are printed with horizontal and vertical polarization, respectively [98].

butadiene styrene (ABS) matrix containing vapor grown carbon nanofibers (VGCF) using a filament made out of the same material [22]. The filaments were prepared using shear processing of the mixture of ABS and VGCF. Owing to the shear forces in filament preparation, there is a degree of alignment in the initial material used for the extrusion process. Including shear-aligned VGCFs in the printed composite structure increase the storage modulus up to 68% than that of unfilled ABS. Same approach was used by Zhong et al. to embed short glass fibers into a ABS matrix by preparing filaments of the matrix and reinforcement materials using shear stress to align the fibers during the extrusion process [18]. Compton and Lewis's work inspired by the cellular structure of balsa wood helped them develop an epoxy-based ink to mimic the remarkable stiffness and bending properties of balsa wood through aligned fiber reinforcement achieved during the extrusion process [19]. In this work, highly oriented fiber-filled epoxy composites of SiC/C-epoxy and SiC-epoxy inks were printed using an extrusion-based process (Fig. 4a). Results of this work show high alignment of SiC whiskers and carbon fibers along the print direction, leading to a considerable increase in the mechanical properties. Expanding on this extrusion-based model, Raney et al. introduced nozzle rotation during the extrusion process (rotational direct ink writing, RDIW) to help enhance the mechanical structures of the manufactured product [72]. Nozzle rotation happens based on the print geometry and toolpath, leading to decoupling the particle orientation from toolpath. Therefore, pure shear leads to orienting the fillers in a more uniform way through different geometrical complexities of the printed part. Implementing a rotational aspect provides extreme control over the material as well as its mechanical properties, yielding much stronger materials with a higher damage tolerance compared to when the nozzle is not rotating (Fig. 4b).

Understanding the particle-fluid interaction is critical in shear field-assisted additive manufacturing. One of the major research gaps in this area is the relationships between shear rate, nozzle size and geometry, rheological behavior of the 3D printed material, and particle properties. Raney et al. studied the particle behavior of gold-platinum nanorods floating in hydrogen peroxide flowing into a Polydimethylsiloxane (PDMS) microchannel [72]. Although in this work polymeric materials are not included, the research framework used by this team can be used when studying the AM of composite materials with polymeric matrix. In another study, a mixture of a polymeric matrix with a high volume fraction of carbon fiber was printed using a micro-extrusion process to develop polymeric composites with tunable mechanical properties [71]. A numerical model was also developed to understand the effect of shear-alignment and optimize the process parameters to reach maximum alignment in the final product. Coupling the methods of smoothed particle hydrodynamics (SPH) and the discrete element method (DEM), Yang et al. developed a new approach for modeling the particle interactions and orientation in extrusion-based AM processes [73]. This approach is helpful in optimizing the AM process and polymeric composites fabricated by such manufacturing methods. In a very unique work, Hausmann et al. experimentally investigated the dynamics of shear-alignment of high volume fraction cellulose-loaded DIW inks, using in situ polarization rheology [74]. In this process, polarization microscopy was devised to take real-time photos of the sample under a rheometer system (Fig. 4c). By changing the shear deformation rate, different yield stress values were measured for different inks. Subsequently, the same inks were exposed to steady-state rheological tests to understand the effect of time on particle alignment under different shear rates. The shear rate difference between these two experiments is used to get an estimation of shear-induced alignment in different inks. As an outcome of this study, combinations of shear rate and nozzle geometry and also design guidelines for DIW inks were proposed to induce proper particle alignment in 3D printed architectures.

One of the topics in material development that has recently drawn a vast deal of attention is developing high energy-density structures with applications in capacitors, batteries, and power transmission systems. A common and efficient strategy in developing these materials is embedding highly aligned nanomaterials inside a polymeric matrix [75–78]. When focusing on the potential of AM to generate these structures, shear-assisted DIW is one of the most widely investigated processes. Most of the studies on shear-assisted DIW for energy and electronic materials focus on developing printable ink with high capability of shear-alignment. Jakus et al. developed a graphene ink used in printing biocompatible and electrically conductive constructs with enhanced mechanical properties [79]. This ink is composed of graphene flakes mixed with hyperelastic polyester polylactide-co-glycolide (PLG), which acts as the binder in the polymeric composites. The printed scaffolds in this study showed highly aligned graphene flakes in-line with the extrusion direction, which is ascribed to the shear-assisted alignment that happens during the DIW process and verified by scanning electron microscopic (SEM) images (Fig. 4d). This work is suggested as a baseline for printing wearable electronics with high electrical conductivity. The same approach was used by Luo et al. to print $BaTiO_3$ nanowires/P(VDF–CTFE) nanocomposites [80]. The shear field during the extrusion process of P(VDF–CTFE)/$BaTiO_3$/dimethylformamide helped with aligning the nanowires in the polymeric matrix. Results of this work show more than 50% improvement in maximum discharged energy of the nanocomposite with aligned nanowires, compared to the nanocomposites with randomly oriented nanowires prepared by the casting method. Liang et al. developed an extrusion-based method for multiscale printing of vertical arrays of 2D structures with highly aligned boron nitride nanorods (Fig. 4e) [81]. The alignment achieved from this study works in favor of increasing the thermal conductivity, which makes the printed structures to be an ideal choice for thermal management purposes. Liu et al. used the FFF of filaments made of thermoplastic polyurethane filled with hexagonal boron nitride (hBN) platelets. Using X-ray diffraction (XRD) and small angle X-ray scattering (SAXS), the degree of filler alignment in 3D printed composite was estimated [82]. Due to the shear effect in extrusion, the hBN platelets are reported to align along the extrusion direction, leading to 2.5 times higher thermal conductivity compared to the samples prepared by hot pressing with the same platelet loading.

One of the aspects of shear-assisted extrusion-based AM is adding materials to the ink that can modify the viscosity of the ink and enable a better shear-assisted behavior. Following the work done by Lewis et al., Kokkinis et al. used fumed silica in 3D printable inks for shear-assisted alignment because of silica's natural behavior as a viscosity modifier [33]. Based on the studies by Jin et al., another material used to modify the viscosity of DIW inks [83] and print self-supporting structures [84] is laponite nanoclay. Additionally, cellulose nanofiber is another additive that enhances the printability of DIW inks. Owing to the high aspect ratio, excellent mechanical properties, and electrostatic repulsive forces of cellulose nanofibers, these materials have played a critical role in developing printable inks and developing tailored composites with desired properties [85]. Since cellulose nanofiber is one of the major reinforcements in wood, using it as a reinforcing element in polymeric composites leads to developing mechanically stronger materials [86, 87]. A CNT/cellulose composite was developed by Li et al., yielding excellent electrical conductivity and mechanical strength in 3D printed structures [88]. In this study, cellulose nanofibers work as the surfactant for CNTs, helping with uniform dispersion of carbon nanotubes in a water solution. A similar approach is also used to print pure cellulose nanocrystals and cellulose-reinforced composites using DIW of aqueous and monomer-based inks [89].

One of the major applications of extrusion-based AM processes is in bioprinting, where the systems are based on dispensing cell-loaded ink. Since shear stress is an inseparable part of the dispensing system, it has an immense effect on 3D bioprinting processes. Due to the biological concerns about the living cells, there is a range of acceptable shear stress for bioprinting. Moderate amounts of shear stress play a positive role in biological processes such as cell differentiation [90] and maturation [91]. On the other hand, excess shear stress on the cell leads to dispatching the cells. In bioprinting where hydrogels with high viscosities

are being extruded out of a nozzle with a small diameter, the shear stress becomes a more crucial phenomenon [92]. Using the DIW bioprinting of hydrogels containing C2C12 myoblast cells, it was observed that the cells were aligned after printing and started to grow along the main axis of printed filaments of the hydrogel. One of the effects of this shear-assisted alignment, which is not observed in previous 2D cell culture studies, was cell maturation after 21 days of culture [93]. Longitudinal formation of myofibers and alignment of cells is also observed by bioprinting human muscle progenitor cells in fibrin ink (Fig. 4f) [94]. In another study from the same team, it is shown that bioengineering can also be utilized in shear force alignment extrusion applications to create cornea tissue and pre-orient the tissue prior to growing in vivo to allow for a viable specimen [95]. Using shear-assisted additive manufacturing and by successfully controlling collagen fibrils orientation, this group successfully created a lattice pattern of a human cornea, using a bioink of cellularized corneal extracellular matrix (ECM) keratocytes.

Extrusion-based shear-alignment of particles and fibers have also played an important role in developing smart and stimuli-responsive materials. Shear induced alignment of fibrils in DIW process led to localized anisotropic swelling behavior, and as a result, the printed filaments showed anisotropic stiffness in longitudinal and transverse directions (Fig. 4g) [96]. A hydrogel composite and acrylamide matrix such as *N,N*-dimethylacrylamide reinforced by nanofibrillated cellulose (NFC) was printed, and by controlling geometrical parameters such as filament size, shape morphing structures programmed to be stimulated by hydration into different shapes were formed. Fast and reversible shape morphing composites were also developed by using DIW and embedding shear-aligned graphene oxide (GO) flakes into a sodium alginate matrix [97]. Due to the controlled alignment of GO flakes, structural local deformation is directed in a single direction, leading to programmed responsive shape changing with multiple stimuli such as water, heat, and light (Fig. 4h). DIW of nanocomposite inks was performed to control the alignment and composition of perovskite blocks made from cesium lead halide ($CsPbX_3$, X = Cl, Br, and I) nanowires, filled block copolymer matrices, and shape polarized optical structures [98]. In these nanocomposites, local environment and alignment of the nanowires define the angular emission pattern of the light. As a result, with controlled pattern of the nanowires, the materials will emit different colors of light when exposed to ultraviolet (UV) beams with certain polarization angles. Applications of such materials can be in information storage and encryption, mechano-optical sensing, and optical displays.

3.2. Shear field-assisted vat photopolymerization AM

Owing to the natural shear-induced particle alignment in extrusion-based processes, most of the research in shear-assisted AM is done on DIW and FFF. In these studies, a nearly laminar and mostly continuous flow of the print material is used to ensure the filler alignment along extrusion direction. For vat photopolymerization, however, using shear field to align the fillers is a little more challenging, since this technology does not possess the intrinsic shear generation during the process. Yunus et al. developed a resin vat which is subjected to lateral oscillation, induced by a linear oscillatory mechanics is installed under the vat (Fig. 5a) [99]. For the reinforcing material, interfacial bonding of the aluminum oxide nanofibers and the resin was enhanced using a silane bonding agent. This oscillation leads to generation of Couette flow and shear forces in both vertical and horizontal directions (Fig. 5b), which results in re-orienting the aluminum oxide nanofibers in the resin vat [100]. Shear-induced alignment of aluminum oxide nanowires led to improving the tensile strength up to 25%. The effect of frequency in the oscillator is studied and it was concluded that a frequency of 1 Hz will yield the maximum shear rate of 314 s^{-1}, leading to the best mechanical behavior in the final product. In order to have better control over local flow in the print area, it is suggested that some wall patterns need to be printed. Same approach of shear patterning was also used to prepare nanocomposites reinforced with silica, alumina, alumina-silica mix, and nickel-coated carbon fibers [101]. An important aspect of this work is the ability of the process to generate green bodies of ceramic-matric composites and generate fully-ceramic parts after burning out the binders and sintering the green bodies (Fig. 5c), which is an industrial approach that is being used by some of the 3D printer manufacturing companies such as Formlabs. A team of researchers at the University of Buffalo has contributed to understanding and applying the shear-induced alignment of particles and molecules in vat photopolymerization process [102–107]. One of the major effects of shear stress during vat photopolymerization process is molecular alignment in print area, which affects the structures and properties of the 3D printed parts. It is suggested by this team that having a delay in printing each layer after positioning the print bed leads to lower degree of molecular alignment in 3D printed product. The findings of these studies is utilized in developing more sensitive polymeric piezoelectric devices.

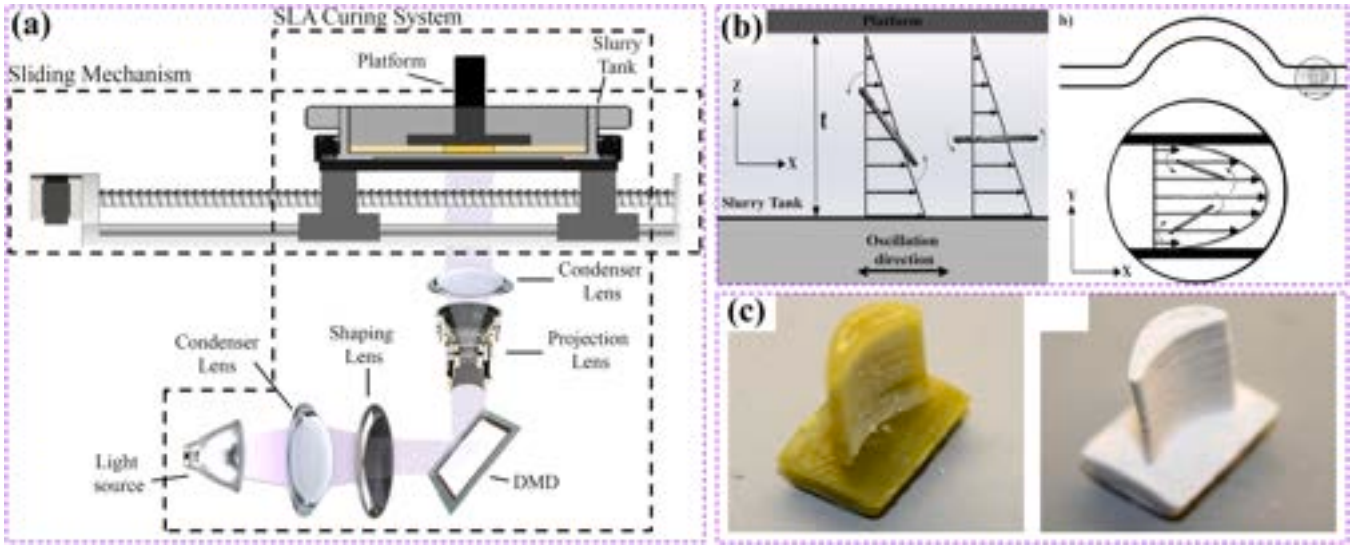

Fig. 5. Shear-assisted alignment in vat photopolymerization: [101] (a) Mechanism used to move the vat back and forth, and introduce shear force in the print area, (b) Schematic of shear alignment process in the proposed method, (c) Green and sintered ceramic part built by the shear-assisted vat photopolymerization.

3.3. Potentials and limitations of shear field-assisted AM

In comparison to other fields that have been paired with AM technologies to re-orient particles and fibers, shear forces can devise a wider range of materials, since the shear forces work in direct contact with the fillers. While among other force fields discussed in this review, generating the shear force in extrusion-based AM is the least challenging, using shear forces to align the fillers is not always the most efficient methods unless the optimized process parameters and material properties are selected.

Compared to other fields, the simplicity of generating the shear field comes with some drawbacks. One of these drawbacks is the current inability in spatial control over the shear field. To this date there is a lack of research is controlling the degree of orientation and concentration within a single AM process in a real-time fashion. When using other field-assisted AM processes, by changing the spatial profile of the field, particle orientation and in some case particle concentration can be locally controlled. However, current approaches in shear-assisted AM do not offer such an ability, and they work the best only in controlling the filler orientation.

3.4. Future perspectives of shear field-assisted AM

From the process and materials parameters point of view, there is a lack of research in predicting the process parameters in order to get to the best shear-alignment. For example, in terms of efficiently devising the shear-alignment in AM technologies, materials development plays an important role in shear-assisted alignment of particles in AM. In this sense, using the potential of colloidal assembly, studying rheological behaviors of print material, and utilizing particle-ink interactions seems to be the main areas that needs more attention. From the theoretical point of view, more comprehensive studies on understanding the effects of nozzle geometry and nozzle wall friction are needed to establish the framework for optimizing the effective shear forces that align the fillers. There is also a close relationship between print material behavior and nozzle characteristics that needs to be understood.

Shear field has been successfully used to partially align fibers and particles due to the material flow in extrusion-based AM; however, there is a relative lack of research endeavor on shear-assisted alignment in AM of polymeric composites using vat photopolymerization. Although it is harder to implement effective shear field in vat photopolymerization, because of the potential of this process in building parts with a higher resolution, shear-assisted vat photopolymerization is also another area that needs to be explored and formulated.

4. Acoustic field-assisted AM

Acoustic field is one of the most widely used external sources of energy for material manipulation in manufacturing processes [108–111]. This field creates moderate forces by producing waves of varying magnitude and frequency to drive materials towards equilibrium states with the potential of not having any direct physical contact [112–115]. Similar to the shear field, acoustic field-assisted AM has the advantage of working with any material regardless of their physical properties, shapes, anisotropy, and sizes. Materials that can be moved or assembled by acoustic fields range from nanometer to millimeter size in solid, liquid, gas, and even tissue or living cells [113,114,116–119]. With such a wide scope of applications, acoustic waves are demonstrated to be effective tools for particle trapping [120], separation, detection, focusing, assembling, and fluid mixing and purification [42,100,121]. However, there are certain limitations associated with the acoustic field. Compared to magnetic or electric field-assisted techniques, acoustic field-assisted techniques have been reported to be challenging in terms of controlling the materials with spatial precision [122,123]. Moreover, while acoustic fields can assemble the solid particles into certain patterns, increased volume can cause poor results. Considering all these unique properties, acoustic field is still one of the most versatile external fields to be used in AM for orienting and patterning nanometer to millimeter sized particles of different shapes and properties into ordered arrays in a polymer matrix, which allows for printing composites with locally varied material compositions, particle alignments, and engineered properties.

There are primarily four distinct approaches that can be adopted to generate acoustic radiation forces to manipulate materials: focused beams [119,124], switching mode [117,118], linear arrays of transducers facing reflective surfaces [125–127], and emission of counter-propagating travelling waves [128–131]. The first approach generally uses an acoustic device constructed with a transducer together with a focusing crystal or concave lens, which can trap and manipulate a single liquid droplet in a manner similar to optical tweezers [119,124]. The second approach, the switching mode method, utilizes a transducer-reflector pair, and by rapidly switching between half and quarter wavelength frequencies, this technique can establish a new agglomeration position that enables particles to be moved to any arbitrary location between the half and quarter wave nodes [117,118]. Using a similar strategy as switching, instead of using one transducer against a reflector, the third method uses a linear array of transducers facing the reflectors. By using multiple transducers with different widths and driving frequencies, this method provides better ability to control the particle assembly in different locations [125–127]. The fourth approach uses pairs of opposing transducers to create counter-propagating waves, in which the pressure node positions are not fixed. By altering the relative phases of the counter propagating waves, the particle assembly can be controlled within the chamber [128,129]. Among the four methods of acoustic force generation, the switching and counter-propagating travelling wave-based methods have been widely studied and used in field-assisted AM.

In order to generate acoustic waves in all of the four methods explained previously, transducers are connected to functional generators and amplifiers which control both the wave frequency and amplitude. The standing waves generated by the transducers lead to steep acoustic pressure gradients within the substrate. These gradients lead to generation of forces which act on suspended materials, moving them towards the pressure nodes or anti-nodes, depending on the densities of fluid and solid materials [130–132]. As long as there is a difference in compressibility and density between the fillers and the surrounding medium which in this case is acoustic contrast, any combination of the host material and filler materials are suitable, which makes the acoustic control quite versatile. When the materials are deposited through an extrusion printhead in an AM process, transducers are attached on the printhead to generate vibrations during extrusion of filaments, solid particles, pastes, or liquid suspensions. This vibration creates better flow control within the nozzle and also increases filler concentration in printed patterns. In vat photopolymerization AM, the solid particles and fibers are pre-dispersed in the resin vat. Piezoelectric transducers are attached either to the resin vat inner walls or outside the resin vat, generating acoustic waves in the dispersion to rearrange the fillers to form desired patterns in the liquid resin [133,134].

Since an extensive range of materials are responsive to the acoustic field, researchers have investigated fillers including: various metal powders, polymer particles such as PDMS spheres or hollow SiO_2 spheres, inorganic particles such as $BaTiO_3$ spheres, ceramic powders such as silicon carbide, SiC, and glass particles. Among different fillers, nano- and micro- sized, continuous and discontinuous glass fibers are most often used to print reinforced polymer composites. Researchers also investigated carbon nanofibers, carbon microfibers, SiC fibers, nickel coated fibers, and silver coated particles. Moreover, a wide range of liquid materials have been studied as host materials, including photocurable polymers, acetone, agar, polyester, silicone and its composites, extremely viscous materials such as polymer clay, hydrogels, and bioinks. In the literature, two categories of AM processes, extrusion-based AM and vat photopolymerization AM, have utilized the acoustic field

to redistribute and assemble particles for productions of composites or multi-material objects with spatially varied material compositions. In this section, the integration of acoustic fields in these 2 AM categories is reviewed.

4.1. Acoustic field-assisted extrusion-based AM

In an extrusion-based AM process, liquid or paste-like ink is dispensed from a nozzle with a controlled flow rate onto a substrate along digitally defined paths for fabricating 3D structures in a layer-by-layer manner. Most commonly, the liquid inks are reinforced with materials such as glass or carbon fibers for the 3D printing of composite structures. In the extrusion process, the internal microstructure of the ink changes because of the deposition, relaxation, and shear force generated during the printing. Although the shear force is favorable in some occasions to naturally align the fillers, it does not have the capability to position or align high concentration of particles/fibers, or separate and manipulate different types of fillers simultaneously.

As a potential solution to address this challenge, acoustic field has been widely utilized in extrusion-based AM, especially in DIW methods, to align multi-scale particles or fibers within fluid inks. Acoustic field has also been effectively used for filler concentration and separation in target positions within the composite ink simultaneously during printing. Particles and fibers of different shapes such as spherical or cylindrical, different sizes from nano- to micro-meter, and different material properties have been investigated in acoustic field-assisted extrusion-based AM processes. Piezoelectric ceramic transducers and ultrasonic probes have been utilized for acoustic field generation in extrusion techniques. The generated acoustic waves are ultrasonic standing waves, such as surface acoustic waves (SAW) and bulk acoustic waves (BAW) for 2D and 3D patterning of particles in the printed traces, respectively.

Depending on the methodology of the extrusion process, acoustic field can be applied before or after the extrusion of the ink. In the first approach, a setup primarily consisting of ultrasonic transducers, a signal generator, and an amplifier is connected to the extruding nozzle. By generating the standing acoustic waves within the nozzle, the system is able to re-orient, align, separate, concentrate, or assemble fillers in the liquid ink inside the nozzle. The desired particle distribution patterns in the liquid ink are generated by the acoustic field within the nozzle immediately before extrusion and then retained in the printed traces. In the second approach, the acoustic setup is attached to the substrate, and acoustic waves were generated within the printed traces to pattern particles in the liquid ink after the deposition but before the full solidification.

A considerable fraction of the research following the first approach, which applies the acoustic field before extrusion, is reported by a group from UC Santa Barbara, led by Begley et al [135–138]. They investigated acoustic focusing of fillers within nozzles in DIW processes to extrude multi-phase composite materials with retained patterns in the printed traces. The multi-phase composite materials printed by their process were comprised of epoxy matrix and fillers including both particles and fibers (silver-coated glass microspheres, hollow SiO_2 spheres and solid $BaTiO_3$ spheres, SiC fibers). In their experimental setup, the extrusion nozzle consisted of a rectangular glass-capped silicon microfluidic channel with a piezoelectric transducer attached to the nozzle using ultrasonic coupling gel [135]. The piezoelectric actuator generated standing half-waves in the silicon channel, establishing standing BAW across the channel width. Particles flowing through the channel were assembled at the nodes of the BAW and subsequently extruded onto a glass substrate. The transducer was thermally coupled to a cooling stage using thermal joint compound to maintain at 20^{o} C temperature. It was observed that increasing the acoustic wave amplitude decreased the particles focusing width.

In another study performed by this group, two different types of nozzles were investigated: a single-channel nozzle and a branched-channel nozzle which produced different local volume fractions of fillers in the printed composites [137]. For the single-channel nozzle, a lead zirconate titanate (PZT) transducer was attached to the outlet of the silicon channel using ultrasonic coupling gel, whereas for the branched-channel nozzle, a second PZT transducer was coupled at the outlet channel near the nozzle exit (Fig. 6a). In the branched-channel nozzle, the second transducer at the outlet was tuned to the half-wave frequency to induce a second stage of focusing, which further concentrated and increased the local volume fractions of the particles during extrusion. The nodes/anti-nodes created by the half-wave pressure also facilitated particle separation in the channel. The denser solid spheres were focused to the center pressure node, whereas the less-dense hollow sphere was driven to the pressure anti-node, close to the channel walls (Fig. 6a). The particle separation and alignment were further retained in the printed traces.

A group from Nanyang Technological University at Singapore used a similar principle of filler focusing but with a slightly different setup to print biological materials [139–142]. Instead of using a silicon microfluidic channel, they glued parallel PZT transducers on the same side of the external wall of a glass tube, which worked as the extrusion print head. The vibration provided by the parallel PZT transducers to the glass tube containing C2C12 cells and human umbilical vein endothelial cells (HUVECs) enabled the nozzle to position and focus the cells before the extrusion process. By exerting high amplitude vibrations to the glass tube nozzle, this study was able to effectively accumulate the biological cells in a short period of time at the center of the cylindrical tube and the pattern were further retained within the printed constructs.

Aside from transducers attached on the outer surface of the nozzle using ultrasonic gel at one side, researchers have also attached pairs of transducers on two opposing outer side surfaces of the nozzle so that a more uniform and stronger acoustic field can be formed in the particle-resin mixture. In a study reported by Wadsworth et al., the extrusion nozzle of a commercial 3D printer was replaced with a custom syringe nozzle [143]. Two PZT transducers were attached to the nozzle external walls, generating standing SAW which aligned the dispersed fillers into discontinuous line patterns in the liquid ink within the nozzle, which were also successfully retained in the printed traces (Fig. 6b).

Utilizing the second approach for acoustic field assistance in extrusion processes, which is acoustic manipulation after extrusion, Shirwaiker et al. presented multiple studies for extrusion-based bioprinting. A common issue in bioprinting is the low concentration of cells in the bio-ink, which results in weak cell-to-cell interaction and slow cell proliferation in the printed construct [144,145]. Achieving high concentrations of cells in 3D printed constructs is usually challenging since it is difficult to accumulate them at the nozzle during extrusion. To solve this problem, this group used acoustic waves to align cells after the extrusion to a bio-ink vat [144,145]. They used opposing transducer-reflector pairs placed in the inner side walls of a bio-ink vat, to generate standing BAWs to pattern human adipose-derived stem (hASC) cells in single/multi-layered hydrogel (Fig. 6c). They found that the spacing between adjacent cell strands was governed only by the acoustic wave frequency and not the cell type, while the strand width was dependent on the transducer frequency and cell type. Furthermore, it was observed that the cell viability was at least 80%, highlighting the adequacy of the developed acoustic field-assisted extrusion AM process for tissue engineering applications.

In addition to particle or fiber focusing and assembling, a study reported by Gunduz et al. demonstrated the utilizaiton of high-amplitude (Ap-p $>$ 1 μm) ultrasonic vibrations (HUAV) in extrusion-based AM processes for reducing flow resistance and improving flow rates, especially for extruding heterogeneous materials with a high fraction of solids ($>$ 60 vol%) and extremely high viscosities ($>$10,000 Pa.s) [146]. Researchers attached a custom PZT transducer-steel probe assembly to the syringe extruder (Fig. 6d). The probe assembly had a resonant frequency of 30 kHz matched to the nozzle resonant vibration mode, generating vibrations with amplitudes of up to 20 μm at the probe tip. A small fan and a vibration duty cycle in the range of 50–80% were used to

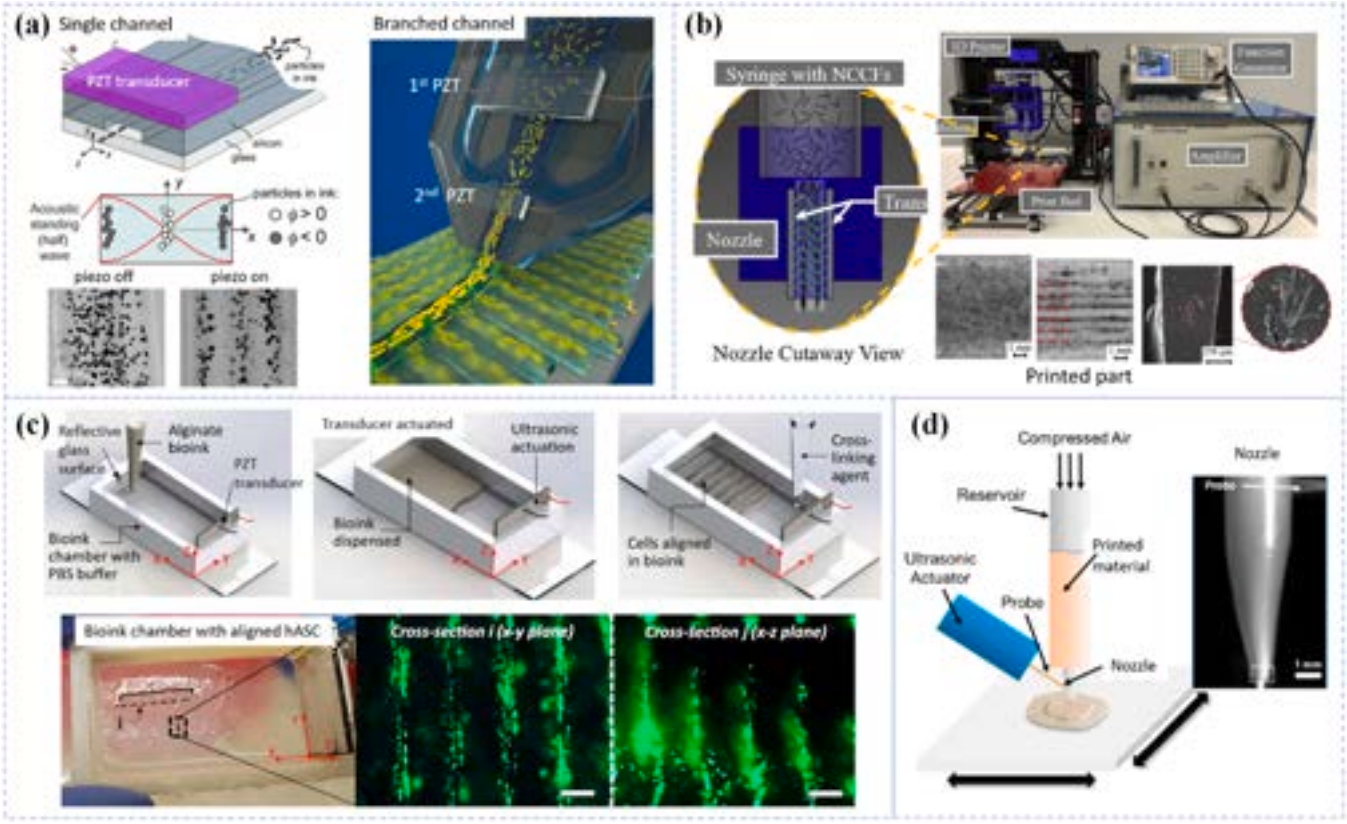

Fig. 6. Acoustic field-assisted extrusion-based AM devices and test cases: (a) One (for single channel) or two (for branched channel) PZT transducers are attached with the nozzle of a DIW setup, creating standing BAW to separate and focus particles to the center of the nozzle [135]. (b) Two PZT transducers attached to the nozzle outside walls, which generate standing SAWs to align the dispersed fibers into discontinuous line patterns [143]. (c) A pair of PZT transducer-glass reflectors are placed on inner walls of the vat, creating standing BAWs which patterned hASC cells in hydrogel into unidirectional lines [145]. (d) A custom PZT transducer-steel probe attached to a syringe extruder which creates high-amplitude ultrasonic vibrations within the nozzle, imparting sufficient inertial forces to enable extrusion of highly viscous composite materials [146].

keep the nozzle temperature below 30 °C. Various parts were successfully printed by the developed HUAV-assisted extrusion AM process using an aluminum-polymer composite or a stiffened fondant with viscosities up to 14,000 Pa·s. This study showed that high-amplitude ultrasonic vibrations within the nozzle generated and applied sufficient inertial forces to highly viscous materials, enabling extrusion of highly viscous composite materials for 3D printing of functional parts at a high fraction of solids, high rates, and with precise flow control.

4.2. Acoustic field-assisted vat photopolymerization AM

Extensive efforts have been made on integrating the acoustic field into vat photopolymerization AM to print polymeric composites with controlled particle dispersion patterns. The photocurable liquid resin is usually contained in a vat or a fluid channel. Particles of different types and shapes, with different sizes ranging from nano- to micrometers have been investigated in this process. In the acoustic field-assisted vat photopolymerization AM, particles are premixed with liquid resin, acoustically assembled to form a pattern, and then consolidated in the resin through photopolymerization [34,100,111,122,147].

All of the related work in this section employed ultrasonic standing waves. For 2D patterning, standing surface acoustic waves (SAW) are usually employed, whereas for bulk 3D and 2D patterning in a high-viscosity medium, standing bulk acoustic waves (BAW) are more commonly used. In most of these studies, ceramic piezoelectric (PZT) transducers were used since, compared to the electrostatic transducers with a metal membrane, they can be sealed without any damage in harsh environments. To integrate transducers in a photopolymerization AM system, direct and non-direct contact approaches have been reported in the literature. In direct-contact approaches, the transducer is mounted on the inner wall of the resin vat, while non-contact approaches place transducers outside of the resin vat. Integration of a single, a pair, and two or multiple orthogonal pairs of PZT transducers in vat photopolymerization AM systems have been demonstrated. By increasing the number of PZT transducers, the complexity of the acoustic standing waves and therefore the variety of particle patterns can be increased. Compared to other field-assisted particle patterning approaches that are paired with vat photopolymerization AM, the acoustic field-assisted patterning works for a broad range of particles in the liquid resin, however, it is limited to patterns of unidirectional lines, curves, or simple shapes with uniform spacing. The time for acoustic field-assisted particle patterning in liquid resin can range from a few milliseconds to minutes, depending on the properties of the particle and the resin, the particle concentration, and the acoustic field properties.

Asif et al. generated standing bulk acoustic waves by placing two PZT transducers facing glass reflectors on the inner walls of a rectangular resin vat to pattern short carbon fibers in liquid resin (Fig. 7a), in which mechanically anisotropic composites were developed and characterized [111]. Aside from PZT transducer-glass reflector pairs, researchers have also employed pairs of opposing transducers to generate ultrasonic standing acoustic waves in vat polymerization AM. Niendorf et al. placed a pair of PZT transducers on opposing inner walls of the resin vat to pattern micro-sized carbon fibers (Fig. 7b) [122]. The authors developed dimensionless parameters using Buckingham Pi analysis for acoustic patterning modeling. They found that microscale alignment of the fillers was primarily driven by the microfiber weight fraction only, whereas the macroscale alignment was significantly affected by the microfiber weight fraction, dimensionless ultrasound transducer input

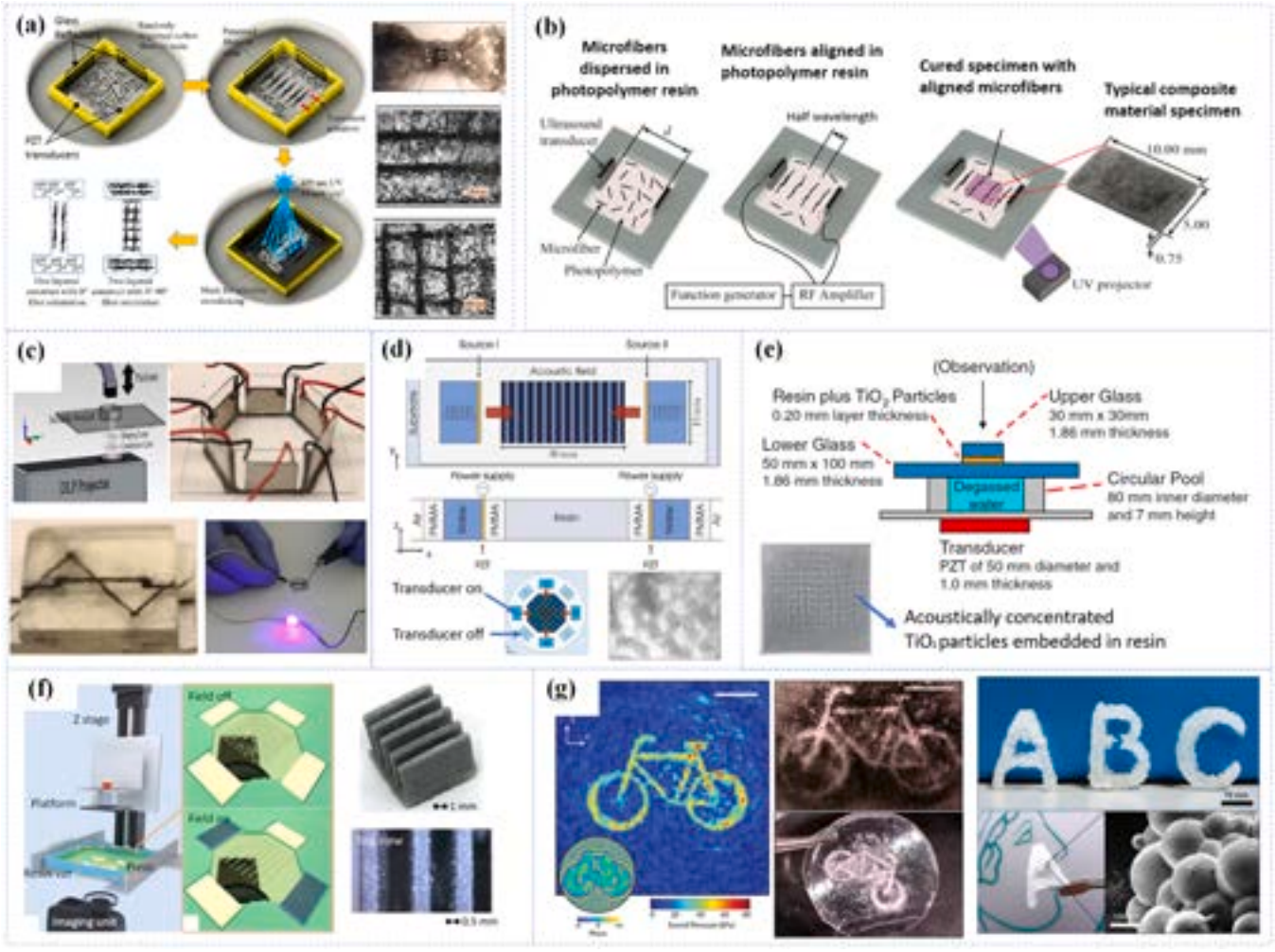

Fig. 7. Acoustic field-assisted photopolymerization based AM devices and test cases: (a) Two pairs of PZT transducer-glass reflectors are placed on inner walls of the resin vat, creating standing bulk acoustic waves which patterned short carbon fibers in liquid resin into unidirectional lines [111]. (b) A pair of PZT transducers is placed on inner walls, creating counter-propagating waves which formed surface standing acoustic waves. Carbon microfibers were patterned to lines in liquid resin [122]. (c) Schematic and the setup of acoustic-assisted stereolithography 3D printer with 6 PZT transducers placed on the inner side walls of the resin vat. A complex 3D object embedded with a zigzag stitch pattern of copper nanoparticles was demonstrated as a test case and the zigzag stitch pattern can work as two separate conductive wires [123]. (d) A pair of PZT transducers are placed on the two sides of the central cavity which contains particle-resin mixture, submerged in water and held in place by springs [147,148]. The device was upgraded by extending to 4 pairs of PZT transducers. A honeycomb pattern of glass microfibers was formed in low viscous liquid resin by driving four orthogonal transducers in phase. (e) Acoustic waves propagating through the degassed water and the glass plate at the lower side and applied to the TiO2-resin mixture layer sandwiched between the two glass plates. The glass at upper side was excited by the ultrasound waves propagating through the mixture [150]. (f) Two orthogonal pairs of PZT transducers were attached beneath the resin vat bottom surface which was a PET film. The PET film vibrated and induced acoustic waves in the particle-resin mixture. Composite object with multi-dimensional particle filler network was printed and demonstrated efficient heat dissipation [151]. (g) Acoustic hologram enabled arbitrary complicated pressure field and assembly of silicone particles with complex patterns including bike and letters [152].

power, and dimensionless ultrasound transducer separation distance. By increasing the number of transducer pairs, particles can be assembled into lines or curves with more angles or even other shapes. Yunus et al. developed a hexagon resin vat with six PZT transducers (three pairs of opposing transducers) placed on the inner side walls (Fig. 7c) [123]. By actuating different pairs of opposing transducers, the propagation direction of acoustic standing waves can be changed. As a result, horizontal 60° and 120° particle alignments of line patterns could be formed. Greenhall et al. reported a study with a similar acoustic field-assisted vat polymerization AM setup, which utilized an octagonal resin vat with eight ultrasound transducers around its perimeter [130,131]. These studies show that by curing the resin layer in multiple sections, each of which contains a line pattern of particles with a specified orientation angle, 3D composite objects embedded with complicated particle patterns could be produced. For example, Yunus et al. presented a zig-zag stitch pattern of copper nanoparticles as a complex 3D form (Fig. 7c) and an electromagnetic coil pattern as an embedded electronic component [123]. Greenhall et al. fabricated macroscale multilayer engineered materials containing a Bouligand microstructure and 3D structures with embedded insulated electrical wiring [131].

In all of the acoustic field-assisted vat photopolymerization AM processes discussed so far, the PZT transducers are in direct contact with the liquid resin and particles, which posed potential challenges including heat generated from transducers, especially at high voltages, which may damage the print quality and cause difficulties in replacing or recycling transducers. To address those challenges, researchers investigated non-contact approaches for integrating PZT transducers [132,148]. In the studies reported by Thomas et al. [132] and Scholz et al. [147,148], two PZT transducers were placed on the opposite outer walls of the resin vat and held in place with small springs (Fig. 7d). The transducers were submerged in water for cooling purposes. Counter-propagating waves were generated by two opposing

transducers, which together formed a standing wave field inside the particle-resin mixture in the central cavity (Fig. 7d). The transducers were operated at the first three resonances, which were calculated by an electro-acoustic transmission line model. Anisotropic composite objects were printed from short glass fibers and low viscosity resins using the developed system. Acoustic assembling in less than 100 ms was demonstrated by Scholz et al [147]. The same research group extended their work to acoustic patterning with 8-transducers and presented more patterns of glass microfibers, including a honeycomb-like pattern formed by driving four orthogonal transducers in phase (Fig. 7d) [148].

In addition to placing transducers on the side walls of the resin vat and propagating acoustic waves on the printing plane, acoustic patterning could also be achieved by placing the transducers on the bottom or top walls of the resin vat [149–151]. Tuziuti et al. sandwiched a layer of particle-resin mixture between two 1.86 mm thick glass plates, one of which was adhered to a PZT transducer (Fig. 7e) [150]. Both plates vibrated normal to their surfaces, and the wave propagating in the liquid mixture formed standing waves, forming two-dimensional particle patterns. Similarly, Lu et al. attached PZT actuators beneath the resin vat bottom surface, which was made of a thin Polyethylene terephthalate (PET) film (Fig. 7f). Two pairs of PZT actuators were used to produce different structural deformations of the PET film, which subsequently induced different acoustic pressure patterns in the particle-resin mixture and assembled particles to varied patterns. Different particles with sizes ranging from 70 nm to 75 μm were successfully patterned into line, curve, and crisscross patterns with more than seven times higher particle concentrations than the concentration of the feedstock. Composites with two-dimensional and three-dimensional filler networks were produced, and multi-dimensional heat dissipation with a high efficiency was demonstrated [151].

Despite all the progress with the existing methods based on PZT actuators, it has not been feasible to generate acoustic fields for particle assembly with truly arbitrary shapes. Only unidirectional parallel lines or curves, crisscross, honeycomb, or their combinations, were reported in acoustic field-assisted vat polymerization AM. A possible solution is to replace the standing acoustic waves with an acoustic hologram, which can generate a complex 3D sound pressure field. Instead of the traditional phased array transducers (PATs), which have limited resolutions and bulky setup, Fischer's group reported a novel acoustic holography approach that creates complex sound waves by using a single transducer and a hologram plate which is characterized by spatially varied thickness [152,153]. They demonstrated silicone microparticles assembled in deionized water by the acoustic intensity gradient, where complex assembly shapes including a bicycle and letters were formed (Fig. 7g). To integrate this acoustic holography method in vat polymerization AM processes, future work may need to focus on device design, material selections, and hologram plate design for increased assembly pattern variety and pattern accuracy.

4.3. Potentials and limitations of acoustic field-assisted AM

Compared with other field-assisted AM technologies, acoustic field-assisted AM provides benefits in material choice freedom and versatile material manipulation capabilities. Acoustic field has been successfully integrated into AM for manipulating solid fillers with arbitrary anisotropy from spherical particles to long fibers, size from nano- to micro-scale, and living cells in polymer matrix to produce polymer composites or bio-constructs. In addition to re-orientation, alignment, and patterning that other external fields are typically capable of, the acoustic field can also focus, separate, and concurrently pattern different types of fillers, enabling additive manufacturing of composites with a higher loading fraction of fillers, denser filler patterns, and separate assemblies of different fillers not possible with other external fields. With those advantages, acoustic field-assisted AM has been demonstrated for fabrications of biomimetic anisotropic composites with enhanced mechanical properties, functional multi-material objects embedded with focused filler lines which could work as thermally or electrically conductive wires, and hydrogels with accumulated and patterned living cells for bio applications.

4.4. Future perspectives of acoustic field-assisted AM

Despite the advances, the use of acoustic fields in AM for productions of composites still face many challenges that need to be addressed, three of which are reviewed.

First, from the machine development perspective, acoustic transducers need to be attached to the resin vat in a photopolymerization AM system or the nozzle surface in an extrusion AM system. Factors including the transducer placement, attachment, bonding, and acoustic transmission efficiency all affect the acoustic manipulation effectiveness and efficiency, process reliability, and the machine lifetime. In addition, a high acoustic radiation force is needed to pattern a high loading fraction of fillers with a high anisotropy or in a viscous liquid matrix, and therefore a high voltage is required to be applied to the acoustic transducer. As a result, a large amount of impedance heating can be generated, and the transducer temperature can rise to severely impact the AM process performance and even damage the transducer. This hardware design challenge also limits the loading fraction of the fillers, the viscosity of the matrix, and the volume of materials that can be processed by the acoustic field-assisted AM technology. High amplitude vibration has been shown effective for decreasing the friction and extruding highly viscous composites with high loading fractions of fillers. One potential research direction is to develop acoustic field AM technology which combines acoustic focusing, assembling, and high amplitude vibration by integrating multiple types of acoustic energy sources. Continuous efforts in improvements and innovations in machine design and development will be needed in the future.

Second, from the product complexity perspective, only simple line, curve, and honeycomb patterns of fillers or their combined patterns of fillers have been achieved in acoustic field-assisted AM. Due to the inherent simplicity of acoustic fields generated by arrays of transducers, arbitrary complex patterns are impossible. To overcome this limitation, development of innovative approaches to generating arbitrary complicated acoustic fields freely and quickly is a critical task in the future. An acoustic hologram based on a hologram plate proposed by Fischer group [152,153] might be worthwhile to investigate as a potential solution. Future advancement in the field of acoustic holography may provide further insight into the development of novel acoustic hologram-assisted AM technology, to produce composites with arbitrary filler distribution patterns.

Furthermore, although extensive research in acoustophoresis has shown the capability of acoustic field in controlling liquid and gaseous materials, the research of acoustic field-assisted AM technology investigated only solid particle fillers. Little work investigated acoustic field-assisted additive manufacturing of composites out of liquid-liquid mixtures or gas-liquid-solid multi-phase mixtures. If the emulsion and gas-liquid-solid multi-phase mixture manipulation capabilities can be unlocked and fully utilized in AM processes in future studies, the versatility of the acoustic field-assisted AM technology will be significantly increased to open up a wide variety of potential applications.

Overall, understanding the acoustic field generation approaches, acoustic manipulation mechanisms, and additive manufacturing processes will lead us to innovations in hardware design and development innovations, driving the acoustic field-assisted AM technology forward. The future study will further exploit the advantages of acoustic fields including material choice flexibility, minimal damage to living cells, and versatile material controllability, leading to breakthroughs in constructing next-generation functional materials and structures for a broad range of bio-applications and engineering applications.

5. Magnetic field-assisted AM

Compared to the other fields discussed in this work, magnetic field has certain properties such as the ability of manipulating the materials in small stimulation timeframe and easier field generation, which makes it distinct and easier to use in field-assisted additive manufacturing. Magnetic field can apply spatial forces in a non-contact mode with a small response time [154–156]. Even with small field magnitudes, ferromagnetic materials have a fast response when exposed to this field. Moreover, generation of magnetic field is cheaper and easier compared to other fields, as it can be produced by using simple, permanent magnets. However, there are also certain limitations in using the magnetic field. Only certain materials are responsive to this field, which limits the material choice that can be used in magnetic field-assisted AM. Considering all these properties, magnetic field has been reported in a number of studies to build shape-shifting structures and composite materials such as graphite electrodes for Li-ion batteries [157], shape-shifting liquid molds for optical lens manufacturing [158], magnetic displays [159], soft [160] and continuum robots [161], or bio-inspired ceramic composites [162]. It has also been widely devised in driving biomedical devices [163], drug delivery devices [164], environmental applications [165], and soft robot actuation [154].

There are two methods used to generate magnetic field: electromagnetic systems and permanent rare-earth magnets. The main component in an electromagnetic system is an electromagnetic coil made of electrically conductive wire wound in turns. The magnetic field is generated when an electrical current passes through the coil. The intensity of the magnetic field is controllable by varying the amperage of electrical current. Large and spatially homogenous magnetic fields are generated using electromagnets, and because of the high-amperage electrical current that is needed for this purpose, electromagnetic systems also require an effective cooling system which can be expensive to integrate [166]. Electromagnetic systems that are used in field-assisted AM are divided into two main categories based on their magnetic field distribution [167]. The first category consists of more established systems such as Helmholtz coils and Maxwell coils, which are normally used to generate uniform or gradient magnetic fields, respectively. In the Helmholtz systems, the uniform field leads to torque generation, and the constant gradient from Maxwell coils generates the magnetic force. The second category of electromagnetic systems are more customized coil systems such as OctoMag [168] and MiniMag [169], that can generate non-uniform or variable gradient fields [170]. Permanent magnets, on the other hand, are materials with a broad magnetic hysteresis loop [171] and have the ability to deliver magnetic flux without continuous energy input [172]. These materials usually consist of rare-earth elements. Alnico and hard ferritic materials have been previously used as permanent magnets; however, thanks to the efficiency and performance of NdFeB alloys, Alnico and hard ferrites are being replaced by these materials [173]. Compared to the electromagnetic systems, permanent magnets are not able to generate large spatial fields; however, certain properties such as being small, having the capability to generate large fields in nearby areas, and the ability to locally control the field, leads to a more common use of these magnets. Rather than individually using the permanent magnets, different arrangements of permanent magnets such as Halbach array, can also be used to generate controllable magnetic fields [171].

There is a limited range of materials including nickel [30] and its alloys [174], carbon nanotubes [175], iron and its oxides [176], cobalt [177], neodymium [161] and PrFeB [178]. that are responsive to magnetic field and used in magnetic field-assisted manufacturing of composite structures. One of the major drawbacks in AM of metals is the expensive equipment and process complexities. To address this challenge and due to their outstanding properties such as being lightweight, chemically stable, biocompatible, and ease of synthesis, polymeric composites with metallic reinforcements have opened up their way to replace the complex metallic parts [179]. To utilize the potential of magnetic field in developing such composite structures, fillers composed of magnetic metals or oxides, and non-magnetic fibers attached to clusters of magnetic-responsive materials are embedded into the polymeric matrices. Researchers have also utilized particle coating methods to pair magnetic materials with non-magnetic or less-magnetic materials such as short carbon fibers [180], ceramics such as alumina [181], and calcium phosphate [10].

In general, two major categories of AM technologies are paired with magnetic field to generate polymeric composites and will be discussed in this section: extrusion-based processes and vat photopolymerization. This section will also include a brief overview of using casting methods along with magnetic field for aligning the fillers in composite structures. Although there is an increasing number of research reports available on additive manufacturing of composite magnetic materials [182–184], due to the scope of this review, only those using AM and magnetic field concurrently are included in the following sections.

5.1. Magnetic field-assisted extrusion-based AM

As discussed previously, in extrusion-based processes, shear force plays an important role in aligning the particles along the extrusion direction. Although in some cases this might be a favorable phenomenon, it also might not induce enough alignment into the process. The 3D printed product might require additional materials to be aligned in the extrusion direction, or conversely, the alignment might need to be in a direction rather than that of the extrusion. Magnetic field has been added to extrusion-based AM processes to address this issue by controlling the fillers that are responsive to the magnetic field [185]. This method has been used by Hone et al. to build carbon nanotube films from deposition under strong magnetic fields. Carbon nanotubes are responsive to magnetic field, and their direction aligns with the field lines under considerable, strong magnetic torques. Aligning CNTs has been devised to achieve polymeric composites with tailored properties in other non-AM works using magnetic fields with magnitudes of 7–25 T [175]. Considering the strong fields required to control carbon nanofibers, there are limitations in using CNTs as magneto-responsive materials in additive manufacturing. Generating such sizeable fields require complex systems which normally need large spaces and can have conflicts with the AM system. Therefore, in magnetic field-assisted AM of polymeric composites, materials with higher magnetic remanence are more commonly used. Moreover, in some cases, fillers that are not responsive to the magnetic field are paired with magnetic materials to enable the magnetic field to control their density or orientation.

In order to control the fillers in magnetic field-assisted extrusion-based AM, magnetic field can be applied during or after the extrusion process. In the first approach, a field-generating setup is devised around the extruding nozzle and, by generating a magnetic field, helps re-orient the fillers during the print process. In this approach, particle alignment occurs at the same time as material flows inside the nozzle. Due to the effects of the shear alignment, filler alignment in a direction other than the direction of flow movement will be difficult. Kim et al. used this approach to print elastomer composite ink containing ferromagnetic particles (neodymium-iron-boron) through a DIW process (Fig. 8a) [186]. A tunable electromagnet is installed around the nozzle to control the particle orientation during the extrusion process. Changing the magnetic field through the electromagnet, multiple magnetic domains were printed in each part. Reorientation of ferromagnetic particles was also studied by Aguilera et al. during material jetting of photocurable resins [187]. The experimental setup developed in this work was capable of positioning the permanent magnets and had real-time control on the magnetic field direction around the nozzle. Roy et al. used permanent magnets during extrusion-based AM of composite structures with convergent nozzles [188]. A combination of magnetic force and changes in nozzle geometries are studied in this work, and their effects on alignment of nickel nanowires is investigated. The theoretical study on particle alignment in this work shows that without the external

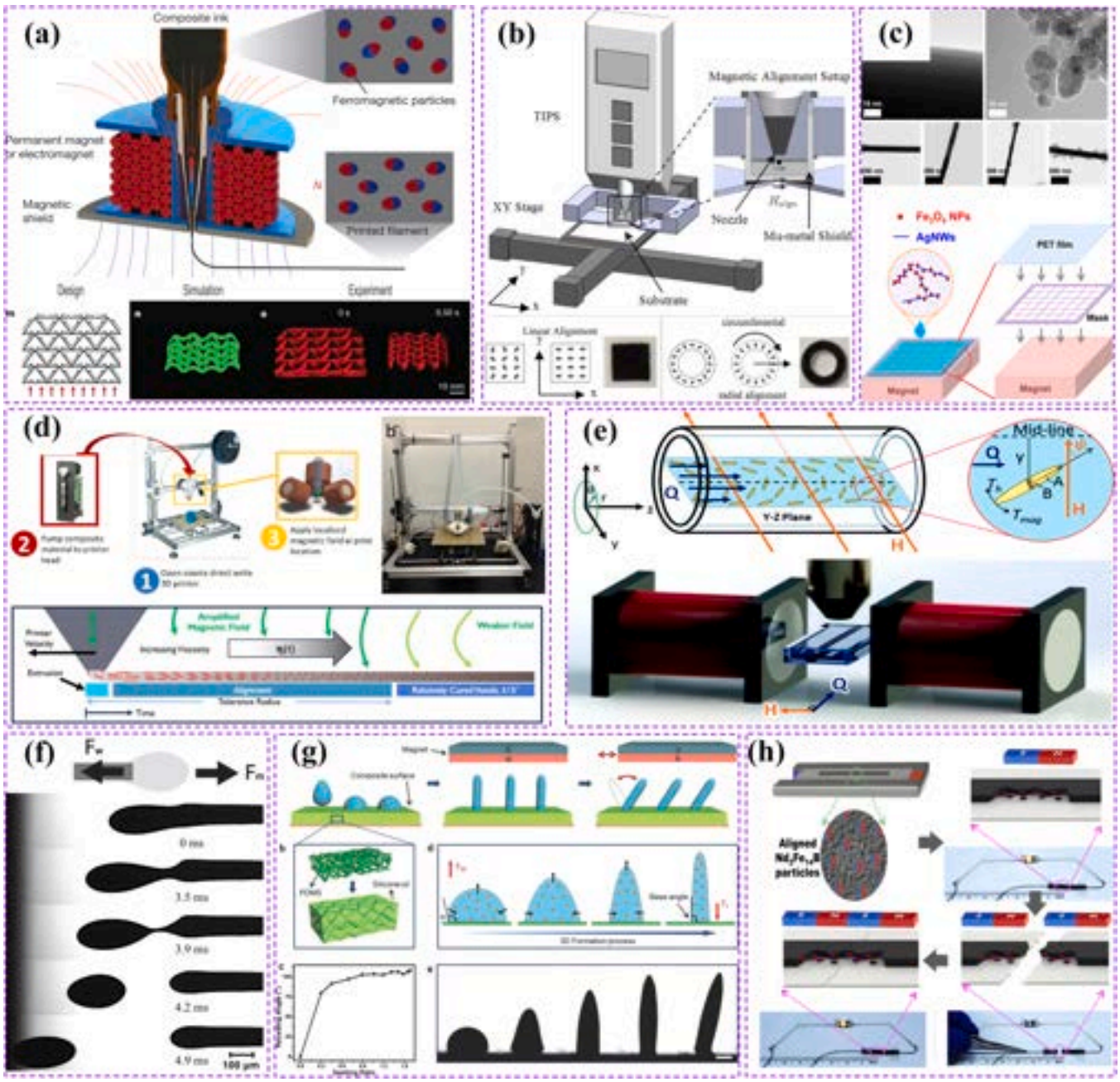

Fig. 8. Magnetic field-assisted extrusion-based AM: a) Example of using magnetic field during the extrusion-based process to print magnetic domains and build smart and functional structures [186]. b) Example of using magnetic field after extrusion of the material to align particles in different directions [189]. c) 3D printing and magnetic patterning of silver nanowires [190]. d) Extrusion-based magnetic AM to align particles and their real-time orientation [192]. e) Extrusion setup and schematic basis of studying the magnetic torque for fiber alignment [196]. f) Force balancing during the magnetic droplet manipulation for 3D printing purposes [36]. g) Precise microstructures controlled by magnetic field [200]. h) Self-healing structures by magnetic alignment after printing [201].

magnetic field, fillers would be randomly aligned in the nozzle.

Due to the challenges in dealing with the shear alignment during the extrusion process, researchers have also tried to control the filler materials after the print material is extruded which eliminated the complexities of concurrently dealing with shear and magnetic forces. Song et al. used inkjet printing to build thin films and components from magnetic particles while an external magnetic field was applied to the print area after the material was extruded [189]. With a printer equipped to a magnetic alignment setup surrounding the nozzle, they produced functional structures by ferromagnetic Cobalt-based high particle content suspensions. An innovation in their work is using Mu-metal as a shield around the nozzle, which causes the magnetic field not to affect the nozzle and the material that is being extruded. As a result, the material is minimally affected by the magnetic field during the extrusion process (Fig. 8b), and magnetic-field induced alignment happens after extrusion. The fiber alignment leads to enhanced functionality of their printed parts, in terms of high frequency permeability and decreases in hysteresis losses in the alignment-induced hard axis. Ahn et al. used a magnetic printing method to pattern silver nanowires [190]. Using magnetite-silver nanowire hybrids, they created a pattern of conductive silver nanowire gridlines on a flexible substrate, which is generated by a controlled magnetic field (Fig. 8c). Their printed product exhibits significant improvement in electrical and optical properties and looks promising for building energy storage devices and

nano/opto-electronics. Clay et al. used magnetic field coupled with the inkjet printing process of photocurable inks to build parts with arbitrary anisotropy [191]. After inkjet printing of the UV-curable ink, an electromagnet moved under the print bed by a two-axis stage to re-orient the particles, and while the particles were frozen in their location, UV light cured the resin. Martin et al. also used an array of permanent magnets around the nozzle to align the extruded particles along the print direction (Fig. 8d) [192]. In another research work, using static magnetic field and PLA filaments loaded with iron particles, the extruded struts of a FDM printer were manipulated to re-orient the particles inside the printed structure [193]. The approach used in this work led to developing active structures with increased attenuation of the transmitted signal power, making them a promising choice to be used in electronics and antenna applications.

Recent developments in colloidal assembly techniques have made a great contribution to field-assisted AM. As a basis to this process, a great deal of research has been done by Yellen's group, which consists of using a uniform magnetic field to control the orientation or concentration of magnetic particles, as well as assembling the magnetic and diamagnetic microparticles [177,194,195]. Martin et al. developed the theoretical basis of this process and studied the feasibility of using magnetic field in the print area to control particle alignment during the extrusion process (Fig. 8e) [196]. Their magnetic energetics model is verified through experimental extrusion results and includes Jeffery orbits and the random rotation of the dipoles in extrusion process. This work provides a strong theoretical basis for similar research studies by quantifying the required magnetic field that is needed to overcome the effects of shear-force in aligning the particles in extrusion-based processes. Having the support of this study, other research groups started using magnetic field to align fillers in extrusion-based processes. In another work from the same group, magnetic field is incorporated into a customized direct write 3D printer for in-process particle re-orientation [192]. Ultra-high magnetic response (UHMR) particles synthesized from alumina doped with iron oxide nanoparticles are aligned after extrusion using three localized electromagnets.

Magnetic field has been also widely used for droplet manipulation, leading to additional potential applications of AM processes [197–199]. Vekselman et al. used a coilgun in a drop-on-demand printing process of the inks loaded with magnetic particles (Fig. 8f) [36]. As the coilgun generates a non-uniform magnetic field around the material jetting nozzles, it will counteract the internal tension forces in the ink and helps the droplet to separate from the nozzle. Wang et al. introduced a magnetically-controlled approach to print fine 3D structures in micron dimensions [200]. In this approach, a droplet of the magnetic ink consisted of magnetite nanoparticles, polyvinylalcohol, and ethylene glycol is deposited on the print area. After deposition, using print beds with controlled hydrophobicity, external magnetic fields are used to manipulate the droplets in different directions. A combination of surface wetting properties and magnetic field strength and direction yields a droplet that is manipulated in different directions with different shapes (Fig. 8g).

With the emergence of the 4D printing concept, one of the most promising applications of magnetic field-assisted AM is in building shape-shifting structures and untethered robots that are capable of being controlled by external magnetic forces. Researchers have used extrusion-based processes paired with external magnetic field to build such smart structures. Zhu et al., 3D printed magnetically responsive 3D structures with a fast response to external magnetic fields [184]. In this work, soft iron nanoparticles were incorporated into a PDMS elastomeric matrix. This ink with a low magnetic remanence was used to print magnetic field responsive terahertz photonic crystal. Using the ferromagnetic iron particles in the printed parts, leads to achieving fast, shape-shifting responses induced by external magnetic field. The potential applications of their work are discussed to be in the fields of biomedical devices and smart textiles. Kim et al. used DIW to embed programmed ferromagnetic domains into soft composite structures [186]. It was proved that through this process, complex and rapid shape transformation in 2D and 3D structures could be programmed.

One of the interesting properties of a permanent magnet is that if broken into two pieces, each piece becomes an independent magnet, and they will be attracted to each other in the broken boundary. This property is used by Bandodkar et al. in building self-healing electrochemical structures that fix themselves when a defect happens in their structure [201]. A conductive self-healing ink was prepared by adding a mixture of carbon black powders and permanent magnetic $Nd_2Fe_{14}B$ microparticles to a polystyrene-block-polyisoprene-block-polystyrene suspension. Using a thin flexible polyester substrate on the semi-automatic screen printer, this ink was printed on the substrate. During the print process, permanent magnets were located under the print bed in such a way that the magnetic field was parallel to the print path. To demonstrate a self-healing capability of the printed ink, a wearable circuit was printed into a T-shirt. After repeatedly inducing microcracks into the circuit, it instantaneously recovered its function (Fig. 8h). The proposed process can be used in building electrical circuits, batteries, and electrochemical sensors.

5.2. Magnetic field-assisted vat photopolymerization AM

The idea of using magneto-responsive materials in SLA was first used by Kobayashi and Ikuta [202]. In their work, ferromagnetic magnetite particles were mixed with a photocurable resin, and this mixture was used to build magnetic parts. Although in this work, magnetic field was not used during the printing process, it is one of the earliest studies to use SLA in building polymeric composites with embedded ferromagnetic fillers. A predominant share of the research in the area of magnetic field-assisted vat photopolymerization is related to the work done by two groups at ETHZ and Northeastern University [10,181,203,204]. Erb et al. analyzed the theories behind functionalized UHMR ceramic particle alignment in a suspension due to magnetic field [181]. These particles are composed from ceramics such as alumina [181], calcium sulfate hemihydrate [181], silica [10], and calcium phosphate [10], which are coated by iron oxide particles. The minimum required magnetic field to align the particles is calculated from the theoretical framework and verified through experiments. Martin and Erb developed the 3D magnetic printing [10,204], in which after global reorientation of the particles in the resin vat, photopolymerization happens in the active voxels and partially cures the resin in selective areas of a layer [10]. The proposed process in these works utilizes a moving rare-earth magnet or solenoids to change the orientation of the particles, and while the magnetic field keeps the particles in a desired orientation, a DLP projector polymerizes each layer section based on the voxel data (Fig. 9a).

Two major approaches for inducing the magnetic field in magnetic field-assisted vat photopolymerization are applying a local or global field to re-orient the particles. When a local field is applied, particles in the entire vat will adapt the same orientation, and in the next stage, the resin is selectively cured by laser-scanning or DLP methods. Nakamoto and Kojima used an array of five electromagnets around their vat to globally re-orient the particles inside the vat and scanned the desired areas with a laser beam to cure the resin loaded with 0.5% of ferromagnetic short fibers [205]. Their methodology led to strengthening the structure of the thin films built by this process. Global magnetic field has also been used in the works done by Erb and Martin [10,204]. One main drawback of using global magnetic field is that during the process, the particles need to be homogeneously distributed inside the entire vat and, as a result, there will be very limited control over the particle concentration in certain regions. Therefore, other researchers have used a local magnetic field in this process, in which a magnetic field source is moved along the vat in a path, which depends on the desired particle profile in the final product [33,35,176,191,206–208]. Using this method, there will be an improved probability to control the orientation and concentration of the particles locally.

Magnetic vat photopolymerization has a great potential in reaching

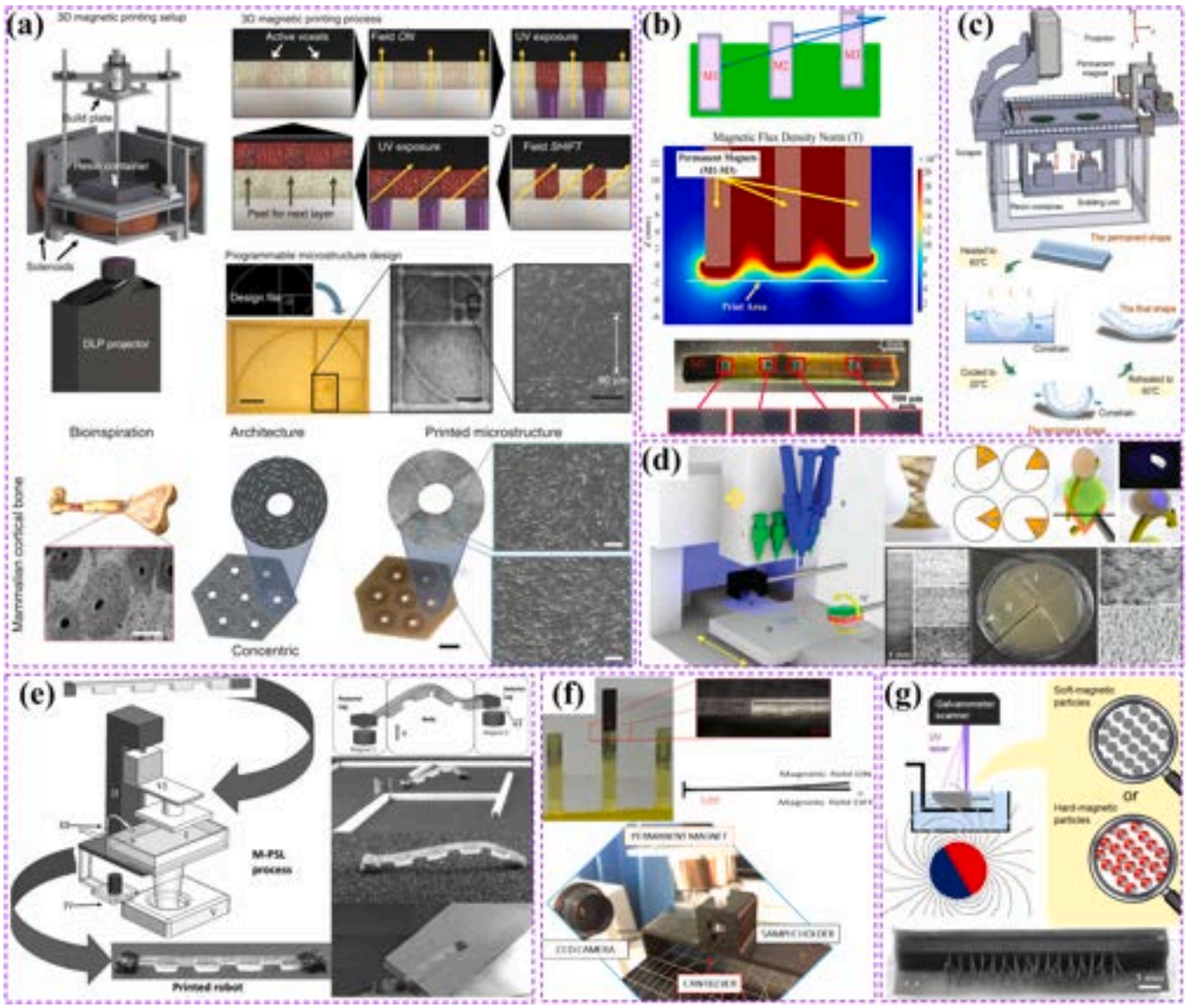

Fig. 9. Magnetic field-assisted vat photopolymerization: a) The 3D printer setup used for voxel-based magnetic vat photopolymerization of simplified bioinspired structures [10]. b) Using different magnetic field strengths and customized printers, gradient distribution and alignment of ferromagnetic particles are achieved and matched with theoretical frameworks [176]. c) Structural gradients can be achieved by using magnetic field and DLP printing to build bioinspired temperature-induced shape shifting structures [33]. d) Multi-technology magnetically assisted vat photopolymerization is used to generate complex biomimetic structures [208]. e) Soft untethered robotic inchworm is printed in a single process and can move along complex paths, and rough and inclined surfaces [35]. f) 3D printed microcantilever MEMS sensor is triggered by external magnetic field [209]. g) 3D printing of a ferrogel with selective filler orientation leads to generating artificial cilia that can be actuated in fluid media [213].

3D structures with different local particle concentrations and orientations as moving and reorienting the particles in a liquid media is less challenging. However, using the liquid media also brings up the biggest drawback of using vat photopolymerization, as the additive process in magnetic field-assisted AM: once the particles are dispersed in the resin, there will be a limited concentration of the particles that can be achieved in each area. Moreover, photocurable resins cannot be solidified when containing a high particle ratio. To address these problems, multi-technology processes has been developed, which basically consist of an extrusion-based system that selectively adds droplets of particle-loaded resin into a vat of pure photocurable resin. This process is used by Kokkinis et al., where multiple nozzles are used to extrude different materials inside the vat and then UV light is used to cure the entire extruded layer (Fig. 9c) [33]. The same process is also used by Credi et al. to 3D print micro-cantilever beams for polymeric micro-electromechanical (MEMS) or nanoelectromechanical (NEMS) applications (Fig. 9f) [209].

Pan and Lu developed Magnetic Field-assisted Projection Stereolithography (M-PSL) to build magneto-responsive smart polymeric structures [206]. In their suggested process, a programmable micro-deposition nozzle locally extrudes the ferromagnetic particles into the vat, and a permanent magnet automatically moves around the resin vat to place the particles into the desired region [210]. Next, the photocuring process happens by applying a digital image with certain patterns. In another work from the same group, they studied the products of this process in terms of microscale particle distribution parameters and how these parameters affect the part response to an external magnetic field that is used for actuation purposes [207]. As shown in Fig. 9e, they also utilized this process to 3D print untethered inchworm soft robots with the capability of linear locomotion and crawling [35,211,212]. Potential applications of soft shape-shifting multidomain structures are in soft robots and wearable electronics. This approach is

used by Shinoda et al. in building a worm-type-actuator and artificial cilia [213]. In this work, magnetic field is applied to a UV-curable gel loaded with two hard and soft magnetic particles, strontium-ferrite and carbonyl iron, to induce the anisotropy during the curing process (Fig. 9g). By changing the direction of the applied magnetic field during the printing process, the orientation of the particles was defined. The final structures showed the ability for magnetic actuation by crossing a narrow gap and reproducing a bioinspired metachronal phase propagation wave.

Magnetic field gradients have been used to generate functionally graded materials (FGMs) [29,162,214,215]. FGMs, in which the composition and micro/macro- structure of building elements are spatially controlled based on the functional requirements, are of an immense importance among different types of composites. Nature has used different FGMs to overcome complicated challenges that exist within biological constructs such as connecting soft and hard tissue structures [216], enamel [217], and bone [218], which are only a few examples in which FGMs are used to implement biomimetic designs [38]. Generally, graded materials show enhanced promising fatigue behavior due to their increased control over the stress distribution as well as smoother transition in areas with stress concentration [219,220]. Moreover, in these materials, cracks propagate without any bridging, which leads to a better fatigue life and mechanical behavior [221]. Generating field gradients with magnets appears to be another potential avenue that can be explored in magnetic field-assisted vat photopolymerization. Safaee and Chen used this approach coupled with a customized DLP process to build 3D functional FGMs with embedded magnetite particles in an acrylic-based commercial resin [176]. Permanent magnets with different distances with respect to the print bed were used to generate field gradients to eventually control the material concentration in different areas (Fig. 9b). Microscopic images were taken from the samples, and material gradients were characterized by analyzing the grey-scale value of these images along the graded areas. Using the data acquired from this work, a framework for design, manufacturing, and characterization of FGMs using magnetic field-assisted DLP printing is established [222]. Results show that controlling the material gradients in vat photopolymerization is a promising method of generating complex 3D FGM structures. Moreover, by selecting proper process parameters, macroscale and microscale test methods can be used interchangeably.

With recent developments in manufacturing processes, achieving more complex structures has turned into a more accessible reality. As a result of these developments, biomimicry and inspiration by nature in developing more efficient and functional structures have received a lot of attention [38]. Magnetic field-assisted AM is a proven tool to reach biomimetic composites owing to its ability in selective particle re-orientation. Ren et al. used magnetic field-assisted SLA to induce structural gradients and develop bioinspired soft actuators [208]. Short steel fibers were mixed with commercial photocurable resins, and concurrently with the DLP printing process, permanent magnets were used to change the magnetic field orientation/magnitude to induce field-gradients (Fig. 9d). The heat-actuated shape memory behavior of graded actuators developed in this work were evaluated. One of the challenges in additive manufacturing is building overhang architectures, which normally require printing extra support structures or external fast-curing of the printed material [223]. Using external magnetic field coupled with DLP printing of photocurable resins mixed with silica (as a viscosity controller) and steel fibers (as the reinforcing component), Ma et al. developed bioinspired overhang structures with locally controlled particle orientation along the printed layers [224]. Using this manufacturing process, it was further proved that local changes the particle orientation can be devised to change the failure mechanisms and enhance the local directional fracture toughness. Being inspired by nature, multi-material surfaces were developed using the ability of magnetic field to form spatial variations in material compositions, leading to development of multi-scale hierarchical hydrophobicity [225]. Using the same concept and inspired by the hierarchical surface structure of the limpet teeth, painless microneedles were developed using magnetic field-assisted of composites loaded with Iron oxide [226].

As stated in the previous section, colloidal assembly is another technique associated with magnetic printing. In vat photopolymerization, this technique emerges with a great importance, as it helps keep the particles suspended in the resin during the print process and achieves a more homogeneous part with better control over particle concentration and orientation. This area, however, has untapped potential and can be of great interest for further research. In fact, the behavior of a particle-resin system is of a considerable importance in field-assisted SLA. Nagarajan et al. developed the magnetic field-assisted SLA process [227] and evaluated the effect of particle content and resin rheology on sedimentation behavior of the particles during the DLP printing process [228]. In a more recent study by the same group [229], a mixture of NdFeB and SrFeO particles is mixed with epoxy-based photocurable resin with a goal of building a stable magnetic particle-loaded resin able to withstand particle settlements and can be used for magnetic field-assisted vat photopolymerization processes. In another study, in order to develop stable particle-resin systems for magnetic field-assisted vat photpolymerization of elastic and tough polymeric composite, silanization of magnetite particles were shown to be a potential method to control the dispersion of particles inside the resin systems during 3D printing process [230].

5.3. Magnetic field-assisted casting

Among the conventional manufacturing processes, casting has also benefitted from using magnetic field to align the particles inside a matrix. In casting, a liquid material, which can be molten metal, ceramic slurry, or curable polymeric resin, flows into a mold cavity and forms into the shape of an unfinished part. In the next step, using a stimulus such as cooling or UV light, the liquid solidifies into the desired final shape. A magnetic freeze casting process was developed by Porter et al. to establish hierarchical particle alignment in anisotropic ceramic scaffolds [162]. In their approach, a controlled rotating magnetic field of 0.12 T was applied with a rotational speed of 0.05 rpm in the direction of ice formation and enabled manipulation of magnetite nanofibers. Depending on how the magnetic field is controlled, the pores generated by this approach were either aligned or perpendicular to the freeze direction. In another study, Chen et al. developed a magnetic roll-to-roll alignment process to build polystyrene films in which nanocolumns of nickel nanofibers were grown along the thickness of the film [30]. Using the magnetic field in this process led to enhancement in light transmission and conductivity of the patterned films in the columnar direction, which makes the process suitable for producing flexible electronics (Fig. 10a).

Magnetic-assisted slip casting (MASC) is another process developed to add the material in a layerwise manner [231]. Using a magnetic field, this very promising fast additive method employs a conventional slip-casting process along with the control of the building blocks (Fig. 10b). In order to mimic the biological constructs of nacre, magnetically assisted vacuum casting is utilized [232]. Their proposed process is composed of using a rotating magnetic field to align the platelets, using vacuum to consolidate these platelets into the ceramic structure, infiltration of the pores among the aligned platelets with a polymeric matrix, and selectively sintering the structure to achieve a nacre-like material (Fig. 10c).

5.4. Potentials and limitations of magnetic field-assisted AM

Although adding the magnetic field to AM processes adds up another dimension to the design space, there are also some limitations with this approach in terms of material and process development. Based on the literature, currently there are a few filler materials that are responsive to

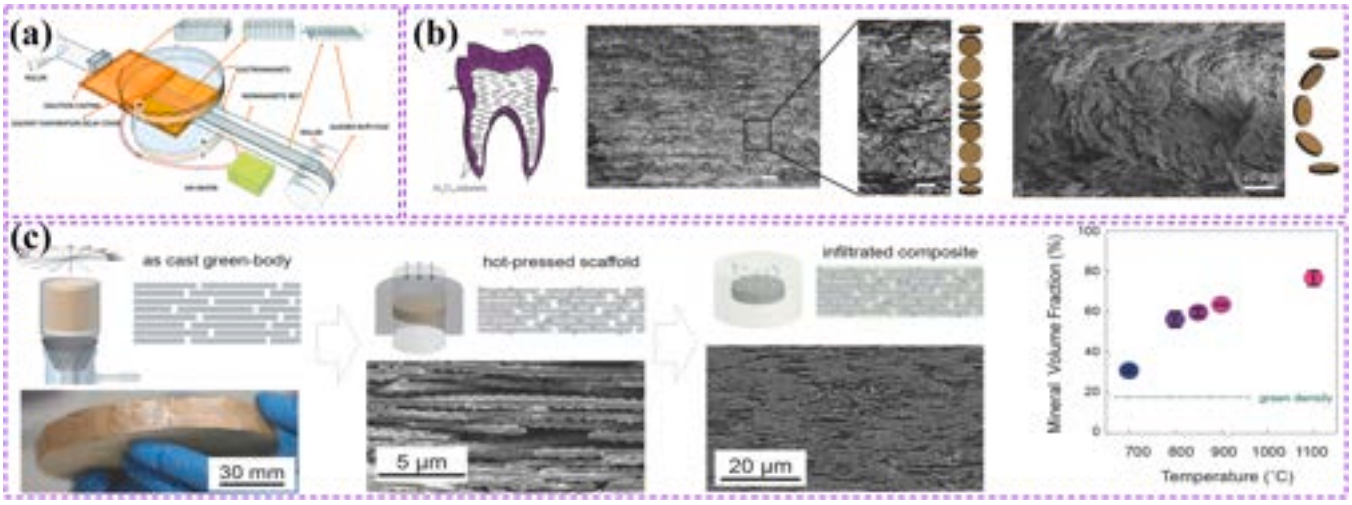

Fig. 10. a) Schematic model for showing the roll-to-roll magnetic alignment [30]. b) MASC is used to build bioinspired tooth-like structure by changing the magnetic field in different regions to reach periodic platelet orientation patterns [231]. c) Schematic of vacuum-assisted magnetic alignment to generate nacre-like structures [232].

the magnetic field. Although some researchers have tried coating other fillers with magnetic materials and make them responsive to the magnetic field, there are still limitations within this highly complex coating process. Another issue within the realm of material development in magnetic field-assisted AM is related to the matrix materials, which are mostly composed of polymers that have limitations such as low tensile strength and low temperature resistance. From the process development perspective, generating and controlling large magnetic fields that affect the materials within the AM process needs advanced technologies, which increases process cost and complexity. Another challenge that comes with adding large magnetic fields is the ability of locally control the field and process components that are surrounding the print area.

5.5. *Future perspectives of magnetic field-assisted AM*

Despite the notable amount of research explored in magnetic field-assisted AM, it appears to still be at its infancy, and there are many potential applications that need to be explored for future research projects. Untethered robotics is another area in which magnetic field has been widely used. Complex robots [154], electromagnetic systems [168], and control approaches [233] are developed using conventional manufacturing processes to perform different tasks using magnetic field, and it seems that magnetic additive manufacturing can also be used to build more complex robots with different geometries and better control over the materials properties. In order to print smaller robots, more precise AM methods like aerosol jet printing can be used to print magnetic filler-loaded inks, while using magnetic field to control the filler orientation during the print process. As suggested by Bandodkar et al., flexible electronics can also be considered as another potential product made by magnetic AM, therefore expanding the ceiling for its applications [201]. Aligning the conductive nanomaterials such as nickel particles and CNTs in the same direction often leads to better electrical conductivity and can be considered an outcome of using magnetic field-assisted AM of flexible electronics. Other materials' behaviors such as mechanical [42] and thermal [234] properties can also be enhanced using this class of field-assisted AM processes.

With the rapid development in biomedical industries and the growing need for in vivo/*in vitro* tests, point-of-care (POC), and Lab-on-a-Chip (LOC) devices are becoming of increased importance. In this sense, the role of magnetic particles is very important, leading to great potential applications of incorporating magnetic field in this area. Researchers have developed methods to utilize magnetic field for such devices [235,236]; however, there is currently no research on additively manufactured LOCs with embedded magnetic particles. Due to the high resolution of some AM processes and their ability to be paired with magnetic field and develop FGM structures, this field allows for promising research in the area of magnetic AM. Considering the current trend in using clean energy resources and the role of rare earth magnets in this scenario, additively manufactured magnets are finding their way into the industry, and many research groups are focusing on building free-form magnets with controllable properties by AM-based methods [237]. Although this research area is still in its infancy, it has a bright prospect in coming years [238,239]. During the AM process, and in order to print more efficient magnets, it is beneficial to align the dipoles and consolidate them. This is an area that particularly field-assisted AM can be helpful. Moreover, for developing MEMS engines, having small and efficient magnets can be a huge advantage, and magnetic AM can be an effective segue to reach this goal. This same concept is applicable to additively manufactured piezoelectric devices.

6. Electric field-assisted AM

Electric field is the force-generating element surrounding an electrical charge, causing different electrical charges to exert certain amount of force to each other. This type of field forms the foundation of many industries and is defined by Coulomb's law. Depending on the direction of the electric field, different electric charges show diverse behaviors when exposed to an external electric field. This characteristic is used in field-assisted manufacturing to control particles with varying responses to external electric fields.

Almost five decades after the Maxwell's fundamental laws for electromagnetism was developed, Pohl discovered that particles immersed in a dielectric media will be stimulated by a force when exposed to an electric field [240]. The result from this interaction is known as the dielectrophoresis phenomena, which is defined as the motion of suspended particles in a fluid media due to the polarization forces that are generated from an inhomogeneous electric field. Pohl's work is characterized by dipole-dipole interactions between particles controlled in a viscous media using an external electric field, and has been used as a starting point by many researchers in various fields such as cell separation and sorting [241], microfluidics [242], colloidal assembly processes [243], production of composites with controlled distribution and orientation of reinforcing elements [244–246]. In the context of last application, electric field can be used to build composites with uniform orientation or locally controlled redistribution of the fillers.

Dielectrophoresis can be used to build composite structures with

uniform or graded distribution or orientation of reinforcing components. In this approach, introduced by Bowen et al., electric field with different directions and magnitudes was locally applied to a liquid polymeric mixture loaded with nano- and micron-sized particles with different electrical properties (insulator, semiconductor, or conductor) [245]. The resulting composite after the curing process was a field-aided micro--tailored (FAiMTa) composite [247]. Based on the concepts and methods introduced by these works, more theoretical frameworks for particle reorientation and motion have been developed, which are considered as the basis of more advanced electric field-assisted manufacturing processes. Dielectrophoresis has also been used for particle manipulation and separation of micro- and nano-scale inclusions and bioparticles [242]. A process based on manipulating particles with similar or dissimilar natural frequencies in a liquid media was developed by Urdaneta and Smela and termed multiple frequency dielectrophoresis (MFDEP) [248]. This process is proven to have the ability of on-demand trap or transport of certain particles.

Electric field can be applied in two different manners depending on the type of electric current being used. If direct current (DC) is the basis of the electric field, the electrical charge flows only in one direction. In the case of using alternating current (AC), the direction of the electrical charge changes periodically. Therefore, the direction of the force being applied to a single electric charge in direct field remains constant and changes periodically in the case of using alternating field. Compared to the magnetic field that can affect a material in a completely non-contact mode, for the electric field to be effective in aligning the particles/fibers, it has to pass through an electrically conductive media. Both of these methods can be used to redistribute organic or inorganic materials.

One of the critical parameters that defines the kind of field to be used in electric field-assisted manufacturing is the filler type that is supposed to be affected by the electric field. Depending on the materials and applications, different kinds of electric field might be applied to control the fillers in a composite system. Different materials such as CNTs [249], alumina [28], nickel nanowires [250], piezoelectric ceramics [251], and polymers [252] have been used in electric field-assisted manufacturing of polymeric composites. In the case of having dielectric particles in the polymeric resin mixtures, applying alternating electric field leads to coalescence of dielectric particles and forming chains that are oriented in the field's direction [253]. In the case of using CNTs, research reports show that using DC voltage leads to easier processibility and higher efficiency [254]. In this work, single-walled CNTs (SWNTs) were aligned using electric fields at frequencies as low as 0.001 Hz, which is effectively a DC condition. Although this method is effective in terms of the alignment precision, due to the low frequencies, more time is required to align the fillers. Moreover, selective alignment of carbon nanotubes in the aligned SWNT bundles and clusters embedded in polymeric matrix of urethane dimethacrylate (UDMA) and 1,6-hexanediol dimethacrylate (HDDMA) can be achieved using AC field [254]. Electrical conductivity of these composites can be controlled by changing the AC frequency or magnitude of the field.

Due to the superior properties derived from the process of additive manufacturing, researchers have made an endeavor to pair electric fields with this category of manufacturing to control filler orientation in polymeric composites, and as a result, control the physical properties of 3D printed structures. Like magnetic field-assisted AM, in electric field-assisted AM, the torque applied on each particle is determined by the applied field and acts as the driving force that re-aligns the particle in the direction of the electric field. Viscosity of the resin mixture or extruded material in electric field-assisted AM is the parameter defining the magnitude and time for the applied electric field threshold to re-orient the fillers. Kim et al. suggested a viscosity of 1 Pa.s for an ideal re-orientation time of different particles in epoxy resins [255]. Although this research is based on conventional manufacturing processes, the same concept is applicable to AM. Based on the research by Kim et al. [249,256–258] and Holmes [28,259–263], different works have subsequently been done to integrate electric field with AM to build polymeric composites with tailored properties. In this section, the progress and developments in this field are reviewed.

6.1. Electric field-assisted extrusion-based AM

Electrospinning, although mostly used for generating 2D structures and not considered an additive manufacturing method, has been used to generate 3D structures in an additive fashion [264]. Electrospun structures are prone to bending instabilities [265], and as a result, this process is typically suitable for generating randomly arranged 2D meshes [266]. This is a limiting factor on developing functional materials and structures from electrospinning process, and researchers have tried to overcome this problem by generating 3D electrospun structures. Because of using of electrostatic forces in electrospinning, this process has a natural ability to use electric field for fiber alignment [267]. Luo et al. devised a near-field electrospinning process to direct-write arbitrary 2D patterns and build arbitrary 3D shaped structures [264]. Using traditional printing paper as a collector in the electrospinning process, this group could print self-aligned particles from poly(vinylidene) fluoride (PVDF) solutions (Fig. 11a). The results of this work can also be used in MEMS and NEMS applications.

Among all the extrusion-based AM processes, DIW has been widely paired with electric field. One of the challenges in the DIW process is control and manipulation of the droplets coming out of the nozzle. Droplet wetting and spreading behavior play an important role in achieving precise geometry and low surface roughness [268]. A research group from the University of Illinois at Chicago used an electric field to achieve better control over droplet behavior and modify the DIW process [269,270]. Different silicone-based and photosensitive inks were deposited on various dielectric substrates such as glass, wood, Kapton tape, superhydrophobic coating surfaces, and ceramic surfaces, while electric field was applied to the substrate to reach better electrowetting behavior between droplets and substrates, and fast curing was induced into the process [269]. Moreover, electrowetting was also used to control and manipulate the droplets from different inks such as pure liquid inks, aqueous polymer solution inks, and carbon fiber suspension inks, by using embedded electrodes on the substrate (Fig. 11b) [270]. Adhesion forces between the droplets and electrodes under different electric fields were analyzed and it was concluded that applying an electric field with the correct magnitude can effectively lead to a more accurate and lower surface roughness of the DIW-printed parts.

For the past several decades, electrophoretic deposition (EPD) has been known for its effectiveness and ease of implementation in industrial applications. EPD is a two-step process, in which charged particles suspended in stable colloidal solutions are directed toward the substrate with electrical potential and finally deposited on this surface [271]. This process is often used for surface coating purposes. Tabellion and Clasen explored applications of this approach for near-shape manufacturing of aqueous solutions containing silica glass and ceramic particles [272]. Sullivan et al. used a combination of DIW and EPD to build composite structures of thermite films [273]. Using DIW, silver nanoparticle inks were printed into self-supporting structures on which Al/CuO thermite composite was coated through EPD. Due to the physical basics of EPD, chances of ignition during the process were eliminated and composite thermites were successfully coated on the DIW-built electrodes (Fig. 11c). The results of this work were used to study the mechanism of combustion reaction. EPD has also been investigated as a ceramic AM process [274]. In this work, particles are extruded close to a membrane, which works as the print bed, using a hollow electrode. Using this process, different geometries including dots, straight lines, and curved lines were deposited with variable height and thickness. Considering the dimensional resolution of the deposited profiles, it was proven by this study that the proposed approach can be used as a basis for AM of 3D structures.

One of the exciting applications of electric field-assisted manufacturing is related to building composite structures from

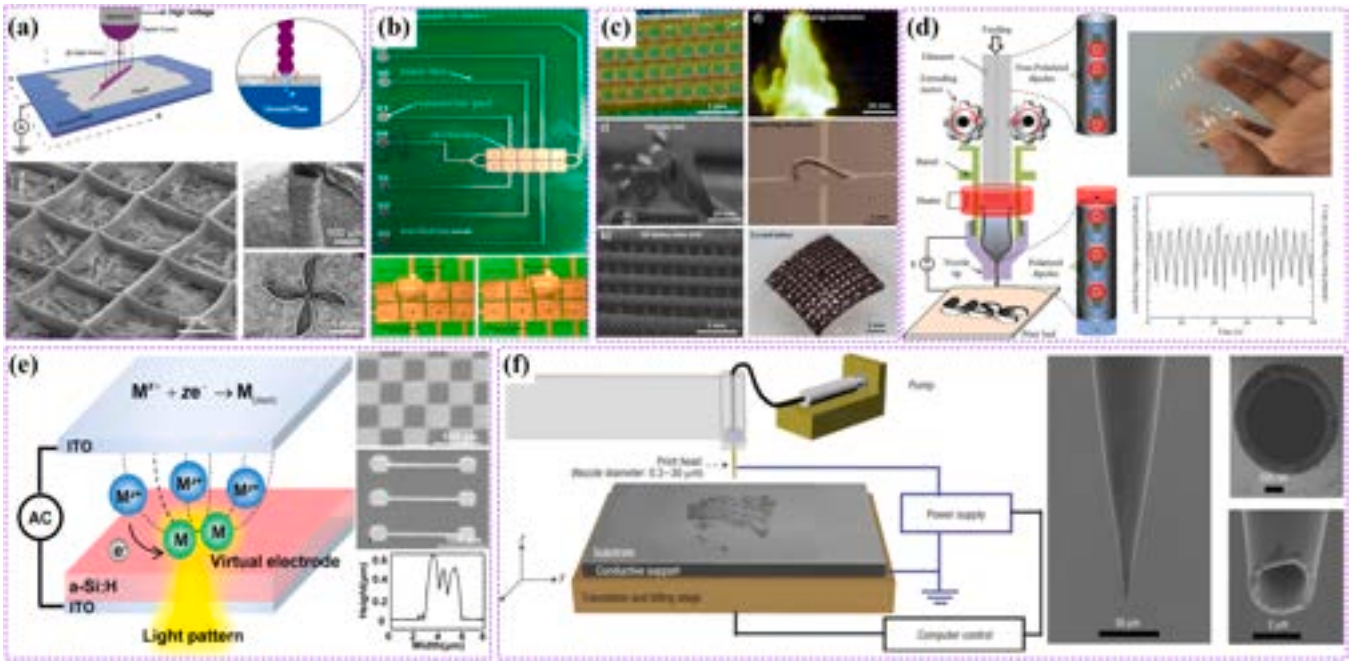

Fig. 11. Electrical field-assisted extrusion-based AM: a) 3D electrospinning process schematic SEM image of stacked 3D grid structures on a paper substrate [264]. b) Electrode array and droplet motion control using electrowetting [270]. c) 3D printed electrode samples for EPD of thermite [273]. d) Electric field-assisted printing of PVDF structures with subsequent poling of the extruded material can be used to build flexible electronics [252]. e) Mechanism of the ODE technique to produce metal electrodes, some of the additively manufactured electrodes, and the smallest geometry that can be obtained [282]. f) Mechanism of the electrohydrodynamic jet printing and the micro capillary nozzle shape for this process [287].

piezoelectric materials. PVDF polymer is one of the polymeric piezoelectric materials which can be used in sensing and energy harvesting applications by converting mechanical to electrical energy [275]. This material shows up in four different phases of α, β, γ, and δ. Due to having the largest dipole moment, β-phase has gained the greatest attention compared to other phases [276]. A well-established process to convert PVDF from its natural α-phase to the most efficient β-phase is by applying axial stretching followed by applying large electric fields that align the dipole structures in the polymeric chains [277]. Researchers have used electric poling-assisted AM to eliminate the complex and time-consuming process of α-to-β transformation in PVDF structures [252]. During this process, molten PVDF filaments are subjected to mechanical stresses resulting from the shear field from the flow inside the extruding nozzle, and then electrically polarized by applying large electric fields (Fig. 11d). The same process has been used for additive manufacturing of piezoelectric polymer-ceramic composites [251]. Barium Titanate (BTO or $BaTiO_3$) ceramic fillers are embedded in PVDF polymeric matrix to enhance the piezo effect. PVDF and BTO powders were mixed via solvent casting, and the mixture was extruded during a heating process to achieve the BTO/PVDF composite filaments. The composite additively manufactured structures from this process possessed acceptable piezoelectric properties, along with toughness, tensile, and fatigue behavior. Alignment of piezoelectric ceramics has also been investigated by other researchers. Using the dielectrophoresis concepts, Van den Ende et al. studied the in situ 2D alignment of PZT short fibers in polyurethane resin [253].

A potential application of electric field-assisted AM is in building thin metallic films on free-form surfaces. This approach is especially useful when patterning conductive layers on top of different free-form substrates. To be more specific, patterning of conductive metallic layers on semiconductor materials is a critical fabrication step in manufacturing of MEMS. Different 3D printing processes such as laser-induced printing [278], inkjet printing [279], screen printing [280], and micro-contact printing [281] have been used in this field and show serious limitations. For example, although inkjet printing can be a fast and single-step process, due to the limitations in nozzle size and droplet formation mechanisms, it lacks the required high resolution. Micro-contact printing has eliminated these problems; however, it still requires the master molds that need to be generated in conventional photolithography processes. Laser-induced printing is still relatively complex, requiring various consecutive steps to process the parts into the final product. Because of these shortcomings, researchers have used different approaches to address the metal patterning problem on semiconductor substrates. Liu et al. addressed these problems by developing a process called optically-controlled digital electrodeposition (ODE) [282]. In this approach, light patterns corresponding to the parts shape are projected into hydrogenated amorphous silicon layer electrode (ODE chip), causing the illuminated areas to become more electrically conductive. After this step, owing to the electrophoresis effect, metal ions are directed and deposited towards the substrate. Using this method, micro-electrodes were fabricated with different geometries, high electrical conductivity, and geometrical resolution of 2.7 μm (Fig. 11e). The same methodology is used by Pascall et al., leading to effectively eliminating the need for photo masks, enhancing the process dimensional resolution, and developing the first projector-based light-directed EPD to control the external electric field during the AM process [283–285].

Electrohydrodynamic jet (e-jet) printing is another electric field-assisted AM process in which high resolution of printing is achieved through using electric field to drive liquid out of micronozzles. Fundamentals of this process were first investigated by Kawamoto et al. [286] However, the process was first introduced by Park et al. as an AM method achieving a resolution less than 10 μm [287]. Nozzles with a tip diameter of approximately 2 μm were prepared by gold-coating the external wall and a small fraction of the internal wall of a glass pipette extruding tip (Fig. 11f). The extruding tip also benefits from a hydrophobic coating, which prevents the nozzle from clogging. In order to provide the ink, this nozzle is connected to a microsyringe pump. An external voltage is applied between the nozzle wall and the print bed, which drives the electrohydrodynamic phenomena and causes the fluid to be extruded out of the nozzle into the substrate. X-Y motion of the

print substrate provides the required area for patterning different 2D shapes into the substrate. Due to its high resolution and ability to print a wide range of materials, the e-jet printing method has also been used to build fine structures such as polymeric composites with embedded aligned silver nanowires [288], printed transistors using reduced graphene oxide [289], organic light-emitting diodes (OLEDs) for small displays [290], and scaffolds for tissue engineering applications with enhanced cell alignment and proliferation [291].

6.2. Electric field-assisted vat photopolymerization AM

Compared to extrusion-based processes, in the case of using vat photopolymerization AM, the application of electric field is slightly different. In extrusion-based processes the electric field is achieved by applying an electrical potential between the nozzle and print bed or at the two sides on the print area on the print bed. However, due to use of a resin vat in the vat photopolymerization, the electric field is generally applied to the liquid resin and re-orients the fillers in the resin while the curing process happens. Electrical-filed alignment of particles suspended in a photocurable resin was initially studied by Park and Robertson [292]. Nakamoto et al. used electrical-assisted laser SLA to build polymeric composite parts with selective alignment of the fillers [293]. Unidirectional TiC whiskers were dispersed into the photocurable resin and used to reinforce microparts along their load bearing axis (Fig. 12a). This work also developed the theoretical framework for calculating the required electric field to generate sufficient moment to rotate the whiskers and align them with the field. When the shear stress on the surface of the whiskers becomes equal to the yield shear stress of the resin, the liquid resin starts flowing. This characteristic, called Bingham property, is measured in this study. As another basis for the electric field-assisted vat photopolymerization, Kim et al. used traditional methods for developing polymeric composites that are reinforced by single-wall CNTs [249]. Electric field was used to control the electrical conductivity of composite structures by aligning the particles under an AC electric field and subsequent photopolymerization of the liquid polymeric mixture. This process was developed to align the fillers in the polymeric matrix without the drawbacks of shear-alignment such as low filler content, which leads to developing composites which are not reinforced beyond increasing the mechanical properties.

Holmes et al. at Army Research Laboratory in collaboration with a research team at the University of Wisconsin-Madison, developed a process called Field-Aided Laminar Composite (FALCom), to create three-dimensionally reinforced polymer composites through using electric field in SLA process [28,259]. In their work, different filler materials such as multi-walled carbon nanotubes (MWCNTs) [259], alumina microparticles [259], and aluminum microparticles [28,259] were used. Based on the previous works completed by Kim et al., a maximum resin viscosity of 1000 cP was selected for efficient particle alignment under an electric field [249,256,258]. An important aspect of this work is that the electrical non-conductivity of the matrix monomer material. However, most of the time, the photoinitiators in photocurable resins turn out to be electrically conductive. Another important point that should always be considered in electric field-assisted AM is that aside from the process that is being used, the fillers do not necessarily need to be electrically conductive. The research done by Holmes and his collaborators is considered to be one of the first comprehensive studies on electric field-assisted vat photopolymerization which is used as the basis for other research done in recent years.

Similar to the extrusion-based processes, vat photopolymerization has also been paired with electric field to build 3D composite structures with piezoelectric properties. Kim et al. used microscale digital projection printing (DPP) to incorporate barium titanate ($BaTiO_3$, BTO) nanofibers into photocurable polymer solutions of polyethylene glycol diacrylate (PEGDA) (Fig. 12b) [294]. Using colloidal assembly and surface modification on BTO nanoparticles, acrylate groups were added to the particles, which led to improving the piezoelectric properties of the 3D printed composites by a factor of 10.

Using the Projection-based Electro-Stereolithography (PES), Pan et al. printed composite structures with controlled distribution of particles into the print vat (Fig. 12c) [295,296]. In the PES process, two technologies, vat photopolymerization and electrostatic deposition, are integrated together to form the final product. During this process, the

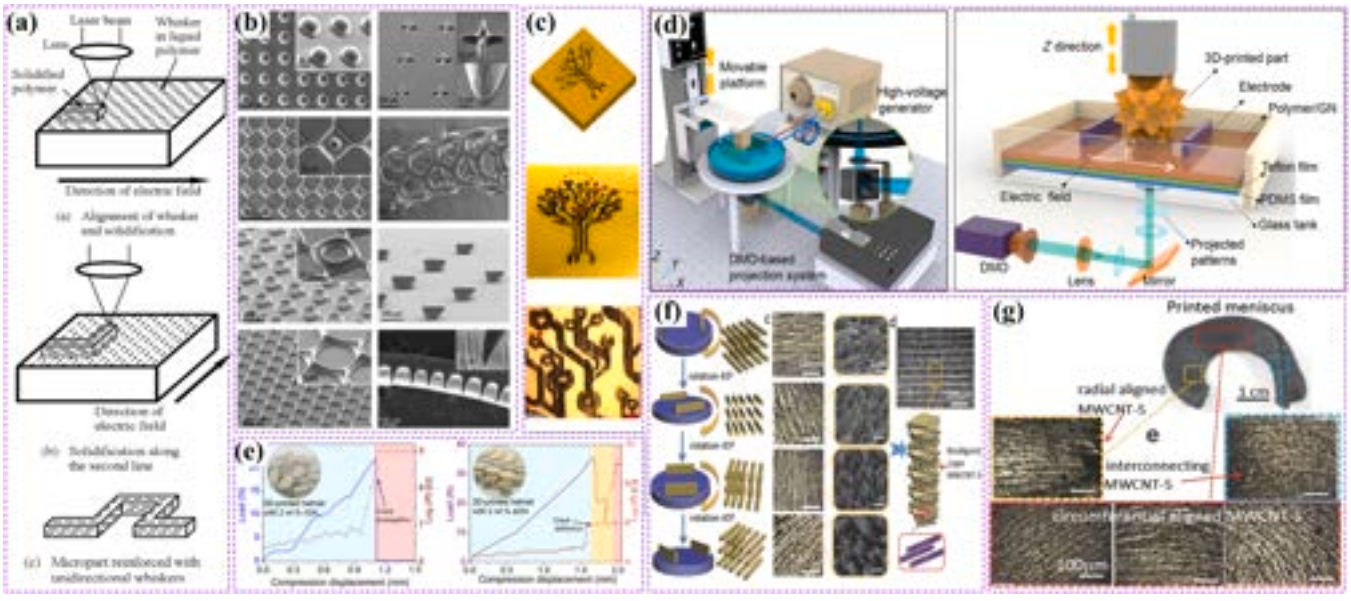

Fig. 12. Electric field-assisted extrusion-based AM: a) Schematic of filler alignment using electric field in laser stereolithography [293]. b) Piezoelectric microstructures built by digital projection printing (right column) and 3D structures manufactured by dynamic optical projection stereolithography (left column) [294]. c) CAD model, 3D view, and microscopic image of part manufactured by projection electro-stereolithography [296]. d) Illustration of the electric field-assisted additive manufacturing process and the SLA setup used for this purpose [301]. e) 3D printed composites of random and aligned graphene nanoplatelets show different behaviors, complete disconnection vs. self-healing properties, under compression tests and simultaneous electrical potential [301]. f) Schematic, SEM, and surface optical microscopic images of MWCNTs in 3D printed to mimic natural materials [300]. g) Electric field-assisted additive manufacturing is used to build an artificial meniscus with selective alignment of MWCNTs in different areas [300].

resin is sensitized using a corona charging device, and particles are deposited from a positively charged plate onto the surface of the resin. In the meantime, the resin is exposed to the curing light, which builds the final product during a top-down SLA approach. In addition to developing this method, this group also developed the physical model for the curing and deposition process.

Biological structures have been significantly inspiring the way researchers look at developing different materials and reinforcements for different applications [297]. However, building the complicated organic natural architectures are currently far beyond the capabilities of traditional manufacturing processes [298,299]. Being considered a process that can handle more complicated designs, additive manufacturing has evolved to help reach this goal by manipulating and modeling the multi-scale/material structures. Due to the importance of reinforcements and control on their dispersion in biological composites, field-assisted AM has been used to mimic these structures for real-life applications [38]. In an effort from researchers at the University of Southern California, alignment of MWCNTs was actively controlled during a DLP process to mimic the reinforcements of biological architectures [300]. In their proposed process, two electrodes are used on the two opposite sides of the resin vat to induce the electric field along the vat, and consequently align the nanofibers. This resin vat along with the electrodes has the ability of rotating during the process, and as a result, the printed parts experience fiber orientation in different directions along different layers. The load-bearing capabilities of the additively manufactured composites was significantly enhanced, and because of the similarities of constructed structures with biological constructs, future applications in printing artificial menisci is predicted for the proposed process (Fig. 12f,g). In another work from the same group, devising the electric field-assisted DLP printing, nacre-inspired hierarchical structures were built using aligned graphene nanoplatelets (aGNs) to reinforce mechanical properties (Fig. 12d,e) [301]. The anisotropic electrical properties of the GNs helped the researchers build self-sensing miniature helmets with the ability of crack detection.

6.3. Electric field-assisted conventional manufacturing processes

Similar to magnetic field-assisted AM, the fundamental concepts of electric field-assisted AM have been developed through conventional manufacturing processes. In this section, a brief overview of these works is presented, which can also be used in conjunction with additive manufacturing methods. Several research groups have worked on particle manipulation using an electric field to generate advanced composites. In 1998, Bowen et al. used the dielectrophoresis phenomena to build composite structures with various filler materials aligned using an electric field in a thermoset polyurethane matrix [245]. Two years later, Vyakarnan and Drzal patented an electric field-assisted approach to fabricate composites with discontinuous fibers aligned in a desired direction [302].

Ryan et al. used electric field during the slow evaporation of a mixture of semiconductor nanorods and toluene to generate superlattices made out of nanorods (Fig. 13a,b) [303]. The direction of the DC field in this work is perpendicular to the substrate, leading to the assembly of the nanorods in this direction. Centrifugal casting is also another conventional method paired with electric field to manipulate fillers in a composite matrix and build semiconducting structures. Decker and Gan used a centrifugal casting method in conjunction with electrical and magnetic fields to manufacture semiconducting polymer structures from polyaniline (PANi) as the matrix and TiO_2 nanotubes as the reinforcing elements [304]. In this method, a rotary chamber generated the mechanical forces required for forming the multilayered structures into a mold, and electrical and magnetic forces were added by a DC field and permanent magnets, respectively. The function of electrical forces polymerized the aniline solution on the surface of the nanotubes by eliminating the hydrophobicity, and the mechanical centrifugal forces pushed the aniline solution towards the nanotubes. The fabricated structures were characterized as an n-type material by measuring their semiconducting properties such as Seebeck coefficient and electrical resistance.

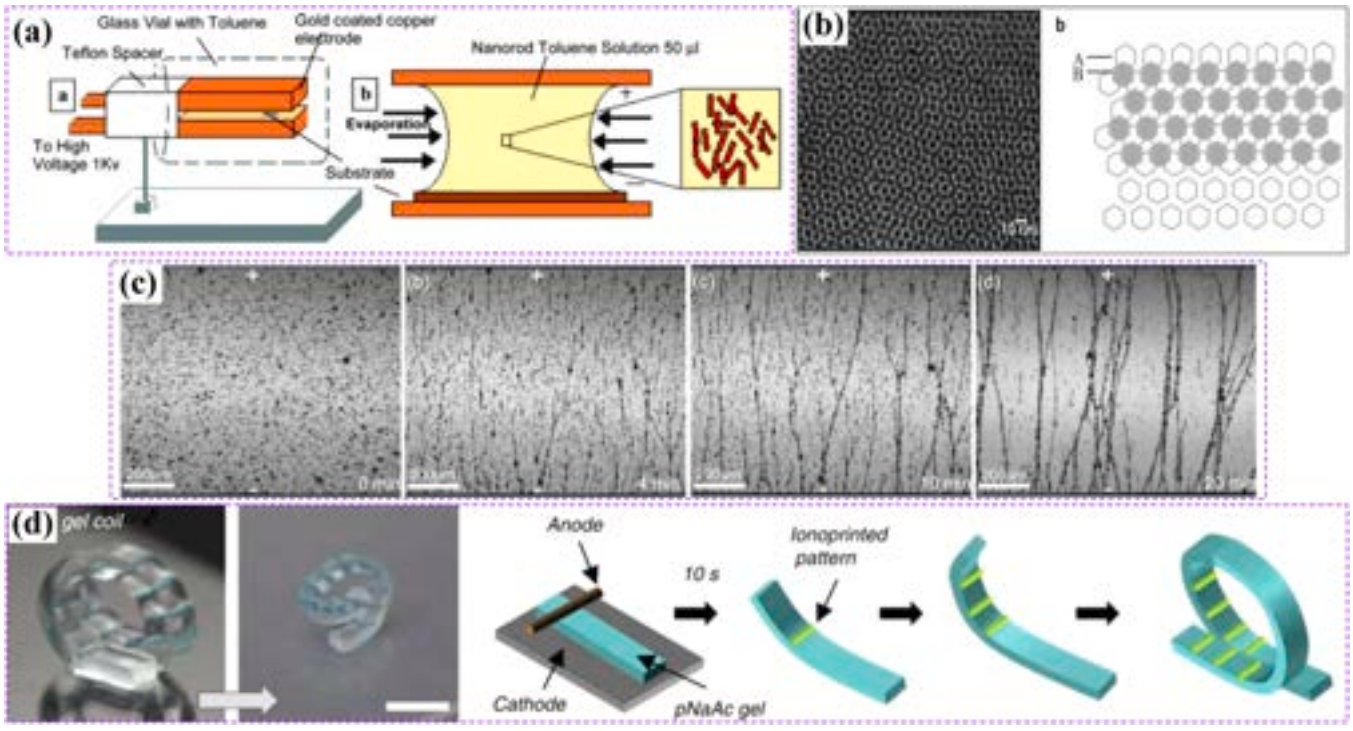

Fig. 13. Electric field-assisted alignment in conventional manufacturing processes: a) schematic of the filler alignment using electric-filed-assembly [303]. b) Nanorods of cadmium sulfide (CdS) are aligned in 3D and deposited under electric field [303]. c) Application of electric field to graphene nanoparticles suspended in epoxy resins leads to orienting the particles in the time span of 20 s [306]. d) Unfolding a 3D gel coil by ionprinted lines and recovery to its original shape by dehydration [307].

A fraction of the research on electric field-assisted manufacturing has also been focused on deriving the theoretical frameworks for particle alignment. Daniel et al. developed the theoretical formulation of carbon fiber alignment under an electric field and validated their equations through experimental results [305]. In another work, the effect of AC electric field on alignment of graphene nano-platelets in epoxy resins was investigated, and a relationship was established to correlate the particle alignment and electrical/thermal conductivity of the resulting composites [306]. Application of the electric field to the resin loaded with graphene platelets significantly led to alignment of the particles in the same direction (Fig. 13c). Smart materials and structures are also another area of interest for electric field-assisted manufacturing processes. Ion printing is used to pattern and embed ions in hydrogels in 2D and 3D fashions [307]. In this process, the ions are injected into the structure of the hydrogels while their orientation is controlled using an external electric field. Due to the responsiveness of the embedded ions and mechanical compliance of the fabricated structures, this method can be used to build soft robots and flexible actuators (Fig. 13d).

6.4. Potentials and limitations of electric field-assisted AM

Compared to magnetic field, electric field-assisted manufacturing has the advantage of using a more extensive range of filler materials. Due to increased research on the electrophoresis phenomena, this class of field-assisted manufacturing processes is investigated more comprehensively. However, using an electric field has its own challenges, such as the need for using high voltage, which leads to a smaller number of works pairing it with AM. A significant amount of work has been explored on changing the material properties using electric field-assisted AM. As an example, improved mechanical properties have been reported by different researchers using this approach [42]. By changing the direction and magnitude of the applied electric field during the manufacturing process, material properties such as electrical conductivity or mechanical strength can be tailored.

6.5. Future perspectives of electric field-assisted AM

Considering all the advantages and disadvantages of electric field-assisted AM, there is still a plethora of applications that remain to be explored using this method. Aligning electrically conductive fillers in the same direction will increase the chance of electrical current passing through the material. As a result, it can be reasonably said that building conductive polymeric structures is a challenge that can be overcome by using AM with electric field [301]. Additively manufactured electromagnetic interference (EMI) shielding devices can also be developed by electric field-assisted processes [308–310].

A promising avenue for using electric field-assisted AM is building 3D structures from piezoelectric polymers such as PVDF or by embedding piezoelectric dipoles in a polymeric matrix and using the generated structure as sensors [251], actuators [252], or energy storage and harvesting devices [276,311]. The electric field applied subsequently to the additive process will help the piezoelectric materials become polarized, which eliminates the need for extra post-processing steps and results in a more efficient device [253]. Customized self-sensing 3D structures have been challenging to fabricate in-house, and additive manufacturing of piezoelectric composites or conductive polymers play an essential role in this field [301]. In general, one of the applications of the electric field is re-orienting the dipoles inside a structure [312], which has opened up new avenues in developing sensors and actuators [313]. The same concept has also been coupled with additive manufacturing; however, one of the challenges in using the electric field in manufacturing processes is the need for applying high electrical voltages to orient dipoles. Aside from the safety issues, large electric fields have undesired effects on the subsystems that are used for process implementation. A topic that can be considered as a future research area electric field assisted AM is developing materials more sensitive to the electric field and as a result do not require large fields for dipole reorientation.

Optically controlled electrodeposition is also a promising process for metal film patterning on freeform surfaces and can be used in placing micro-sensors, solar cells, and field effect transistors [282]. Ion-planting has been effectively used to pattern ions into polymeric structures. Considering hydrogels mechanical properties and their ability to entrap the ions, this approach is efficient for building stimuli-responsive structures for soft and untethered robots [307]. Another process that has been used widely in the industry is field-assisted sintering technology (FAST), where an electric field is used to sinter powders in a green sample [314,315]. Although this technology has not been applied to powder-bed AM processes, incorporating FAST with AM could open up new research areas for developing polymeric composites with controlled anisotropy.

7. Conclusion

Fig. 14 summarizes the matrix materials, reinforcing fillers, and potential applications and limitations of each reviewed field, including shear, acoustic, magnetic, and electric field. In this figure, moving from left to right, more material constraints is imposed on the filler/matrix and as a result, smaller choice of material will exist. Therefore, the need to expanding materials range while moving from shear-assisted process to electric field-assisted processes exists and needs to be addressed in future research works. As another limitation in field-assisted AM, increasing the volume fraction of fillers inside the polymeric matrix in all of the reviewed processes is a limiting factor in terms of materials and process development that can be explored in future studies.

Although there has been a significant number of research published on pairing external fields with 3D printing processes, many challenges remain to be tackled in future in order to establish these class of manufacturing processes for practical and industrial applications. Fig. 15 (a) summarizes the current level of development in areas related to field-assisted AM for each field. A higher score indicates more development is still needed. Generally, shear and acoustic fields are more developed than magnetic and electric fields. Fig. 15 (a) also provides a general direction and guideline for future studies. Fig. 15 (b) characterizes the limitations and flexibility of each field in different categories. A higher score indicates it is more flexible and has less limitations. Shear and acoustic fields work for a wide range of materials but provide less spatial control. On the other hand, magnetic and electric field, although only work for magnetic and electrically conductive materials, respectively, offer a greater and more flexible control of anisotropy orientation and distribution.

This paper provided a state-of-the-art review on field-assisted additive manufacturing processes of polymeric composites. In summary, advances in AM methods and technologies and deep understanding of required filler-matrix material properties along with the potential applications are areas for exploring field-assisted AM for polymeric composites. Different material systems for polymeric composites can benefit from field-assisted AM in a variety of directions such as improving local and global physical properties of the composite materials, creating smart structures, and developing efficient sensors and actuators with customized shapes and functionalities. The anisotropic alignment introduced by field-assisted AM can lead to fabrication of structures that can mimic the functionality of natural materials and help with achieving tunable properties in 3D printed components. Despite all the progress that has happened in this area for the past few years, field-assisted AM is still in its infancy and to have a meaningful progress toward advancements in this field, collaborative research between different disciplines such as physics, mechanics, and materials science is required. For example, studies on predicting and understating the material behavior under external fields have emerged recently. Integrating these studies with 3D printing process leads to better understanding on manufacturing process control and help with creating more optimized structures that are capable to efficiently perform a functional task. From

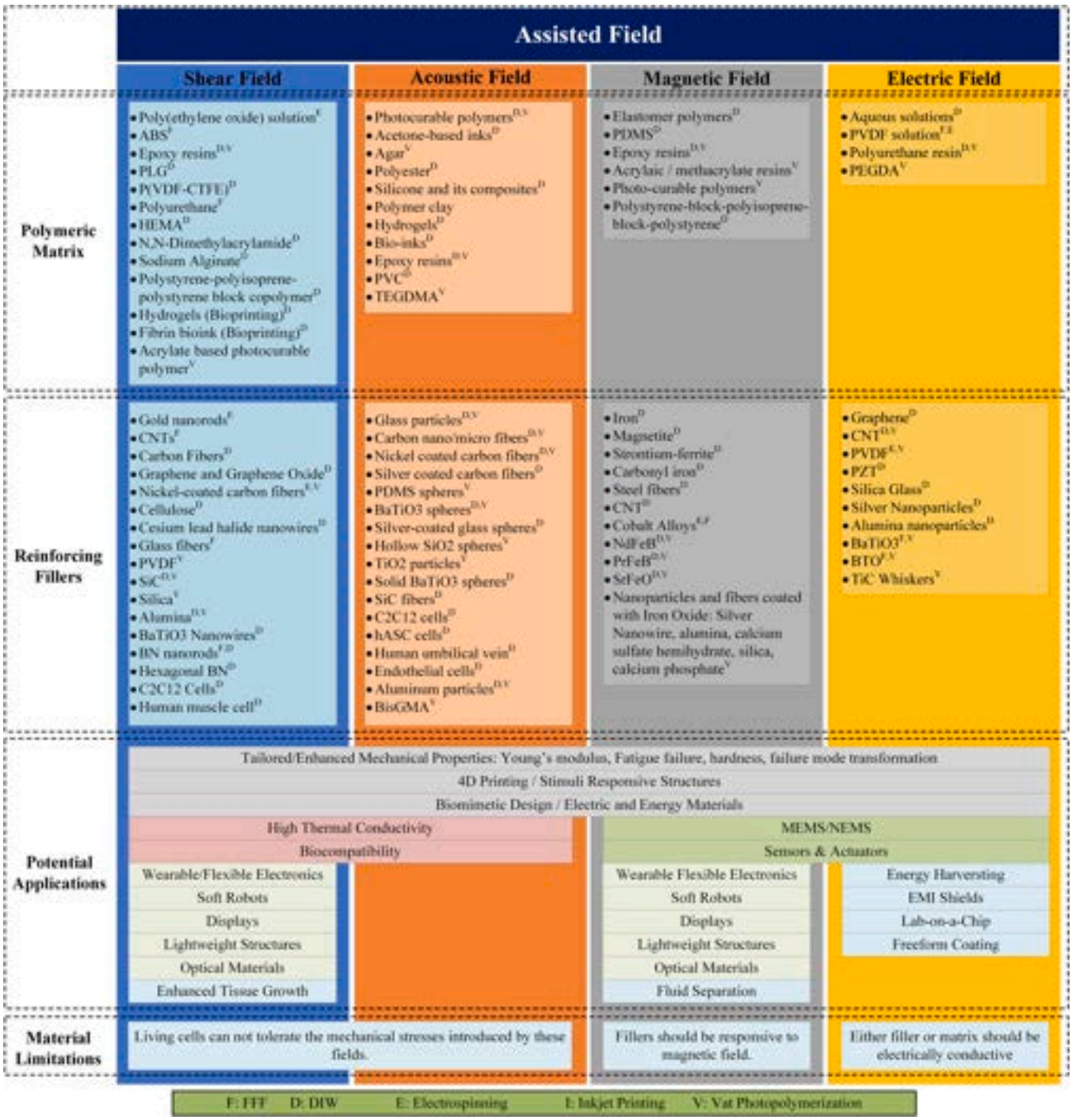

Fig. 14. Summary of the matrix and filler materials used in field-assisted additive manufacturing of polymeric composites, and the potential applications and limitations for each process.

another perspective, developing frameworks that helps with implementing a desired design into the final products is another area that needs to be explored in field-assisted AM. We predict that in future, more research in these areas will be performed and multiscale relationships between properties of raw materials, manufacturing process mechanisms, and performance of the fabricated polymeric composites will be extracted. As it is discussed for each field-assisted process, a major area of research is developing easier and more optimized methods to induce the assistive field into 3D printing processes. By developing more versatile field generation devices, establishing new paradigms in field generation, and creating materials that are more responsive to external fields, field-assisted AM can be developed into further steps. Moreover, a limited number of additive technologies, materials extrusion and vat photopolymerization, are widely paired with external field to control anisotropy in polymer-matrix composites. The authors believe that other AM technologies of polymeric materials are also viable candidates in this field and need to be further explored. Future studies can explore the use of multiple assisted fields, by leveraging the advantages of each field, while overcoming the limitations of each own to achieve a greater functionality of the composite material. There is also a great potential when combining field-assisted AM with smart materials. These processes enable and open up new opportunities for design and manufacturing of

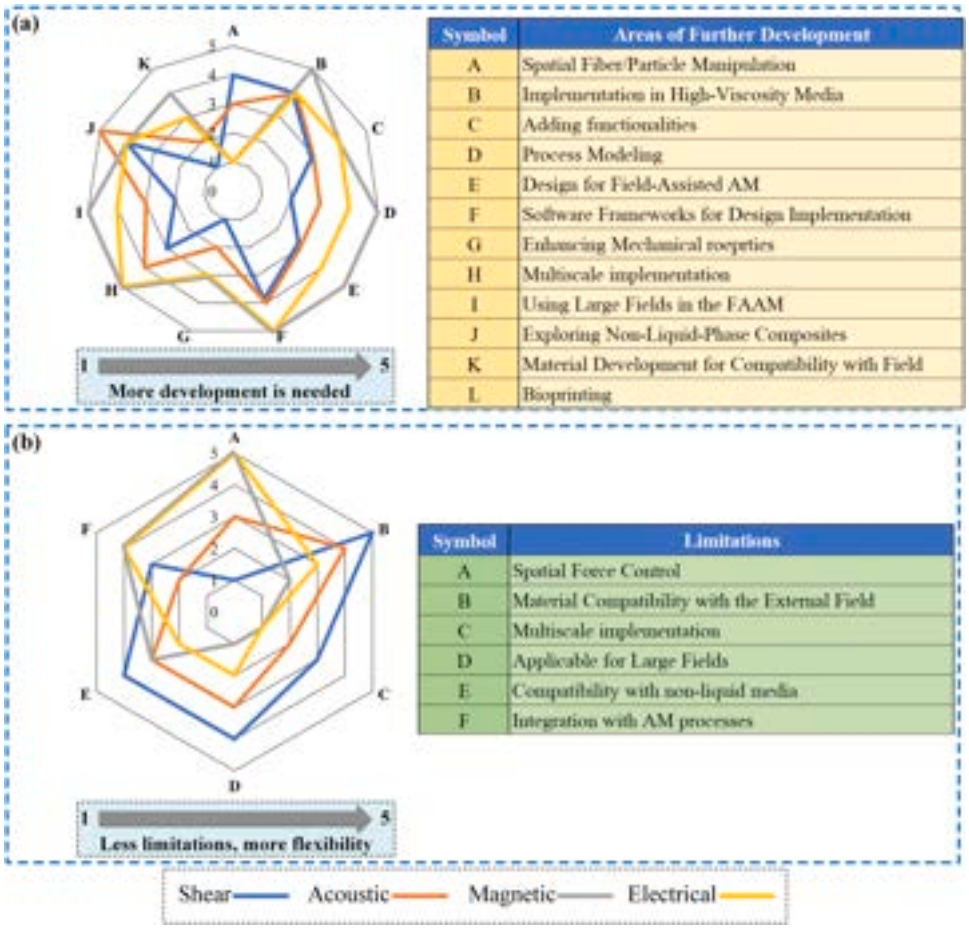

Symbol	Areas of Further Development
A	Spatial Fiber/Particle Manipulation
B	Implementation in High-Viscosity Media
C	Adding functionalities
D	Process Modeling
E	Design for Field-Assisted AM
F	Software Frameworks for Design Implementation
G	Enhancing Mechanical roeprties
H	Multiscale implementation
I	Using Large Fields in the FAAM
J	Exploring Non-Liquid-Phase Composites
K	Material Development for Compatibility with Field
L	Bioprinting

Symbol	Limitations
A	Spatial Force Control
B	Material Compatibility with the External Field
C	Multiscale implementation
D	Applicable for Large Fields
E	Compatibility with non-liquid media
F	Integration with AM processes

Fig. 15. Guidelines for future research in field-assisted additive manufacturing of polymeric composites: (a) Potential areas of further development, and (b) Limitations for each field-assisted process.

novel materials and structures for a variety of applications.

CRediT authorship contribution statement

Matthew Schock: Methodology, Writing – original draft, Writing – review & editing, Investigation. **Shahriar Safaee:** Methodology, Investigation, Writing – review & editing, Writing – original draft, Visualization, Conceptualization. **Yayue Pan:** Writing – review & editing, Writing – original draft. **Erina B. Joyee:** Methodology, Writing – original draft, Writing – review & editing, Investigation. **Roland K. Chen:** Conceptualization, Funding acquisition, Investigation, Methodology, Project administration, Writing – original draft, Writing – review & editing.

Declaration of Competing Interest

The authors declare that they have no known competing financial interests or personal relationships that could have appeared to influence the work reported in this paper.

Acknowledgements

This research was in part supported by the U.S. Department of Defense Congressionally Directed Medical Research Programs (W81XWH18-1-0137).

References

[1] B. Berman, 3-D printing: the new industrial revolution, Bus. Horiz. 55 (2012) 155–162, https://doi.org/10.1016/j.bushor.2011.11.003.
[2] J. Yang, E.C. Baker, H.O.T. Ware, F. Zhou, C. Sun, G.A. Ameer, R. Van Lith, 3d Printing of Biomedical Implants, 20180117219, 2018. ⟨http://www.freepatentsonline.com/y2018/0117219.html⟩ (Accessed 17 January 2022).
[3] D. Sheynin, Y.M. Bovalino, This Is What A 3D Printed Jet Engine Looks Like, GE Reports, 2017. ⟨https://www.ge.com/reports/treat-avgeeks-inside-look-ges-3d-printed-aircraft-engine/⟩ (Accessed 17 January 2022).
[4] The perfect fit: Carbon + adidas collaborate to upend athletic footwear, Carbon. (n.d.). ⟨https://www.carbon3d.com/case-studies/adidas/⟩ (accessed January 17, 2022).
[5] L.D. Sturm, C.B. Williams, J.A. Camelio, J. White, R. Parker, Cyber-physical vulnerabilities in additive manufacturing systeMs: A Case study attack on the.STL file with human subjects, J. Manuf. Syst. 44 (2017) 154–164, https://doi.org/10.1016/j.jmsy.2017.05.007.
[6] F.L. Matthews, R.D. Rawlings, Composite Materials: Engineering and Science, CRC Press, 1999.
[7] S. Weiner, H.D. Wagner, The material bone: structure-mechanical function relations, Annu. Rev. Mater. Sci. 28 (1998) 271–298, https://doi.org/10.1146/annurev.matsci.28.1.271.
[8] J.C. Weaver, G.W. Milliron, A. Miserez, K. Evans-Lutterodt, S. Herrera, I. Gallana, W.J. Mershon, B. Swanson, P. Zavattieri, E. DiMasi, D. Kisailus, The stomatopod dactyl club: a formidable damage-tolerant biological hammer, Science 336 (2012) 1275–1280, https://doi.org/10.1126/science.1218764.
[9] Y. Politi, M. Priewasser, E. Pippel, P. Zaslansky, J. Hartmann, S. Siegel, C. Li, F. G. Barth, P. Fratzl, A spider's fang: how to design an injection needle using chitin-based composite material, Adv. Funct. Mater. 22 (2012) 2519–2528, https://doi.org/10.1002/adfm.201200063.
[10] J.J. Martin, B.E. Fiore, R.M. Erb, Designing bioinspired composite reinforcement architectures via 3D magnetic printing, Nat. Commun. 6 (2015), https://doi.org/10.1038/ncomms9641.
[11] M. Hofmann, 3D printing gets a boost and opportunities with polymer materials, ACS Macro Lett. 3 (2014) 382–386, https://doi.org/10.1021/mz4006556.

[12] M. Falahati, P. Ahmadvand, S. Safaee, Y.-C. Chang, Z. Lyu, R. Chen, L. Li, Y. Lin, Smart polymers and nanocomposites for 3D and 4D printing, Mater. Today 40 (2020) 215–245, https://doi.org/10.1016/j.mattod.2020.06.001.

[13] D.N. Saheb, J.P. Jog, Natural fiber polymer composites: a review, Adv. Polym. Technol. 18 (1999) 351–363, https://doi.org/10.1002/(SICI)1098-2329(199924)18:4<351::AID-ADV6>3.0.CO;2-X.

[14] P. Parandoush, D. Lin, A review on additive manufacturing of polymer-fiber composites, Compos. Struct. 182 (2017) 36–53, https://doi.org/10.1016/j.compstruct.2017.08.088.

[15] A. Bandyopadhyay, B. Heer, Additive manufacturing of multi-material structures, Mater. Sci. Eng.: R: Rep. 129 (2018) 1–16, https://doi.org/10.1016/j.mser.2018.04.001.

[16] A.R. Studart, Additive manufacturing of biologically-inspired materials, Chem. Soc. Rev. 45 (2016) 359–376, https://doi.org/10.1039/C5CS00836K.

[17] E.J. Garcia, B.L. Wardle, A. John Hart, Joining prepreg composite interfaces with aligned carbon nanotubes, Compos. Part A: Appl. Sci. Manuf. 39 (2008) 1065–1070, https://doi.org/10.1016/j.compositesa.2008.03.011.

[18] W. Zhong, F. Li, Z. Zhang, L. Song, Z. Li, Short fiber reinforced composites for fused deposition modeling, Mater. Sci. Eng.: A 301 (2001) 125–130, https://doi.org/10.1016/S0921-5093(00)01810-4.

[19] B.G. Compton, J.A. Lewis, 3D-printing of lightweight cellular composites, Adv. Mater. 26 (2014) 5930–5935, https://doi.org/10.1002/adma.201401804.

[20] J.P. Bell, Flow orientation of short fiber composites, J. Compos. Mater. 3 (1969) 244–253, https://doi.org/10.1177/002199836900300204.

[21] K.N. Murty, G.F. Modlen, Experimental characterization of the alignment of short fibers during flow, Polym. Eng. Sci. 17 (1977) 848–853, https://doi.org/10.1002/pen.760171207.

[22] M.L. Shofner, K. Lozano, F.J. Rodríguez-Macías, E.V. Barrera, Nanofiber-reinforced polymers prepared by fused deposition modeling, J. Appl. Polym. Sci. 89 (2003) 3081–3090, https://doi.org/10.1002/app.12496.

[23] D.K. Rajak, D.D. Pagar, P.L. Menezes, E. Linul, Fiber-reinforced polymer composites: manufacturing, properties, and applications, Polymers 11 (2019) 1667, https://doi.org/10.3390/polym11101667.

[24] A.N. Dickson, J.N. Barry, K.A. McDonnell, D.P. Dowling, Fabrication of continuous carbon, glass and Kevlar fibre reinforced polymer composites using additive manufacturing, Addit. Manuf. 16 (2017) 146–152, https://doi.org/10.1016/j.addma.2017.06.004.

[25] S. Biswas, B. Deo, A. Patnaik, A. Satapathy, Effect of fiber loading and orientation on mechanical and erosion wear behaviors of glass–epoxy composites, Polym. Compos. 32 (2011) 665–674, https://doi.org/10.1002/pc.21082.

[26] J.-W. Kim, D.-G. Lee, Effect of fiber orientation and fiber contents on the tensile strength in fiber-reinforced composites, J. Nanosci. Nanotechnol. 10 (2010) 3650–3653, https://doi.org/10.1166/jnn.2010.2303.

[27] A. Tezvergil, L.V.J. Lassila, P.K. Vallittu, The effect of fiber orientation on the thermal expansion coefficients of fiber-reinforced composites, Dent. Mater. 19 (2003) 471–477, https://doi.org/10.1016/S0109-5641(02)00092-1.

[28] L.R. Holmes, J.C. Riddick, Research summary of an additive manufacturing technology for the fabrication of 3D composites with tailored internal structure, JOM 66 (2014) 270–274, https://doi.org/10.1007/s11837-013-0828-4.

[29] R.M. Erb, D.S. Sebba, A.A. Lazarides, B.B. Yellen, Magnetic field induced concentration gradients in magnetic nanoparticle suspensions: theory and experiment, J. Appl. Phys. 103 (2008), 063916, https://doi.org/10.1063/1.2901140.

[30] Y. Chen, Y. Guo, S. Batra, E. Wang, Y. Wang, X. Liu, Y. Wang, M. Cakmak, Transparent and through thickness conductive polystyrene films using external magnetic fields for " Z " alignment of nickel nanoparticles, Nanoscale 7 (2015) 14636–14642, https://doi.org/10.1039/C5NR03328D.

[31] Y. Guo, S. Batra, Y. Chen, E. Wang, M. Cakmak, Roll to roll electric field "Z" alignment of nanoparticles from polymer solutions for manufacturing multifunctional capacitor films, ACS Appl. Mater. Interfaces 8 (2016) 18471–18480, https://doi.org/10.1021/acsami.6b05435.

[32] Z. Qiang, Y. Guo, H. Liu, S.Z.D. Cheng, M. Cakmak, K.A. Cavicchi, B.D. Vogt, Large-scale roll-to-roll fabrication of ordered mesoporous materials using resol-assisted cooperative assembly, ACS Appl. Mater. Interfaces 7 (2015) 4306–4310, https://doi.org/10.1021/am5086275.

[33] D. Kokkinis, M. Schaffner, A.R. Studart, Multimaterial magnetically assisted 3D printing of composite materials, Nat. Commun. 6 (2015) 8643, https://doi.org/10.1038/ncomms9643.

[34] L. Lu, X. Tang, S. Hu, Y. Pan, Acoustic field-assisted particle patterning for smart polymer composite fabrication in stereolithography, 3D Print. Addit. Manuf. 5 (2018) 151–159, https://doi.org/10.1089/3dp.2017.0157.

[35] E.B. Joyee, Y. Pan, A fully three-dimensional printed inchworm-inspired soft robot with magnetic actuation, Soft Robot. (2019), https://doi.org/10.1089/soro.2018.0082.

[36] V. Vekselman, L. Sande, K.G. Kornev, Fully magnetic printing by generation of magnetic droplets on demand with a coilgun, J. Appl. Phys. 118 (2015), 224902, https://doi.org/10.1063/1.4937152.

[37] O. Trotsenko, A. Tokarev, A. Gruzd, T. Enright, S. Minko, Magnetic field assisted assembly of highly ordered percolated nanostructures and their application for transparent conductive thin films, Nanoscale 7 (2015) 7155–7161, https://doi.org/10.1039/C5NR00154D.

[38] Y. Yang, X. Song, X. Li, Z. Chen, C. Zhou, Q. Zhou, Y. Chen, Recent Progress in Biomimetic Additive Manufacturing Technology: From Materials to Functional Structures, Advanced Materials. 0 (n.d.) 1706539. https://doi.org/10.1002/adma.201706539.

[39] G.D. Goh, Y.L. Yap, S. Agarwala, W.Y. Yeong, Recent progress in additive manufacturing of fiber reinforced polymer composite, Adv. Mater. Technol. 4 (2019) 1800271, https://doi.org/10.1002/admt.201800271.

[40] B. Elder, R. Neupane, E. Tokita, U. Ghosh, S. Hales, Y.L. Kong, Nanomaterial patterning in 3D printing, Adv. Mater. 32 (2020) 1907142, https://doi.org/10.1002/adma.201907142.

[41] Y. Hu, Recent progress in field-assisted additive manufacturing: materials, methodologies, and applications, Mater. Horiz. (2020), https://doi.org/10.1039/D0MH01322F.

[42] M. Roy, P. Tran, T. Dickens, A. Schrand, Composite reinforcement architectures: a review of field-assisted additive manufacturing for polymers, J. Compos. Sci. 4 (2020) 1, https://doi.org/10.3390/jcs4010001.

[43] ASTM International, ASTM52900–15 standard terminology for additive manufacturing—general principles—terminology, ASTM International, West Conshohocken, PA 2015., n.d. ⟨https://doi.org/10.1520/F2792–12A⟩.

[44] S.S. Crump, Apparatus and method for creating three-dimensional objects, 1992.

[45] O.A. Mohamed, S.H. Masood, J.L. Bhowmik, Optimization of fused deposition modeling process parameters: a review of current research and future prospects, Adv. Manuf. 3 (2015) 42–53, https://doi.org/10.1007/s40436-014-0097-7.

[46] F. Ning, W. Cong, J. Qiu, J. Wei, S. Wang, Additive manufacturing of carbon fiber reinforced thermoplastic composites using fused deposition modeling, Compos. Part B: Eng. 80 (2015) 369–378.

[47] C.W. Hull, Apparatus for production of three-dimensional objects by stereolithography, (1986).

[48] P. Bártolo (Ed.), Stereolithography: Materials, Processes and Applications, Springer, New York, 2011.

[49] F.P.W. Melchels, J. Feijen, D.W. Grijpma, A review on stereolithography and its applications in biomedical engineering, Biomaterials 31 (2010) 6121–6130, https://doi.org/10.1016/j.biomaterials.2010.04.050.

[50] J. Choi, R.B. Wicker, S. Cho, C. Ha, S. Lee, Cure depth control for complex 3D microstructure fabrication in dynamic mask projection microstereolithography, Rapid Prototyp. J. 15 (2009) 59–70, https://doi.org/10.1108/13552540910925072.

[51] K. Jerald, Kay, Fluid Mechanics, CUP Arch. (1963).

[52] Z. Csuka, R. Olšiak, The profile of shear stress in the liquid at turbulent flow, Šamorín Čilistov, Slovak Repub. (2016), 020032, https://doi.org/10.1063/1.4963054.

[53] G.B. Jeffery, L.N.G. Filon, The motion of ellipsoidal particles immersed in a viscous fluid, Proc. R. Soc. Lond. Ser. A Contain. Pap. A Math. Phys. Character 102 (1922) 161–179, https://doi.org/10.1098/rspa.1922.0078.

[54] T.D. Papathanasiou, D.C. Guell, Flow-Induced Alignment in Composite Materials, Woodhead Publishing, 1997.

[55] X. Chen, J.F. Dobson, C.L. Raston, Vortex fluidic exfoliation of graphite and boron nitride, Chem. Commun. 48 (2012) 3703–3705, https://doi.org/10.1039/C2CC17611D.

[56] E. Varrla, K.R. Paton, C. Backes, A. Harvey, R.J. Smith, J. McCauley, J. N. Coleman, Turbulence-assisted shear exfoliation of graphene using household detergent and a kitchen blender, Nanoscale 6 (2014) 11810–11819, https://doi.org/10.1039/C4NR03560G.

[57] K.R. Paton, E. Varrla, C. Backes, R.J. Smith, U. Khan, A. O'Neill, C. Boland, M. Lotya, O.M. Istrate, P. King, T. Higgins, S. Barwich, P. May, P. Puczkarski, I. Ahmed, M. Moebius, H. Pettersson, E. Long, J. Coelho, S.E. O'Brien, E. K. McGuire, B.M. Sanchez, G.S. Duesberg, N. McEvoy, T.J. Pennycook, C. Downing, A. Crossley, V. Nicolosi, J.N. Coleman, Scalable production of large quantities of defect-free few-layer graphene by shear exfoliation in liquids, Nat. Mater. 13 (2014) 624–630, https://doi.org/10.1038/nmat3944.

[58] G.L. Goh, S. Agarwala, W.Y. Yeong, Directed and on-demand alignment of carbon nanotube: a review toward 3D printing of electronics, Adv. Mater. Interfaces 6 (2019) 1801318, https://doi.org/10.1002/admi.201801318.

[59] H. Zhao, Z. Zhou, H. Dong, L. Zhang, H. Chen, L. Hou, A facile method to align carbon nanotubes on polymeric membrane substrate, Sci. Rep. 3 (2013) 3480, https://doi.org/10.1038/srep03480.

[60] D. Wang, P. Song, C. Liu, W. Wu, S. Fan, Highly oriented carbon nanotube papers made of aligned carbon nanotubes, Nanotechnology (2008) 7.

[61] S. Huang, B. Maynor, X. Cai, J. Liu, Ultralong, well-aligned single-walled carbon nanotube architectureson surfaces, Adv. Mater. 15 (2003) 1651–1655, https://doi.org/10.1002/adma.200305203.

[62] S. Huang, M. Woodson, R. Smalley, J. Liu, Growth mechanism of oriented long single walled carbon nanotubes using "fast-heating" chemical vapor deposition process, Nano Lett. 4 (2004) 1025–1028, https://doi.org/10.1021/nl049691d.

[63] Z. Jin, H. Chu, J. Wang, J. Hong, W. Tan, Y. Li, Ultralow feeding gas flow guiding growth of large-scale horizontally aligned single-walled carbon nanotube arrays, Nano Lett. 7 (2007) 2073–2079, https://doi.org/10.1021/nl070980m.

[64] K.E. Roskov, K.A. Kozek, W.-C. Wu, R.K. Chhetri, A.L. Oldenburg, R.J. Spontak, J. B. Tracy, Long-range alignment of gold nanorods in electrospun polymer nano/microfibers, Langmuir 27 (2011) 13965–13969, https://doi.org/10.1021/la2021066.

[65] K. Thorkelsson, A.J. Mastroianni, P. Ercius, T. Xu, Direct nanorod assembly using block copolymer-based supramolecules, Nano Lett. 12 (2012) 498–504, https://doi.org/10.1021/nl2040089.

[66] D.B. Shinde, J. Brenker, C.D. Easton, R.F. Tabor, A. Neild, M. Majumder, Shear Assisted Electrochemical Exfoliation of Graphite to Graphene, Langmuir 32 (2016) 3552–3559, https://doi.org/10.1021/acs.langmuir.5b04209.

[67] A. Kotula, K. Migler, Simultaneous rheology and crystallinity measures of the shear-assisted crystallization of polycaprolactones, (2017) V11.003.

[68] H. Hu, S. Wang, X. Feng, M. Pauly, G. Decher, Y. Long, In-plane aligned assemblies of 1D-nanoobjects: recent approaches and applications, Chem. Soc. Rev. 49 (2020) 509–553, https://doi.org/10.1039/C9CS00382G.

[69] J.E. Smay, G.M. Gratson, R.F. Shepherd, J. Cesarano, J.A. Lewis, Directed colloidal assembly of 3D periodic structures, Adv. Mater. 14 (2002) 1279–1283, https://doi.org/10.1002/1521-4095(20020916)14:18<1279::AID-ADMA1279>3.0.CO;2-A.

[70] J.A. Lewis, Direct ink writing of 3D functional materials, Adv. Funct. Mater. 16 (2006) 2193–2204, https://doi.org/10.1002/adfm.200600434.

[71] J.P. Lewicki, J.N. Rodriguez, C. Zhu, M.A. Worsley, A.S. Wu, Y. Kanarska, J. D. Horn, E.B. Duoss, J.M. Ortega, W. Elmer, R. Hensleigh, R.A. Fellini, M.J. King, 3D-printing of meso-structurally ordered carbon fiber/polymer composites with unprecedented orthotropic physical properties, Sci. Rep. 7 (2017) 43401, https://doi.org/10.1038/srep43401.

[72] J.R. Raney, B.G. Compton, J. Mueller, T.J. Ober, K. Shea, J.A. Lewis, Rotational 3D printing of damage-tolerant composites with programmable mechanics, PNAS 115 (2018) 1198–1203, https://doi.org/10.1073/pnas.1715157115.

[73] D. Yang, K. Wu, L. Wan, Y. Sheng, A particle element approach for modelling the 3D printing process of fibre reinforced polymer composites, J. Manuf. Mater. Process. 1 (2017) 10, https://doi.org/10.3390/jmmp1010010.

[74] M.K. Hausmann, P.A. Rühs, G. Siqueira, J. Läuger, R. Libanori, T. Zimmermann, A.R. Studart, Dynamics of cellulose nanocrystal alignment during 3D printing, ACS Nano 12 (2018) 6926–6937, https://doi.org/10.1021/acsnano.8b02366.

[75] M. Gao, L. Li, W. Li, H. Zhou, Y. Song, Direct writing of patterned, lead-free nanowire aligned flexible piezoelectric device, Adv. Sci. 3 (2016) 1600120, https://doi.org/10.1002/advs.201600120.

[76] J.H. Kim, S. Lee, M. Wajahat, H. Jeong, W.S. Chang, H.J. Jeong, J.-R. Yang, J. T. Kim, S.K. Seol, Three-dimensional printing of highly conductive carbon nanotube microarchitectures with fluid ink, ACS Nano 10 (2016) 8879–8887, https://doi.org/10.1021/acsnano.6b04771.

[77] D. He, Y. Wang, S. Song, S. Liu, Y. Deng, Significantly enhanced dielectric performances and high thermal conductivity in poly(vinylidene fluoride)-based composites enabled by SiC@SiO2 core-shell whiskers alignment, ACS Appl. Mater. Interfaces 9 (2017) 44839–44846, https://doi.org/10.1021/acsami.7b14751.

[78] X. Zhang, J. Jiang, Z. Shen, Z. Dan, M. Li, Y. Lin, C.-W. Nan, L. Chen, Y. Shen, Polymer nanocomposites with ultrahigh energy density and high discharge efficiency by modulating their nanostructures in three dimensions, Adv. Mater. 30 (2018) 1707269, https://doi.org/10.1002/adma.201707269.

[79] A.E. Jakus, E.B. Secor, A.L. Rutz, S.W. Jordan, M.C. Hersam, R.N. Shah, Three-dimensional printing of high-content graphene scaffolds for electronic and biomedical applications, ACS Nano 9 (2015) 4636–4648, https://doi.org/10.1021/acsnano.5b01179.

[80] H. Luo, X. Zhou, R. Guo, X. Yuan, H. Chen, I. Abrahams, D. Zhang, 3D printing of anisotropic polymer nanocomposites with aligned BaTiO 3 nanowires for enhanced energy density, Mater. Adv. 1 (2020) 14–19, https://doi.org/10.1039/D0MA00045K.

[81] Z. Liang, Y. Pei, C. Chen, B. Jiang, Y. Yao, H. Xie, M. Jiao, G. Chen, T. Li, B. Yang, L. Hu, General, vertical, three-dimensional printing of two-dimensional materials with multiscale alignment, ACS Nano 13 (2019) 12653–12661, https://doi.org/10.1021/acsnano.9b04202.

[82] J. Liu, W. Li, Y. Guo, H. Zhang, Z. Zhang, Improved thermal conductivity of thermoplastic polyurethane via aligned boron nitride platelets assisted by 3D printing, Compos. Part A Appl. Sci. Manuf. 120 (2019) 140–146, https://doi.org/10.1016/j.compositesa.2019.02.026.

[83] Y. Jin, A. Compaan, W. Chai, Y. Huang, Functional nanoclay suspension for printing-then-solidification of liquid materials, ACS Appl. Mater. Interfaces 9 (2017) 20057–20066, https://doi.org/10.1021/acsami.7b02398.

[84] Y. Jin, C. Liu, W. Chai, A. Compaan, Y. Huang, Self-supporting nanoclay as internal scaffold material for direct printing of soft hydrogel composite structures in air, ACS Appl. Mater. Interfaces 9 (2017) 17456–17465, https://doi.org/10.1021/acsami.7b03613.

[85] L. Heux, G. Chauve, C. Bonini, Nonflocculating and chiral-nematic self-ordering of cellulose microcrystals suspensions in nonpolar solvents, Langmuir 16 (2000) 8210–8212, https://doi.org/10.1021/la9913957.

[86] V. Favier, H. Chanzy, J.Y. Cavaille, Polymer nanocomposites reinforced by cellulose whiskers, Macromolecules 28 (1995) 6365–6367, https://doi.org/10.1021/ma00122a053.

[87] M. Jorfi, M.N. Roberts, E.J. Foster, C. Weder, Physiologically responsive, mechanically adaptive bio-nanocomposites for biomedical applications, ACS Appl. Mater. Interfaces 5 (2013) 1517–1526, https://doi.org/10.1021/am303160j.

[88] Y. Li, H. Zhu, Y. Wang, U. Ray, S. Zhu, J. Dai, C. Chen, K. Fu, S.-H. Jang, D. Henderson, T. Li, L. Hu, Cellulose-nanofiber-enabled 3D printing of a carbon-nanotube microfiber network, Small Methods 1 (2017) 1700222, https://doi.org/10.1002/smtd.201700222.

[89] G. Siqueira, D. Kokkinis, R. Libanori, M.K. Hausmann, A.S. Gladman, A. Neels, P. Tingaut, T. Zimmermann, J.A. Lewis, A.R. Studart, Cellulose nanocrystal Inks for 3D printing of textured cellular architectures, Adv. Funct. Mater. 27 (2017) 1604619, https://doi.org/10.1002/adfm.201604619.

[90] M.F. Potter Claire, Lao Ka Hou, Zeng Lingfang, Xu Qingbo, Role of biomechanical forces in stem cell vascular lineage differentiation, Arterioscler. Thromb. Vasc. Biol. 34 (2014) 2184–2190, https://doi.org/10.1161/ATVBAHA.114.303423.

[91] J. Jiang, D.S. Woulfe, E.T. Papoutsakis, Shear enhances thrombopoiesis and formation of microparticles that induce megakaryocytic differentiation of stem cells, Blood 124 (2014) 2094–2103, https://doi.org/10.1182/blood-2014-01-547927.

[92] A. Blaeser, D.F. Duarte Campos, U. Puster, W. Richtering, M.M. Stevens, H. Fischer, Controlling shear stress in 3d bioprinting is a key factor to balance printing resolution and stem cell integrity, Adv. Healthc. Mater. 5 (2016) 326–333, https://doi.org/10.1002/adhm.201500677.

[93] P. Mozetic, S.M. Giannitelli, M. Gori, M. Trombetta, A. Rainer, Engineering muscle cell alignment through 3D bioprinting, J. Biomed. Mater. Res. Part A 105 (2017) 2582–2588, https://doi.org/10.1002/jbm.a.36117.

[94] J.H. Kim, Y.-J. Seol, I.K. Ko, H.-W. Kang, Y.K. Lee, J.J. Yoo, A. Atala, S.J. Lee, 3D bioprinted human skeletal muscle constructs for muscle function restoration, Sci. Rep. 8 (2018) 12307, https://doi.org/10.1038/s41598-018-29968-5.

[95] H. Kim, J. Jang, J. Park, K.-P. Lee, S. Lee, D.-M. Lee, K.H. Kim, H.K. Kim, D.-W. Cho, Shear-induced alignment of collagen fibrils using 3D cell printing for corneal stroma tissue engineering, Biofabrication 11 (2019), 035017, https://doi.org/10.1088/1758-5090/ab1a8b.

[96] A. Sydney Gladman, E.A. Matsumoto, R.G. Nuzzo, L. Mahadevan, J.A. Lewis, Biomimetic 4D Printing, Nat. Mater. (2016) 413–418, https://doi.org/10.1038/nmat4544.

[97] M. Zhang, Y. Wang, M. Jian, C. Wang, X. Liang, J. Niu, Y. Zhang, Spontaneous alignment of graphene oxide in hydrogel during 3D printing for multistimuli-responsive actuation, Adv. Sci. 7 (2020) 1903048, https://doi.org/10.1002/advs.201903048.

[98] N. Zhou, Y. Bekenstein, C.N. Eisler, D. Zhang, A.M. Schwartzberg, P. Yang, A. P. Alivisatos, J.A. Lewis, Perovskite nanowire–block copolymer composites with digitally programmable polarization anisotropy, Sci. Adv. 5 (2019) eaav8141, https://doi.org/10.1126/sciadv.aav8141.

[99] D.E. Yunus, W. Shi, S. Sohrabi, Y. Liu, Shear induced alignment of short nanofibers in 3D printed polymer composites, Nanotechnology 27 (2016), 495302, https://doi.org/10.1088/0957-4484/27/49/495302.

[100] D. Yunus, Shear Induced Fiber Alignment and Acoustic Nanoparticle Micropatterning during Stereolithography, Theses and Dissertations. (2017). ⟨https://preserve.lehigh.edu/etd/2977⟩.

[101] D.E. Yunus, R. He, W. Shi, O. Kaya, Y. Liu, Short fiber reinforced 3d printed ceramic composite with shear induced alignment, Ceram. Int. 43 (2017) 11766–11772, https://doi.org/10.1016/j.ceramint.2017.06.012.

[102] P. Chakraborty, C. Zhou, D.D.L. Chung, Enhancing the inherent piezoelectric behavior of a three-dimensionally printed acrylate polymer by electrical poling, Smart Mater. Struct. 27 (2018), 115038, https://doi.org/10.1088/1361-665X/aae59d.

[103] P. Chakraborty, C. Zhou, D.D.L. Chung, Piezoelectric behavior of three-dimensionally printed acrylate polymer without filler or poling, J. Mater. Sci. 53 (2018) 6819–6830, https://doi.org/10.1007/s10853-018-2006-0.

[104] N.B. Gundrati, P. Chakraborty, C. Zhou, D.D.L. Chung, Effects of printing conditions on the molecular alignment of three-dimensionally printed polymer, Compos. Part B Eng. 134 (2018) 164–168, https://doi.org/10.1016/j.compositesb.2017.09.067.

[105] N.B. Gundrati, P. Chakraborty, C. Zhou, D.D.L. Chung, First observation of the effect of the layer printing sequence on the molecular structure of three-dimensionally printed polymer, as shown by in-plane capacitance measurement, Compos. Part B: Eng. 140 (2018) 78–82, https://doi.org/10.1016/j.compositesb.2017.12.008.

[106] P. Chakraborty, G. Zhao, C. Zhou, C. Cheng, D.D.L. Chung, Decreasing the shear stress-induced in-plane molecular alignment by unprecedented stereolithographic delay in three-dimensional printing, J. Mater. Sci. 54 (2019) 3586–3599, https://doi.org/10.1007/s10853-018-3047-0.

[107] P. Chakraborty, C. Zhou, D.D.L. Chung, Converse piezoelectric behavior of three-dimensionally printed polymer and comparison of the in-plane and out-of-plane behavior, Mater. Sci. Eng.: B 252 (2020), 114447, https://doi.org/10.1016/j.mseb.2019.114447.

[108] D.B. Möller, Acoustically driven particle transport in fluid chambers, ETH Zur. (2013), https://doi.org/10.3929/ETHZ-A-010080297.

[109] K. Moradi, Acoustic Manipulation and Alignment of Particles for Applications in Separation, Micro-Templating, and Device Fabrication, Doctor of Philosophy Mechanical Engineering, Florida International University, 2015. https://doi.org/10.25148/etd.FI15032198.

[110] C. Witte, Micromanipulation in microfluidics using optoelectronic and acoustic tweezing, (n.d.) 281.

[111] S. Asif, P. Chansoria, R. Shirwaiker, Ultrasound-assisted vat photopolymerization 3D printing of preferentially organized carbon fiber reinforced polymer composites, J. Manuf. Process. (2020), https://doi.org/10.1016/j.jmapro.2020.04.029.

[112] F.G. Mitri, F.H. Garzon, D.N. Sinha, Characterization of acoustically engineered polymer nanocomposite metamaterials using x-ray microcomputed tomography, Rev. Sci. Instrum. 82 (2011), 034903, https://doi.org/10.1063/1.3553207.

[113] M. Saito, T. Daian, K. Hayashi, S. Izumida, Fabrication of a polymer composite with periodic structure by the use of ultrasonic waves, J. Appl. Phys. 83 (1998) 3490–3494, https://doi.org/10.1063/1.366561.

[114] M. Saito, Y. Imanishi, Host-guest composites containing ultrasonically arranged particles, (n.d.) 5.

[115] S. Yamahira, S. Hatanaka, M. Kuwabara, S. Asai, Orientation of fibers in liquid by ultrasonic standing waves, Jpn. J. Appl. Phys. 39 (2000) 3683–3687, https://doi.org/10.1143/JJAP.39.3683.

[116] P. Brodeur, J.L. Dion, J.J. Garceau, G. Pelletier, D. Massicotte, Fiber characterization in a stationary ultrasonic field, IEEE Trans. Ultrason. Ferroelectr. Freq. Control 36 (1989) 549–553, https://doi.org/10.1109/58.31799.

[117] P. Glynne-Jones, R.J. Boltryk, N.R. Harris, A.W.J. Cranny, M. Hill, Mode-switching: a new technique for electronically varying the agglomeration position in an acoustic particle manipulator, Ultrasonics 50 (2010) 68–75, https://doi.org/10.1016/j.ultras.2009.07.010.

[118] P. Glynne-Jones, C.E.M. Demore, Congwei Ye, Yongqiang Qiu, S. Cochran, M. Hill, Array-controlled ultrasonic manipulation of particles in planar acoustic resonator, IEEE Trans. Ultrason. Ferroelectr. Freq. Control 59 (2012) 1258–1266, https://doi.org/10.1109/TUFFC.2012.2316.

[119] J. Lee, S.-Y. Teh, A. Lee, H.H. Kim, C. Lee, K.K. Shung, Single beam acoustic trapping, Appl. Phys. Lett. 95 (2009), 073701, https://doi.org/10.1063/1.3206910.

[120] S. Yang, J.R.G. Evans, A multi-component powder dispensing system for three dimensional functional gradients, Mater. Sci. Eng.: A 379 (2004) 351–359, https://doi.org/10.1016/j.msea.2004.03.047.

[121] L. Johansson, Acoustic Manipulation of Particles and Fluids in Microfluidic Systems, (2009). ⟨http://urn.kb.se/resolve?urn=urn:nbn:se:uu:diva-100758⟩ (accessed January 17, 2022).

[122] K. Niendorf, B. Raeymaekers, Quantifying macro- and microscale alignment of carbon microfibers in polymer-matrix composite materials fabricated using ultrasound directed self-assembly and 3D-printing, Compos. Part A Appl. Sci. Manuf. 129 (2020), 105713, https://doi.org/10.1016/j.compositesa.2019.105713.

[123] D.E. Yunus, S. Sohrabi, R. He, W. Shi, Y. Liu, Acoustic patterning for 3D embedded electrically conductive wire in stereolithography, J. Micromech. Microeng. 27 (2017), 045016, https://doi.org/10.1088/1361-6439/aa62b7.

[124] J. Wu, G. Du, Acoustic radiation force on a small compressible sphere in a focused beam, J. Acoust. Soc. Am. 87 (1990) 997–1003, https://doi.org/10.1121/1.399435.

[125] T. Kozuka, T. Tuziuti, H. Mitome, T. Fukuda, Acoustic micromanipulation using a multi-electrode transducer, in: MHS'96 Proceedings of the Seventh International Symposium on Micro Machine and Human Science, IEEE, Nagoya, Japan, 1996: pp. 163–170. https://doi.org/10.1109/MHS.1996.563418.

[126] K.T. T. T, M.H. F. T, Control of a standing wave field using a line-focused transducer for two-dimensional manipulation of particles, Jpn. J. Appl. Phys. Part 1. Regul. Pap., Short. Notes Rev. Pap. 37 (1998) 2974–2978.

[127] T. Kozuka, T. Tuziuti, H. Mitome, T. Fukuda, F. Arai, Control of position of a particle using a standing wave field generated by crossing sound beams, in: 1998 IEEE Ultrasonics Symposium. Proceedings (Cat. No. 98CH36102), IEEE, Sendai, Japan, 1998: pp. 657–660. https://doi.org/10.1109/ULTSYM.1998.762234.

[128] C.R.P. Courtney, C.-K. Ong, B.W. Drinkwater, A.L. Bernassau, P.D. Wilcox, D.R. S. Cumming, Manipulation of particles in two dimensions using phase controllable ultrasonic standing waves, Proc. R. Soc. A Math. Phys. Eng. Sci. 468 (2012) 337–360, https://doi.org/10.1098/rspa.2011.0269.

[129] C.R.P. Courtney, C.-K. Ong, B.W. Drinkwater, P.D. Wilcox, C. Demore, S. Cochran, P. Glynne-Jones, M. Hill, Manipulation of microparticles using phase-controllable ultrasonic standing waves, J. Acoust. Soc. Am. 128 (2010) EL195–EL199, https://doi.org/10.1121/1.3479976.

[130] J. Greenhall, Three-Dimensional Printing Engineered Materials via Integration of Ultrasound Directed Self-Assembly with Stereolithography, Ph.D. Thesis. (2017). ⟨http://adsabs.harvard.edu/abs/2017PhDT⟩. (accessed January 17, 2022).

[131] J. Greenhall, B. Raeymaekers, 3D printing macroscale engineered materials using ultrasound directed self-assembly and stereolithography, Adv. Mater. Technol. 2 (2017) 1700122, https://doi.org/10.1002/admt.201700122.

[132] T.M. Llewellyn-Jones, B.W. Drinkwater, R.S. Trask, 3D printed components with ultrasonically arranged microscale structure, Smart Mater. Struct. 25 (2016) 02LT01, https://doi.org/10.1088/0964-1726/25/2/02LT01.

[133] A. Hehr, M. Norfolk, A comprehensive review of ultrasonic additive manufacturing, Rapid Prototyp. J. 26 (2019) 445–458, https://doi.org/10.1108/RPJ-03-2019-0056.

[134] S. Piperno, H. Sazan, H. Shpaisman, Simultaneous polymerization and patterning: a one step acoustic directed assembly method, Polymer 173 (2019) 20–26, https://doi.org/10.1016/j.polymer.2019.04.016.

[135] L. Friedrich, R. Collino, T. Ray, M. Begley, Acoustic control of microstructures during direct ink writing of two-phase materials, Sens. Actuators A: Phys. 268 (2017) 213–221, https://doi.org/10.1016/j.sna.2017.06.016.

[136] R.R. Collino, T.R. Ray, R.C. Fleming, C.H. Sasaki, H. Haj-Hariri, M.R. Begley, Acoustic field controlled patterning and assembly of anisotropic particles, Extrem. Mech. Lett. 5 (2015) 37–46, https://doi.org/10.1016/j.eml.2015.09.003.

[137] R.R. Collino, T.R. Ray, R.C. Fleming, J.D. Cornell, B.G. Compton, M.R. Begley, Deposition of ordered two-phase materials using microfluidic print nozzles with acoustic focusing, Extrem. Mech. Lett. 8 (2016) 96–106, https://doi.org/10.1016/j.eml.2016.04.003.

[138] R.R. Collino, T.R. Ray, L.M. Friedrich, J.D. Cornell, C.D. Meinhart, M.R. Begley, Scaling relationships for acoustic control of two-phase microstructures during direct-write printing, Mater. Res. Lett. 6 (2018) 191–198, https://doi.org/10.1080/21663831.2018.1431317.

[139] Y. Sriphutkiat, S. Kasetsirikul, D. Ketpun, Y. Zhou, Cell alignment and accumulation using acoustic nozzle for bioprinting, Sci. Rep. 9 (2019), https://doi.org/10.1038/s41598-019-54330-8.

[140] Y. Sriphutkiat, S. Kasetsirikul, Y. Zhou, Formation of cell spheroids using Standing Surface Acoustic Wave (SSAW), Int. J. Bioprint. 4 (2018), https://doi.org/10.18063/ijb.v4i1.130.

[141] Y. Sriphutkiat, Y. Zhou, Particle accumulation in a microchannel and its reduction by a standing surface acoustic wave (SSAW), Sensors 17 (2017) 106, https://doi.org/10.3390/s17010106.

[142] Y. Sriphutkiat, Y. Zhou, Acoustic manipulation of microparticle in a cylindrical tube for 3D printing, Rapid Prototyp. J. 25 (2019) 925–938, https://doi.org/10.1108/RPJ-10-2017-0191.

[143] P. Wadsworth, I. Nelson, D.L. Porter, B. Raeymaekers, S.E. Naleway, Manufacturing bioinspired flexible materials using ultrasound directed self-assembly and 3D printing, Mater. Des. 185 (2020), 108243, https://doi.org/10.1016/j.matdes.2019.108243.

[144] P. Chansoria, R. Shirwaiker, 3D bioprinting of anisotropic engineered tissue constructs with ultrasonically induced cell patterning, Addit. Manuf. 32 (2020), 101042, https://doi.org/10.1016/j.addma.2020.101042.

[145] P. Chansoria, L.K. Narayanan, K. Schuchard, R. Shirwaiker, Ultrasound-assisted biofabrication and bioprinting of preferentially aligned three-dimensional cellular constructs, Biofabrication 11 (2019), 035015, https://doi.org/10.1088/1758-5090/ab15cf.

[146] I.E. Gunduz, M.S. McClain, P. Cattani, G.T.-C. Chiu, J.F. Rhoads, S.F. Son, 3D printing of extremely viscous materials using ultrasonic vibrations, Addit. Manuf. 22 (2018) 98–103, https://doi.org/10.1016/j.addma.2018.04.029.

[147] M.-S. Scholz, B.W. Drinkwater, R.S. Trask, Ultrasonic assembly of anisotropic short fibre reinforced composites, Ultrasonics 54 (2014) 1015–1019, https://doi.org/10.1016/j.ultras.2013.12.001.

[148] M.-S. Scholz, B.W. Drinkwater, T.M. Llewellyn-Jones, R.S. Trask, Counterpropagating wave acoustic particle manipulation device for the effective manufacture of composite materials, IEEE Trans. Ultrason. Ferroelectr., Freq. Control 62 (2015) 1845–1855, https://doi.org/10.1109/TUFFC.2015.007116.

[149] D.S. Melchert, R.R. Collino, T.R. Ray, N.D. Dolinski, L. Friedrich, M.R. Begley, D. S. Gianola, Flexible conductive composites with programmed electrical anisotropy using acoustophoresis, Adv. Mater. Technol. 4 (2019) 1900586, https://doi.org/10.1002/admt.201900586.

[150] T. Tuziuti, Y. Masuda, K. Yasui, K. Kato, Two-dimensional patterning of inorganic particles in resin using ultrasound-induced plate vibration, Jpn. J. Appl. Phys. 50 (2011), 088006, https://doi.org/10.1143/JJAP.50.088006.

[151] L. Lu, Z. Zhang, J. Xu, Y. Pan, 3D-printed polymer composites with acoustically assembled multidimensional filler networks for accelerated heat dissipation, Compos. Part B Eng. 174 (2019), 106991, https://doi.org/10.1016/j.compositesb.2019.106991.

[152] K. Melde, E. Choi, Z. Wu, S. Palagi, T. Qiu, P. Fischer, Acoustic fabrication via the assembly and fusion of particles, Adv. Mater. 30 (2018) 1704507, https://doi.org/10.1002/adma.201704507.

[153] K. Melde, A.G. Mark, T. Qiu, P. Fischer, Holograms for acoustics, Nature 537 (2016) 518–522, https://doi.org/10.1038/nature19755.

[154] Z. Ren, W. Hu, X. Dong, M. Sitti, Multi-functional soft-bodied jellyfish-like swimming, Nat. Commun. 10 (2019) 2703, https://doi.org/10.1038/s41467-019-10549-7.

[155] J.K. Hamilton, M.T. Bryan, A.D. Gilbert, F.Y. Ogrin, T.O. Myers, A new class of magnetically actuated pumps and valves for microfluidic applications, Sci. Rep. 8 (2018) 933, https://doi.org/10.1038/s41598-018-19506-8.

[156] R. Bernasconi, E. Carrara, M. Hoop, F. Mushtaq, X. Chen, B.J. Nelson, S. Pané, C. Credi, M. Levi, L. Magagnin, Magnetically navigable 3D printed multifunctional microdevices for environmental applications, Addit. Manuf. 28 (2019) 127–135, https://doi.org/10.1016/j.addma.2019.04.022.

[157] J. Billaud, F. Bouville, T. Magrini, C. Villevieille, A.R. Studart, Magnetically aligned graphite electrodes for high-rate performance Li-ion batteries, Nat. Energy 1 (2016) 1–6, https://doi.org/10.1038/nenergy.2016.97.

[158] M. Falahati, W. Zhou, A. Yi, L. Li, Fabrication of polymeric lenses using magnetic liquid molds, Appl. Phys. Lett. 114 (2019), 203701, https://doi.org/10.1063/1.5090511.

[159] S. Sundaram, M. Skouras, D.S. Kim, L. van den Heuvel, W. Matusik, Topology optimization and 3D printing of multimaterial magnetic actuators and displays, Sci. Adv. 5 (2019) eaaw1160, https://doi.org/10.1126/sciadv.aaw1160.

[160] T. Xu, J. Zhang, M. Salehizadeh, O. Onaizah, E. Diller, Millimeter-scale flexible robots with programmable three-dimensional magnetization and motions, Sci. Robot. 4 (2019), https://doi.org/10.1126/scirobotics.aav4494.

[161] Y. Kim, G.A. Parada, S. Liu, X. Zhao, Ferromagnetic soft continuum robots, Sci. Robot. 4 (2019) eaax7329, https://doi.org/10.1126/scirobotics.aax7329.

[162] M.M. Porter, M. Yeh, J. Strawson, T. Goehring, S. Lujan, P. Siripasopsotorn, M. A. Meyers, J. McKittrick, Magnetic freeze casting inspired by nature, Mater. Sci. Eng.: A 556 (2012) 741–750, https://doi.org/10.1016/j.msea.2012.07.058.

[163] L. Sliker, G. Ciuti, M. Rentschler, A. Menciassi, Magnetically driven medical devices: a review, Expert Rev. Med. Devices 12 (2015) 737–752, https://doi.org/10.1586/17434440.2015.1080120.

[164] Y.-L. Liu, D. Chen, P. Shang, D.-C. Yin, A review of magnet systems for targeted drug delivery, J. Control. Release 302 (2019) 90–104, https://doi.org/10.1016/j.jconrel.2019.03.031.

[165] T. Manouras, M. Vamvakaki, Field responsive materials: photo-, electro-, magnetic- and ultrasound-sensitive polymers, Polym. Chem. 8 (2016) 74–96, https://doi.org/10.1039/C6PY01455K.

[166] A.C. Day, P.E. Johnson, B.D. Stanley, Electromagnet having spacer for facilitating cooling and associated cooling method, US7675395B2, 2010. ⟨https://patents.google.com/patent/US7675395B2/en⟩ (Accessed 17 January 2022).

[167] S. Song, H. Yu, H. Ren, Study on mathematic magnetic field model of rectangular coils for magnetic actuation, in: 2015 IEEE 28th Canadian Conference on Electrical and Computer Engineering (CCECE), 2015: pp. 19–24. https://doi.org/10.1109/CCECE.2015.7129153.

[168] M.P. Kummer, J.J. Abbott, B.E. Kratochvil, R. Borer, A. Sengul, B.J. Nelson, OctoMag: an electromagnetic system for 5-DOF wireless micromanipulation, IEEE

Trans. Robot. 26 (2010) 1006–1017, https://doi.org/10.1109/TRO.2010.2073030.
[169] B.E. Kratochvil, M.P. Kummer, S. Erni, R. Borer, D.R. Frutiger, S. Schürle, B.J. Nelson, MiniMag: A. Hemispherical Electromagnetic System for 5-DOF Wireless Micromanipulation, in: O. Khatib, V. Kumar, G. Sukhatme (Eds.), Experimental Robotics: The 12th International Symposium on Experimental Robotics, Springer, Berlin, Heidelberg, 2014: pp. 317–329. https://doi.org/10.1007/978-3-642-28572-1_22.
[170] S. Jeon, G. Jang, H. Choi, S. Park, Magnetic navigation system with gradient and uniform saddle coils for the wireless manipulation of micro-robots in human blood vessels, IEEE Trans. Magn. 46 (2010) 1943–1946, https://doi.org/10.1109/TMAG.2010.2040144.
[171] J.M.D. Coey, Permanent magnet applications, J. Magn. Magn. Mater. 248 (2002) 441–456, https://doi.org/10.1016/S0304-8853(02)00335-9.
[172] R. Skomski, Y. Liu, J.E. Shield, G.C. Hadjipanayis, D.J. Sellmyer, Permanent magnetism of dense-packed nanostructures, J. Appl. Phys. 107 (2010) 09A739, https://doi.org/10.1063/1.3337657.
[173] J.M.D. Coey, Permanent magnets: plugging the gap, Scr. Mater. 67 (2012) 524–529, https://doi.org/10.1016/j.scriptamat.2012.04.036.
[174] L. Ren, X. Zhou, Q. Liu, Y. Liang, Z. Song, B. Zhang, B. Li, 3D magnetic printing of bio-inspired composites with tunable mechanical properties, J. Mater. Sci. 53 (2018) 14274–14286, https://doi.org/10.1007/s10853-018-2447-5.
[175] M.J. Casavant, D.A. Walters, J.J. Schmidt, R.E. Smalley, Neat macroscopic membranes of aligned carbon nanotubes, J. Appl. Phys. 93 (2003) 2153–2156, https://doi.org/10.1063/1.1536732.
[176] S. Safaee, R. Chen, Investigation of a magnetic field-assisted digital-light-processing stereolithography for functionally graded materials, Procedia Manuf. 34 (2019) 731–737, https://doi.org/10.1016/j.promfg.2019.06.229.
[177] B. Yellen, G. Friedman, A. Feinerman, Printing superparamagnetic colloidal particle arrays on patterned magnetic film, J. Appl. Phys. 93 (2003) 7331–7333, https://doi.org/10.1063/1.1555908.
[178] V.K. Venkiteswaran, L.F.P. Samaniego, J. Sikorski, S. Misra, Bio-inspired terrestrial motion of magnetic soft millirobots, IEEE Robot. Autom. Lett. 4 (2019) 1753–1759, https://doi.org/10.1109/LRA.2019.2898040.
[179] S. Anandhan, S. Bandyopadhyay, Polymer nanocomposites: from synthesis to applications, Nanocomp. Polym. Anal. Methods (2011), https://doi.org/10.5772/17039.
[180] J. Ciambella, D.C. Stanier, S.S. Rahatekar, Magnetic alignment of short carbon fibres in curing composites, Compos. Part B: Eng. 109 (2017) 129–137, https://doi.org/10.1016/j.compositesb.2016.10.038.
[181] R.M. Erb, R. Libanori, N. Rothfuchs, A.R. Studart, Composites reinforced in three dimensions by using low magnetic fields, Science 335 (2012) 199–204, https://doi.org/10.1126/science.1210822.
[182] S.J. Leigh, C.P. Purssell, D.R. Billson, D.A. Hutchins, Using a magnetite/thermoplastic composite in 3D printing of direct replacements for commercially available flow sensors, Smart Mater. Struct. 23 (2014), 095039, https://doi.org/10.1088/0964-1726/23/9/095039.
[183] U. D'Amora, T. Russo, A. Gloria, V. Rivieccio, V. D'Antò, G. Negri, L. Ambrosio, R. De Santis, 3D additive-manufactured nanocomposite magnetic scaffolds: Effect of the application mode of a time-dependent magnetic field on hMSCs behavior, Bioact. Mater. 2 (2017) 138–145, https://doi.org/10.1016/j.bioactmat.2017.04.003.
[184] P. Zhu, W. Yang, R. Wang, S. Gao, B. Li, Q. Li, 4D printing of complex structures with a fast response time to magnetic stimulus, ACS Appl. Mater. Interfaces 10 (2018) 36435–36442, https://doi.org/10.1021/acsami.8b12853.
[185] J. Hone, M.C. Llaguno, N.M. Nemes, A.T. Johnson, J.E. Fischer, D.A. Walters, M. J. Casavant, J. Schmidt, R.E. Smalley, Electrical and thermal transport properties of magnetically aligned single wall carbon nanotube films, Appl. Phys. Lett. 77 (2000) 666–668, https://doi.org/10.1063/1.127079.
[186] Y. Kim, H. Yuk, R. Zhao, S.A. Chester, X. Zhao, Printing ferromagnetic domains for untethered fast-transforming soft materials, Nature 558 (2018) 274–279, https://doi.org/10.1038/s41586-018-0185-0.
[187] A.F. Eufracio Aguilera, B. Nagarajan, B.A. Fleck, A.J. Qureshi, Ferromagnetic particle structuring in material jetting - manufacturing control system and software development, Procedia Manuf. 34 (2019) 545–551, https://doi.org/10.1016/j.promfg.2019.06.218.
[188] M. Roy, P. Tran, T. Dickens, B.D. Quaife, Effects of geometry constraints and fiber orientation in field assisted extrusion-based processing, Addit. Manuf. 32 (2020), 101022, https://doi.org/10.1016/j.addma.2019.101022.
[189] H. Song, J. Spencer, A. Jander, J. Nielsen, J. Stasiak, V. Kasperchik, P. Dhagat, Inkjet printing of magnetic materials with aligned anisotropy, J. Appl. Phys. 115 (2014) 17E308, https://doi.org/10.1063/1.4863168.
[190] T. Ahn, H.-J. Kim, J. Lee, D.-G. Choi, J.-Y. Jung, J.-H. Choi, S. Jeon, J.-D. Kim, J.-H. Jeong, A facile patterning of silver nanowires using a magnetic printing method, Nanotechnology 26 (2015), 345301, https://doi.org/10.1088/0957-4484/26/34/345301.
[191] G. Clay, H. Song, J. Nielsen, J. Stasiak, M. Khavari, A. Jander, P. Dhagat, 3D Printing Magnetic Material with Arbitrary Anisotropy, (2015). ⟨https://www.ingentaconnect.com/content/ist/nipdf/2015/00002015/00000001/art00068⟩ (accessed January 17, 2022).
[192] J.J. Martin, A. Caunter, A. Dendulk, S. Goodrich, R. Pembroke, D. Shores, R.M. Erb, Direct-write 3D printing of composite materials with magnetically aligned discontinuous reinforcement, in: T. George, A.K. Dutta, M.S. Islam (Eds.), Anaheim, California, United States, 2017: p. 101941I. https://doi.org/10.1117/12.2263215.
[193] J. Köhler, W. Bösch, E. Leitgeb, R. Teschl, D.J. Pommerenke, Manipulating Iron Filament with Permanent Magnets for FDM Printing for X-Band, in: 2020 International Conference on Broadband Communications for Next Generation Networks and Multimedia Applications (CoBCom), 2020: pp. 1–7. https://doi.org/10.1109/CoBCom49975.2020.9174185.
[194] B.B. Yellen, G. Friedman, Programmable assembly of colloidal particles using magnetic microwell templates, Langmuir 20 (2004) 2553–2559, https://doi.org/10.1021/la0352016.
[195] B.B. Yellen, O. Hovorka, G. Friedman, Arranging matter by magnetic nanoparticle assemblers, Proc. Natl. Acad. Sci. 102 (2005) 8860–8864, https://doi.org/10.1073/pnas.0500409102.
[196] J.J. Martin, M.S. Riederer, M.D. Krebs, R.M. Erb, Understanding and overcoming shear alignment of fibers during extrusion, Soft Matter 11 (2015) 400–405, https://doi.org/10.1039/C4SM02108H.
[197] Z. Long, A.M. Shetty, M.J. Solomon, R.G. Larson, Fundamentals of magnet-actuated droplet manipulation on an open hydrophobic surface, Lab a Chip 9 (2009) 1567–1575, https://doi.org/10.1039/B819818G.
[198] C. Yang, G. Li, A novel magnet-actuated droplet manipulation platform using a floating ferrofluid film, Sci. Rep. 7 (2017) 1–9, https://doi.org/10.1038/s41598-017-15964-8.
[199] Y. Park, J. Jeon, S.K. Chung, Three-dimensional (3D) magnetic droplet manipulation for biomedical applications, 2018 IEEE Micro Electro Mech. Syst. (MEMS) (2018) 1283–1285, https://doi.org/10.1109/MEMSYS.2018.8346799.
[200] L. Wang, F. Li, M. Kuang, M. Gao, J. Wang, Y. Huang, L. Jiang, Y. Song, Interface manipulation for printing three-dimensional microstructures under magnetic guiding, Small 11 (2015) 1900–1904, https://doi.org/10.1002/smll.201403355.
[201] A.J. Bandodkar, C.S. López, A.M.V. Mohan, L. Yin, R. Kumar, J. Wang, All-printed magnetically self-healing electrochemical devices, Sci. Adv. 2 (2016), e1601465, https://doi.org/10.1126/sciadv.1601465.
[202] K. Kobayashi, K. Ikuta, Three-dimensional magnetic microstructures fabricated by microstereolithography, Appl. Phys. Lett. 92 (2008), 262505, https://doi.org/10.1063/1.2954011.
[203] T.P. Niebel, F.J. Heiligtag, J. Kind, M. Zanini, A. Lauria, M. Niederberger, A. R. Studart, Multifunctional microparticles with uniform magnetic coatings and tunable surface chemistry, RSC Adv. 4 (2014) 62483–62491, https://doi.org/10.1039/C4RA09698C.
[204] R. Erb, J.J. Martin, Additive Manufacturing of Discontinuous Fiber Composites Using Magnetic Fields, US20170136699A1, 2017. ⟨https://patents.google.com/patent/US20170136699A1/⟩ (Accessed 17 January 2022).
[205] T. Nakamoto, S. Kojima, Layered thin film micro parts reinforced with aligned short fibers in laser stereolithography by applying magnetic field, J. Adv. Mech. Des. Syst. Manuf. 6 (2012) 849–858, https://doi.org/10.1299/jamdsm.6.849.
[206] Y. Pan, L. Lu, Additive Manufacturing of Magnetic Field-Responsive Smart Polymer Composites, (2016) V001T02A075. https://doi.org/10.1115/MSEC2016–8865.
[207] L. Lu, E. Baynojir Joyee, Y. Pan, Correlation between microscale magnetic particle distribution and magnetic-field-responsive performance of three-dimensional printed composites, J. Micro Nano Manuf. 6 (2017), 010904, https://doi.org/10.1115/1.4038574.
[208] L. Ren, B. Li, Z. Song, Q. Liu, L. Ren, X. Zhou, 3D printing of structural gradient soft actuators by variation of bioinspired architectures, J. Mater. Sci. 54 (2019) 6542–6551, https://doi.org/10.1007/s10853-019-03344-8.
[209] C. Credi, A. Fiorese, M. Tironi, R. Bernasconi, L. Magagnin, M. Levi, S. Turri, 3D printing of cantilever-type microstructures by stereolithography of ferromagnetic photopolymers, ACS Appl. Mater. Interfaces 8 (2016) 26332–26342, https://doi.org/10.1021/acsami.6b08880.
[210] L. Lu, P. Guo, Y. Pan, Magnetic-field-assisted projection stereolithography for three-dimensional printing of smart structures, J. Manuf. Sci. Eng. 139 (2017), 071008.
[211] E.B. Joyee, Y. Pan, Additive manufacturing of multi-material soft robot for on-demand drug delivery applications, J. Manuf. Process. 56 (2020) 1178–1184, https://doi.org/10.1016/j.jmapro.2020.03.059.
[212] E.B. Joyee, A. Szmelter, D. Eddington, Y. Pan, 3D printed biomimetic soft robot with multimodal locomotion and multifunctionality, Soft Robot. (2020), https://doi.org/10.1089/soro.2020.0004.
[213] H. Shinoda, S. Azukizawa, K. Maeda, F. Tsumori, Bio-mimic motion of 3D-printed gel structures dispersed with magnetic particles, J. Electrochem. Soc. 166 (2019) B3235–B3239, https://doi.org/10.1149/2.0361909jes.
[214] T. Liu, Q. Wang, A. Gao, C. Zhang, C. Wang, J. He, Fabrication of functionally graded materials by a semi-solid forming process under magnetic field gradients, Scr. Mater. 57 (2007) 992–995, https://doi.org/10.1016/j.scriptamat.2007.08.011.
[215] Z. Wang, X. Shi, H. Huang, C. Yao, W. Xie, C. Huang, P. Gu, X. Ma, Z. Zhang, L.-Q. Chen, Magnetically actuated functional gradient nanocomposites for strong and ultra-durable biomimetic interfaces/surfaces, Mater. Horiz. 4 (2017) 869–877, https://doi.org/10.1039/C7MH00223H.
[216] N. Lee, M.F. Horstemeyer, H. Rhee, B. Nabors, J. Liao, L.N. Williams, Hierarchical multiscale structure–property relationships of the red-bellied woodpecker (Melanerpes carolinus) beak, J. R. Soc. Interface 11 (2014) 20140274, https://doi.org/10.1098/rsif.2014.0274.
[217] L.-H. He, M.V. Swain, Enamel—a functionally graded natural coating, J. Dent. 37 (2009) 596–603, https://doi.org/10.1016/j.jdent.2009.03.019.
[218] Y.H. Hsu, I.G. Turner, A.W. Miles, Fabrication of porous bioceramics with porosity gradients similar to the bimodal structure of cortical and cancellous bone, J. Mater. Sci: Mater. Med 18 (2007) 2251–2256, https://doi.org/10.1007/s10856-007-3126-2.

[219] V. Birman, L.W. Byrd, Modeling and analysis of functionally graded materials and structures, Appl. Mech. Rev. 60 (2007) 195–216, https://doi.org/10.1115/1.2777164.
[220] E. Willert, A.I. Dmitriev, S.G. Psakhie, V.L. Popov, Effect of elastic grading on fretting wear, Sci. Rep. 9 (2019), https://doi.org/10.1038/s41598-019-44269-1.
[221] Nava Mirzaali, Nouri-Goushki Gunashekar, Zadpoor Doubrovski, Fracture behavior of bio-inspired functionally graded soft–hard composites made by multi-material 3D printing: the case of colinear cracks, Materials 12 (2019) 2735, https://doi.org/10.3390/ma12172735.
[222] S. Safaee, R.K. Chen, Development of a design and characterization framework for fabrication of functionally graded materials using magnetic field-assisted digital light processing stereolithography, J. Manuf. Process. 67 (2021) 314–324, https://doi.org/10.1016/j.jmapro.2021.04.058.
[223] M. Muthusamy, S. Safaee, R. Chen, Additive manufacturing of overhang structures using moisture-cured silicone with support material, J. Manuf. Mater. Process. 2 (2018) 24, https://doi.org/10.3390/jmmp2020024.
[224] Y. Ma, Q. Wu, L. Duanmu, S. Wu, Q. Liu, B. Li, X. Zhou, Bioinspired composites reinforced with ordered steel fibers produced via a magnetically assisted 3D printing process, J. Mater. Sci. 55 (2020) 15510–15522, https://doi.org/10.1007/s10853-020-05092-6.
[225] E.B. Joyee, A. Szmelter, D. Eddington, Y. Pan, Magnetic field-assisted stereolithography for productions of multimaterial hierarchical surface structures, ACS Appl. Mater. Interfaces 12 (2020) 42357–42368, https://doi.org/10.1021/acsami.0c11693.
[226] X. Li, W. Shan, Y. Yang, D. Joralmon, Y. Zhu, Y. Chen, Y. Yuan, H. Xu, J. Rong, R. Dai, Q. Nian, Y. Chai, Y. Chen, Limpet tooth-inspired painless microneedles fabricated by magnetic field-assisted 3D printing, Adv. Funct. Mater. 31 (2021) 2003725, https://doi.org/10.1002/adfm.202003725.
[227] B. Nagarajan, A.F. Eufracio Aguilera, M. Wiechmann, A.J. Qureshi, P. Mertiny, Characterization of magnetic particle alignment in photosensitive polymer resin: A preliminary study for additive manufacturing processes, Addit. Manuf. 22 (2018) 528–536, https://doi.org/10.1016/j.addma.2018.05.046.
[228] B. Nagarajan, M. Arshad, A. Ullah, P. Mertiny, A.J. Qureshi, Additive manufacturing ferromagnetic polymers using stereolithography – Materials and process development, Manuf. Lett. 21 (2019) 12–16, https://doi.org/10.1016/j.mfglet.2019.06.003.
[229] B. Nagarajan, M. Kamkar, M.A.W. Schoen, U. Sundararaj, S. Trudel, A.J. Qureshi, P. Mertiny, Development and characterization of stable polymer formulations for manufacturing magnetic composites, J. Manuf. Mater. Process. 4 (2020) 4, https://doi.org/10.3390/jmmp4010004.
[230] S. Safaee, A. Otero, M. Fei, T. Liu, J. Zhang, R.K. Chen, Particle-resin systems for additive manufacturing of rigid and elastic magnetic polymeric composites, Addit. Manuf. 51 (2022), 102587, https://doi.org/10.1016/j.addma.2021.102587.
[231] H.L. Ferrand, F. Bouville, T.P. Niebel, A.R. Studart, Magnetically assisted slip casting of bioinspired heterogeneous composites, Nat. Mater. 14 (2015) 1172–1179, https://doi.org/10.1038/nmat4419.
[232] M. Grossman, F. Bouville, F. Erni, K. Masania, R. Libanori, A.R. Studart, Mineral nano-interconnectivity stiffens and toughens nacre-like composite materials, Adv. Mater. 29 (2017) 1605039, https://doi.org/10.1002/adma.201605039.
[233] X. Dong, M. Sitti, Controlling two-dimensional collective formation and cooperative behavior of magnetic microrobot swarms, 0278364920903107, Int. J. Robot. Res. (2020), https://doi.org/10.1177/0278364920903107.
[234] L. Ren, X. Zhou, J. Xue, Z. Song, B. Li, Q. Liu, C. Zhao, Thermal metamaterials with site-specific thermal properties fabricated by 3D magnetic printing, Adv. Mater. Technol. 4 (2019) 1900296, https://doi.org/10.1002/admt.201900296.
[235] S. Nayak, N.R. Blumenfeld, T. Laksanasopin, S.K. Sia, Point-of-care diagnostics: recent developments in a connected age, Anal. Chem. 89 (2017) 102–123, https://doi.org/10.1021/acs.analchem.6b04630.
[236] S. Wang, S. Tasoglu, P.Z. Chen, M. Chen, R. Akbas, S. Wach, C.I. Ozdemir, U. A. Gurkan, F.F. Giguel, D.R. Kuritzkes, U. Demirci, Micro-a-fluidics ELISA for rapid CD4 cell count at the point-of-care, Sci. Rep. 4 (2014) 1–9, https://doi.org/10.1038/srep03796.
[237] C.L. Cramer, P. Nandwana, J. Yan, S.F. Evans, A.M. Elliott, C. Chinnasamy, M. P. Paranthaman, Binder jet additive manufacturing method to fabricate near net shape crack-free highly dense Fe-6.5 wt% Si soft magnets, Heliyon 5 (2019), e02804, https://doi.org/10.1016/j.heliyon.2019.e02804.
[238] L. Li, B. Post, V. Kunc, A.M. Elliott, M.P. Paranthaman, Additive manufacturing of near-net-shape bonded magnets: Prospects and challenges, Scr. Mater. 135 (2017) 100–104, https://doi.org/10.1016/j.scriptamat.2016.12.035.
[239] J.M.D. Coey, Perspective and prospects for rare earth permanent magnets, Engineering (2019), https://doi.org/10.1016/j.eng.2018.11.034.
[240] H.A. Pohl, The motion and precipitation of suspensoids in divergent electric fields, J. Appl. Phys. 22 (1951) 869–871, https://doi.org/10.1063/1.1700065.
[241] M.A. Witek, I.M. Freed, S.A. Soper, Cell separations and sorting, Anal. Chem. 92 (2020) 105–131, https://doi.org/10.1021/acs.analchem.9b05357.
[242] K. Khoshmanesh, S. Nahavandi, S. Baratchi, A. Mitchell, K. Kalantar-zadeh, Dielectrophoretic platforms for bio-microfluidic systems, Biosens. Bioelectron. 26 (2011) 1800–1814, https://doi.org/10.1016/j.bios.2010.09.022.
[243] E.M. Freer, O. Grachev, X. Duan, S. Martin, D.P. Stumbo, High-yield self-limiting single-nanowire assembly with dielectrophoresis, Nat. Nanotechnol. 5 (2010) 525–530, https://doi.org/10.1038/nnano.2010.106.
[244] S.A. Wilson, G.M. Maistros, R.W. Whatmore, Structure modification of 0–3 piezoelectric ceramic/polymer composites through dielectrophoresis, J. Phys. D: Appl. Phys. 38 (2005) 175–182, https://doi.org/10.1088/0022-3727/38/2/001.
[245] C.P. Bowen, R.E. Newnham, C.A. Randall, Dielectric properties of dielectrophoretically assembled particulate-polymer composites, J. Mater. Res. 13 (1998) 205–210, https://doi.org/10.1557/JMR.1998.0027.
[246] US20190207079A1 - Fabrication of Piezoelectric Composites Using High Temperature Dielectrophoresis Technique - Google Patents, (n.d.). ⟨https://patents.google.com/patent/US20190207079A1/en⟩ (Accessed 17 January 2022).
[247] G. Kim, Y.M. Shkel, Polymeric composites tailored by electric field, J. Mater. Res. 19 (2004) 1164–1174, https://doi.org/10.1557/JMR.2004.0151.
[248] M. Urdaneta, E. Smela, Multiple frequency dielectrophoresis, ELectrophoresis 28 (2007) 3145–3155, https://doi.org/10.1002/elps.200600786.
[249] G.H. Kim, D.K. Moeller, Y.M. Shkel, Orthotropic polymeric composites with microstructure tailored by electric field, J. Compos. Mater. 38 (2004) 1895–1909, https://doi.org/10.1177/0021998304048415.
[250] L. Zhang, T. Petit, Y. Lu, B.E. Kratochvil, K.E. Peyer, R. Pei, J. Lou, B.J. Nelson, Controlled propulsion and cargo transport of rotating nickel nanowires near a patterned solid surface, ACS Nano 4 (2010) 6228–6234, https://doi.org/10.1021/nn101861n.
[251] H. Kim, F. Torres, D. Villagran, C. Stewart, Y. Lin, T.-L.B. Tseng, 3D printing of BaTiO3/PVDF composites with electric in situ poling for pressure sensor applications, Macromol. Mater. Eng. 302 (2017) 1700229, https://doi.org/10.1002/mame.201700229.
[252] C. Lee, J.A. Tarbutton, Electric poling-assisted additive manufacturing process for PVDF polymer-based piezoelectric device applications, Smart Mater. Struct. 23 (2014), 095044, https://doi.org/10.1088/0964-1726/23/9/095044.
[253] D.A. van den Ende, S.E. van Kempen, X. Wu, W.A. Groen, C.A. Randall, S. van der Zwaag, Dielectrophoretically structured piezoelectric composites with high aspect ratio piezoelectric particles inclusions, J. Appl. Phys. 111 (2012), 124107, https://doi.org/10.1063/1.4729814.
[254] C. Park, J. Wilkinson, S. Banda, Z. Ounaies, K.E. Wise, G. Sauti, P.T. Lillehei, J. S. Harrison, Aligned single-wall carbon nanotube polymer composites using an electric field, J. Polym. Sci. Part B Polym. Phys. 44 (2006) 1751–1762, https://doi.org/10.1002/polb.20823.
[255] G. Kim, Field Aided Technology for Local Micro-tailoring of Polymeric Composites With Multi-functional Response, University of Wisconsin–Madison, 2003, p. 1.
[256] G.H. Kim, Y.M. Shkel, R.E. Rowlands, Field-aided microtailoring of polymeric nanocomposites, in: Smart Structures and Materials 2003: Electroactive Polymer Actuators and Devices (EAPAD), International Society for Optics and Photonics, SPIE, 2003, pp. 442–452, https://doi.org/10.1117/12.484432.
[257] G. Kim, Thermo-physical responses of polymeric composites tailored by electric field, Compos. Sci. Technol. 65 (2005) 1728–1735, https://doi.org/10.1016/j.compscitech.2005.02.013.
[258] G.H. Kim, D.K. Moeller, Y.M. Shkel, Functionally graded polymeric composites having micro-tailored structure formed by electric field, Am. Soc. Mech. Eng. Digit. Collect. (2008) 131–136, https://doi.org/10.1115/IMECE2003-43518.
[259] J. Holmes, Micro-Composite Fabrication via Field-Aided Laminar Composite (FALCom) Processing, Army research lab aberdeen proving ground md weapons and materials research directorate, 2012. https://apps.dtic.mil/docs/citations/ADA567078 (Accessed 17 January 2022).
[260] J. Holmes, J.P. Wolbert, J.M. Gardner, A Method for Out-of-autoclave Fabrication of High Fiber Volume Fraction Fiber Reinforced Polymer Composites, Army research lab aberdeen proving ground md weapons and materials research directorate, 2012. https://apps.dtic.mil/docs/citations/ADA564674 (Accessed 17 January 2022).
[261] L.-S. Turng, L.R.H. JR, Y. Peng, X. Li, Method of orientating fillers in composite materials, US8475703B2, 2013. ⟨https://patents.google.com/patent/US847570303B2/en⟩ (Accessed 17 January 2022).
[262] J.M. Gardner, J. Holmes, J.T. Tzeng, Fabrication of a First Article Lightweight Composite Technology Demonstrator - Exospine, ARMY Research lab aberdeen proving ground md weapons and materials research directorate, 2014. https://apps.dtic.mil/docs/citations/ADA601399 (accessed January 17, 2022).
[263] Z. Quan, A. Wu, M. Keefe, X. Qin, J. Yu, J. Suhr, J.-H. Byun, B.-S. Kim, T.-W. Chou, Additive manufacturing of multi-directional preforms for composites: opportunities and challenges, Mater. Today 18 (2015) 503–512, https://doi.org/10.1016/j.mattod.2015.05.001.
[264] G. Luo, K.S. Teh, Y. Liu, X. Zang, Z. Wen, L. Lin, Direct-write, self-aligned electrospinning on paper for controllable fabrication of three-dimensional structures, ACS Appl. Mater. Interfaces 7 (2015) 27765–27770, https://doi.org/10.1021/acsami.5b08909.
[265] W.E. Teo, S. Ramakrishna, A review on electrospinning design and nanofibre assemblies, Nanotechnology 17 (2006) R89–R106, https://doi.org/10.1088/0957-4484/17/14/R01.
[266] A. Greiner, J.H. Wendorff, Electrospinning: a fascinating method for the preparation of ultrathin fibers, Angew. Chem. Int. Ed. Engl. 46 (2007) 5670–5703, https://doi.org/10.1002/anie.200604646.
[267] A. Theron, E. Zussman, A.L. Yarin, Electrostatic field-assisted alignment of electrospun nanofibres, Nanotechnology 12 (2001) 384–390, https://doi.org/10.1088/0957-4484/12/3/329.
[268] B. Derby, Inkjet printing of functional and structural materials: fluid property requirements, feature stability, and resolution, Annu. Rev. Mater. Res. 40 (2010) 395–414, https://doi.org/10.1146/annurev-matsci-070909-104502.
[269] J.-M. Löwe, J. Plog, Y. Jiang, Y. Pan, A.L. Yarin, Drop deposition affected by electrowetting in direct ink writing process, J. Appl. Phys. 126 (2019), 035302, https://doi.org/10.1063/1.5109385.

[270] J. Plog, J.-M. Löwe, Y. Jiang, Y. Pan, A.L. Yarin, Control of direct written ink droplets using electrowetting, Langmuir 35 (2019) 11023–11036, https://doi.org/10.1021/acs.langmuir.9b01061.
[271] P. Amrollahi, J.S. Krasinski, R. Vaidyanathan, L. Tayebi, D. Vashaee, Electrophoretic deposition (EPD): fundamentals and applications from nano- to microscale structures, in: M. Aliofkhazraei, A.S.H. Makhlouf (Eds.), Handbook of Nanoelectrochemistry: Electrochemical Synthesis Methods, Properties, and Characterization Techniques, Springer International Publishing, Cham, 2016, pp. 561–591, https://doi.org/10.1007/978-3-319-15266-0_7.
[272] J. Tabellion, R. Clasen, Electrophoretic deposition from aqueous suspensions for near-shape manufacturing of advanced ceramics and glasses—applications, J. Mater. Sci. (2004) 803–811, https://doi.org/10.1023/B:JMSC.0000012907.52051.fb.
[273] K.T. Sullivan, C. Zhu, D.J. Tanaka, J.D. Kuntz, E.B. Duoss, A.E. Gash, Electrophoretic deposition of thermites onto micro-engineered electrodes prepared by direct-ink writing, J. Phys. Chem. B 117 (2013) 1686–1693, https://doi.org/10.1021/jp306440t.
[274] L. Vogt, M. Schäfer, D. Kurth, F. Raether, Usability of electrophoretic deposition for additive manufacturing of ceramics, Ceram. Int. 45 (2019) 14214–14222, https://doi.org/10.1016/j.ceramint.2019.04.129.
[275] V. Bharti, T. Kaura, R. Nath, Ferroelectric hysteresis in simultaneously stretched and corona-poled PVDF films, IEEE Trans. Dielectr. Electr. Insul. 4 (1997) 738–741, https://doi.org/10.1109/94.654689.
[276] R. Li, J. Pei, C. Xiong, Preparation and electric property of PA/PVDF blend for energy storage material, Polym. Sci. Ser. A. 58 (2016) 765–775, https://doi.org/10.1134/S0965545X16050126.
[277] S. Lanceros-Méndez, J.F. Mano, A.M. Costa, V.H. Schmidt, FTIR and DSC studies of mechanically deformed β-PVDF films, J. Macromol. Sci., Part B 40 (2001) 517–527, https://doi.org/10.1081/MB-100106174.
[278] M. Makrygianni, I. Kalpyris, C. Boutopoulos, I. Zergioti, Laser induced forward transfer of Ag nanoparticles ink deposition and characterization, Appl. Surf. Sci. 297 (2014) 40–44, https://doi.org/10.1016/j.apsusc.2014.01.069.
[279] M. Singh, H.M. Haverinen, P. Dhagat, G.E. Jabbour, Inkjet printing—process and its applications, Adv. Mater. 22 (2010) 673–685, https://doi.org/10.1002/adma.200901141.
[280] T. Schüler, T. Asmus, W. Fritzsche, R. Möller, Screen printing as cost-efficient fabrication method for DNA-chips with electrical readout for detection of viral DNA, Biosens. Bioelectron. 24 (2009) 2077–2084, https://doi.org/10.1016/j.bios.2008.10.028.
[281] C.-H. Hsu, M.-C. Yeh, K.-L. Lo, L.-J. Chen, Application of microcontact printing to electroless plating for the fabrication of microscale silver patterns on glass, Langmuir 23 (2007) 12111–12118, https://doi.org/10.1021/la7023988.
[282] N. Liu, F. Wei, L. Liu, H.S.S. Lai, H. Yu, Y. Wang, G.-B. Lee, W.J. Li, Optically-controlled digital electrodeposition of thin-film metals for fabrication of nano-devices, Opt. Mater. Express, Ome. 5 (2015) 838–848, https://doi.org/10.1364/OME.5.000838.
[283] A.J. Pascall, F. Qian, G. Wang, M.A. Worsley, Y. Li, J.D. Kuntz, Light-directed electrophoretic deposition: a new additive manufacturing technique for arbitrarily patterned 3D composites, Adv. Mater. 26 (2014) 2252–2256, https://doi.org/10.1002/adma.201304953.
[284] A.J. Pascall, J. Mora, J.A. Jackson, J.D. Kuntz, Light directed electrophoretic deposition for additive manufacturing: spatially localized deposition control with photoconductive counter electrodes, Key Eng. Mater. 654 (2015) 261–267, https://doi.org/10.4028/www.scientific.net/KEM.654.261.
[285] J. Mora, J.K. Dudoff, B.D. Moran, J.R. DeOtte, W.L. Du Frane, J.D. Kuntz, A. J. Pascall, Projection based light-directed electrophoretic deposition for additive manufacturing, Addit. Manuf. 22 (2018) 330–333, https://doi.org/10.1016/j.addma.2018.05.020.
[286] H. Kawamoto, S. Umezu, R. Koizumi, Fundamental investigation on electrostatic ink jet phenomena in pin-to-plate discharge system, J. Imaging Sci. Technol. 49 (2005) 19–27.
[287] J.-U. Park, M. Hardy, S.J. Kang, K. Barton, K. Adair, D. Kishore Mukhopadhyay, C. Y. Lee, M.S. Strano, A.G. Alleyne, J.G. Georgiadis, P.M. Ferreira, J.A. Rogers, High-resolution electrohydrodynamic jet printing, Nat. Mater. 6 (2007) 782–789, https://doi.org/10.1038/nmat1974.
[288] H. Lee, B. Seong, J. Kim, Y. Jang, D. Byun, Direct alignment and patterning of silver nanowires by electrohydrodynamic jet printing, Small 10 (2014) 3918–3922, https://doi.org/10.1002/smll.201400936.
[289] B.W. An, K. Kim, M. Kim, S.-Y. Kim, S.-H. Hur, J.-U. Park, Direct printing of reduced graphene oxide on planar or highly curved surfaces with high resolutions using electrohydrodynamics, Small 11 (2015) 2263–2268, https://doi.org/10.1002/smll.201403131.
[290] K. Kim, G. Kim, B. Ram Lee, S. Ji, S.-Y. Kim, B. Wan An, M. Hoon Song, J.-U. Park, High-resolution electrohydrodynamic jet printing of small-molecule organic light-emitting diodes, Nanoscale 7 (2015) 13410–13415, https://doi.org/10.1039/C5NR03034J.
[291] T. Liu, R. Huang, J. Zhong, Y. Yang, Z. Tan, W. Tan, Control of cell proliferation in E-jet 3D-printed scaffolds for tissue engineering applications: the influence of the cell alignment angle, J. Mater. Chem. B 5 (2017) 3728–3738, https://doi.org/10.1039/C7TB00377C.
[292] C. Park, R.E. Robertson, Alignment of particles by an electric field, Mater. Sci. Eng. A 257 (1998) 295–311, https://doi.org/10.1016/S0921-5093(98)00848-X.
[293] T. Nakamoto, O. Kanehisa, Y. Sugawa, Whisker alignment in microparts using laser stereolithography with applied electric field, J. Adv. Mech. Des. Syst. Manuf. 7 (2013) 888–902, https://doi.org/10.1299/jamdsm.7.888.
[294] K. Kim, W. Zhu, X. Qu, C. Aaronson, W.R. McCall, S. Chen, D.J. Sirbuly, 3D optical printing of piezoelectric nanoparticle–polymer composite materials, ACS Nano 8 (2014) 9799–9806, https://doi.org/10.1021/nn503268f.
[295] Y. Pan, A. Patil, C. Zhou, A novel projection based electro-stereolithography (PES) process for composite printing, in: Annual Solid Freeform Fabrication Symposium, Austin, 2015. ⟨http://sffsymposium.engr.utexas.edu/sites/default/files/2015/2015–1-Pan.pdf⟩ (accessed January 17, 2022).
[296] Y. Pan, A. Patil, P. Guo, C. Zhou, A novel projection based electro-stereolithography (PES) process for production of 3D polymer-particle composite objects, Rapid Prototyp. J. 23 (2017) 236–245, https://doi.org/10.1108/RPJ-02-2016-0030.
[297] J. Aizenberg, P. Fratzl, New materials through bioinspiration and nanoscience, Adv. Funct. Mater. 23 (2013) 4398–4399, https://doi.org/10.1002/adfm.201302690.
[298] B. Wang, W. Yang, J. McKittrick, M.A. Meyers, Keratin: structure, mechanical properties, occurrence in biological organisms, and efforts at bioinspiration, Prog. Mater. Sci. 76 (2016) 229–318, https://doi.org/10.1016/j.pmatsci.2015.06.001.
[299] S.E. Naleway, M.M. Porter, J. McKittrick, M.A. Meyers, Structural design elements in biological materials: application to bioinspiration, Adv. Mater. 27 (2015) 5455–5476, https://doi.org/10.1002/adma.201502403.
[300] Y. Yang, Z. Chen, X. Song, Z. Zhang, J. Zhang, K.K. Shung, Q. Zhou, Y. Chen, Biomimetic anisotropic reinforcement architectures by electrically assisted nanocomposite 3D printing, Adv. Mater. 29 (2017) 1605750, https://doi.org/10.1002/adma.201605750.
[301] Y. Yang, X. Li, M. Chu, H. Sun, J. Jin, K. Yu, Q. Wang, Q. Zhou, Y. Chen, Electrically assisted 3D printing of nacre-inspired structures with self-sensing capability, Sci. Adv. 5 (2019) eaau9490, https://doi.org/10.1126/sciadv.aau9490.
[302] M.N. Vyakarnam, L.T. Drzal, Composite material of aligned discontinuous fibers, US6025285A, 2000. ⟨https://patents.google.com/patent/US6025285A/en⟩ (Accessed 17 January 2022).
[303] K.M. Ryan, A. Mastroianni, K.A. Stancil, H. Liu, A.P. Alivisatos, Electric-field-assisted assembly of perpendicularly oriented nanorod superlattices, Nano Lett. 6 (2006) 1479–1482, https://doi.org/10.1021/nl060866o.
[304] B.Y. Decker, Y.X. Gan, Electric field-assisted additive manufacturing polyaniline based composites for thermoelectric energy conversion, J. Manuf. Sci. Eng. 137 (2015), https://doi.org/10.1115/1.4029398.
[305] J. Daniel, L. Ju, J. Yang, X. Sun, N. Gupta, A. Schrand, C. Xu, Pearl-chain formation of discontinuous carbon fiber under an electrical field, J. Manuf. Mater. Process. 1 (2017) 22, https://doi.org/10.3390/jmmp1020022.
[306] S. Wu, R.B. Ladani, J. Zhang, E. Bafekrpour, K. Ghorbani, A.P. Mouritz, A. J. Kinloch, C.H. Wang, Aligning multilayer graphene flakes with an external electric field to improve multifunctional properties of epoxy nanocomposites, Carbon 94 (2015) 607–618, https://doi.org/10.1016/j.carbon.2015.07.026.
[307] E. Palleau, D. Morales, M.D. Dickey, O.D. Velev, Reversible patterning and actuation of hydrogels by electrically assisted ionoprinting, Nat. Commun. 4 (2013), https://doi.org/10.1038/ncomms3257.
[308] C.-Y. Huang, C.-C. Wu, The EMI shielding effectiveness of PC/ABS/nickel-coated-carbon-fibre composites, Eur. Polym. J. 36 (2000) 2729–2737, https://doi.org/10.1016/S0014-3057(00)00039-2.
[309] Y. Li, Z. Feng, L. Huang, K. Essa, E. Bilotti, H. Zhang, T. Peijs, L. Hao, Additive manufacturing high performance graphene-based composites: a review, Compos. Part A: Appl. Sci. Manuf. 124 (2019), 105483, https://doi.org/10.1016/j.compositesa.2019.105483.
[310] E. Zakar, T. Anthony, M. Dubey, Effects of conductive polymer composite layering on EMI shielding during additive manufacturing, MRS Adv. 4 (2019) 2153–2159, https://doi.org/10.1557/adv.2019.326.
[311] Park Gyuhae, Rosing Tajana, D. Todd Michael, R. Farrar Charles, Hodgkiss William, Energy harvesting for structural health monitoring sensor networks, J. Infrastruct. Syst. 14 (2008) 64–79, https://doi.org/10.1061/(ASCE)1076-0342(2008)14:1(64).
[312] R.H. Baughman, C. Cui, A.A. Zakhidov, Z. Iqbal, J.N. Barisci, G.M. Spinks, G. G. Wallace, A. Mazzoldi, D.D. Rossi, A.G. Rinzler, O. Jaschinski, S. Roth, M. Kertesz, Carbon Nanotube Actuators, Science 284 (1999) 1340–1344, https://doi.org/10.1126/science.284.5418.1340.
[313] T. Lei, L. Yu, G. Zheng, L. Wang, D. Wu, D. Sun, Electrospinning-induced preferred dipole orientation in PVDF fibers, J. Mater. Sci. 50 (2015) 4342–4347, https://doi.org/10.1007/s10853-015-8986-0.
[314] N.S. Weston, B. Thomas, M. Jackson, Processing metal powders via field assisted sintering technology (FAST): a critical review, Mater. Sci. Technol. 35.11 (2019) 1306–1328.
[315] Y. Mao, et al., Influence of the interface strength on the mechanical properties of discontinuous tungsten fiber-reinforced tungsten composites produced by field assisted sintering technology, Compos. Part A Appl. Sci. Manuf. 107 (2018) 342–353.